
Learning from Similarity-Confidence and Confidence-Difference

Tomoya Tate

Waseda University
3-4-1 Okubo, Shinjuku, Tokyo 169-8555, Japan
tomot203@toki.waseda.jp

Kosuke Sugiyama

Waseda University
3-4-1 Okubo, Shinjuku, Tokyo 169-8555, Japan
kohsuke0322@asagi.waseda.jp

Masato Uchida

Waseda University
3-4-1 Okubo, Shinjuku, Tokyo 169-8555, Japan
m.uchida@waseda.jp

Abstract

In practical machine learning applications, it is often challenging to assign accurate labels to data, and increasing the number of labeled instances is often limited. In such cases, Weakly Supervised Learning (WSL), which enables training with incomplete or imprecise supervision, provides a practical and effective solution. However, most existing WSL methods focus on leveraging a single type of weak supervision. In this paper, we propose a novel WSL framework that leverages complementary weak supervision signals from multiple relational perspectives, which can be especially valuable when labeled data is limited. Specifically, we introduce *SconfConfDiff Classification*, a method that integrates two distinct forms of weak labels: similarity-confidence and confidence-difference, which are assigned to unlabeled data pairs. To implement this method, we derive two types of unbiased risk estimators for classification: one based on a convex combination of existing estimators, and another newly designed by modeling the interaction between two weak labels. We prove that both estimators achieve optimal convergence rates with respect to estimation error bounds. Furthermore, we introduce a risk correction approach to mitigate overfitting caused by negative empirical risk, and provide theoretical analysis on the robustness of the proposed method against inaccurate class prior probability and label noise. Experimental results demonstrate that the proposed method consistently outperforms existing baselines across a variety of settings.

1 Introduction

In recent years, machine learning models have achieved remarkable performance across a wide range of applications. However, training high-performance models typically requires large amounts of accurately labeled data. In many real-world scenarios, acquiring such labels is often expensive, time-consuming, or even impractical, thereby limiting the availability of sufficient training data. To address this challenge, various Weakly Supervised Learning (WSL) methods [1] have been

proposed to exploit incomplete supervision, including Positive-Unlabeled Learning [2, 3, 4, 5, 6], Partial-Label Learning [7], Unlabeled-Unlabeled Learning [8], and Complementary-Label Learning [9, 10]. More recently, research has shifted toward learning from labeled pairs of instances rather than individual samples [11, 12, 13], demonstrating promising results. Notable examples include Similarity-Confidence (Sconf) Learning [14] and Confidence-Difference (ConfDiff) Classification [15].

In addition to labeling challenges, there are scenarios where increasing the number of instances is simply not feasible – not due to cost or effort, but because the data pertains to phenomena that are inherently rare, unobservable, or access-restricted. For instance, in predicting the risk of rare diseases, obtaining labels may be challenging due to the need for expert knowledge. Similarly, in domains such as security and privacy, data availability may be constrained by ethical, legal, or technical barriers. When the number of instances is fundamentally limited, increasing the sample size becomes difficult regardless of intent. In such scenarios, there is a critical need for learning frameworks that enhance model performance by enriching limited data with information derived from multiple diverse perspectives.

Conventional WSL methods typically assume that each training instance is annotated with a single type of weak label, and accordingly design risk estimators specific to that label type. In contrast, we investigate a novel setting in which multiple forms of weak supervision are simultaneously available and can be utilized jointly for training. Our objective is to derive risk estimators that aggregate these labels in a unified manner. Our key hypothesis is that leveraging multiple sources of weak supervision can lead to more accurate models, even when the number of labeled instances is limited.

In this paper, we propose an effective training method, *SconfConfDiff Classification*, which learns a binary classifier using two types of weak labels: similarity-confidence, introduced in Sconf Learning [14], and confidence-difference, introduced in ConfDiff Classification [15]. Similarity-confidence is defined as the probability that a pair of data points belongs to the same class, while confidence-difference represents the difference between the probabilities that each point in the pair belongs to the positive class. By leveraging them, we can construct richer supervision that facilitates more effective learning.

The contributions of this paper are summarized as follows. First, we propose two unbiased risk estimators for binary classification, both of which can be computed from similarity-confidence and confidence-difference. In Section 3.1, we construct the first estimator as a convex combination of the unbiased estimators individually derived from Sconf Learning and ConfDiff Classification. While this approach can be effective, as demonstrated in the experiments, it treats similarity-confidence and confidence-difference in isolation, ignoring how they jointly reflect the relationship between labels. To address this limitation, we develop a second estimator in Section 3.2 that directly models the interaction between the two weak supervision signals, thereby capturing their combined influence on label prediction, and we analyze the variance of the estimator in Section 3.3. Furthermore, in Section 3.4, we provide an estimation error analysis and prove that the proposed method achieves the optimal convergence rate, and we investigate the impact of an inaccurate class prior probability and noisy labels on the estimation error bound in Section 3.5. Additionally, to mitigate overfitting resulting from negative empirical risk values, we introduce a risk correction approach and derive the estimation error bound under risk correction in Section 3.6.

To evaluate the effectiveness of the proposed method, we conduct experiments using the settings described in Section 4.1, and assess the classification accuracy and the improvement achieved through the risk correction approach in Section 4.2. Section 4.3 presents experiments with fewer training data, and in Section 4.4, we experimentally investigate the robustness of the proposed method.

2 Preliminaries

In this section, we describe the problem setting and present the formulations of binary classification, Sconf Learning, and ConfDiff Classification.

2.1 Binary Classification

For binary classification, let $\mathcal{X} \subseteq \mathbb{R}^d$ denote the d -dimensional feature space and $\mathcal{Y} = \{-1, +1\}$ denote the label space. Let $p(\mathbf{x}, y)$ denote the unknown joint probability density over random

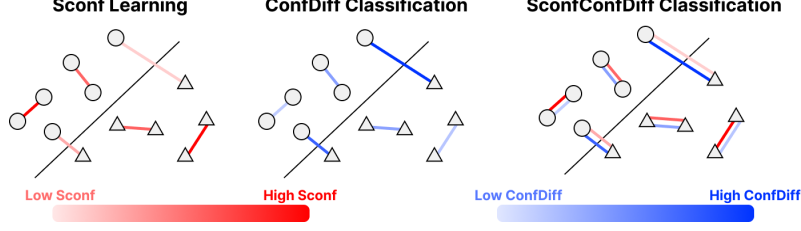


Figure 1: Illustration of Sconf Learning, ConfDiff Classification, and SconfConfDiff Classification

variables (\mathbf{x}, y) . The goal of binary classification is to find a binary classifier $g : \mathcal{X} \rightarrow \mathbb{R}$ that minimizes the following classification risk [16]:

$$R(g) = \mathbb{E}_{p(\mathbf{x}, y)}[\ell(g(\mathbf{x}), y)], \quad (1)$$

where $\ell : \mathbb{R} \times \mathcal{Y} \rightarrow \mathbb{R}^+$ is a non-negative binary classification loss function, such as 0-1 loss and logistic loss. Then, the classification risk $R(g)$ in Eq. (1) can be equivalently expressed as

$$R(g) = \pi_+ \mathbb{E}_{p(\mathbf{x}|y=+1)}[\ell(g(\mathbf{x}), +1)] + \pi_- \mathbb{E}_{p(\mathbf{x}|y=-1)}[\ell(g(\mathbf{x}), -1)], \quad (2)$$

where $\pi_+ = p(y = +1)$ and $\pi_- = p(y = -1)$ denote the class prior probabilities for positive and negative classes, respectively.

2.2 Similarity-Confidence (Sconf) Learning

In Sconf Learning [14], we are given unlabeled data pairs annotated with similarity-confidence, $\mathcal{D}_n = \{(\mathbf{x}_i, \mathbf{x}'_i), s_i\}_{i=1}^n$, without ordinary class labels. Here, $s_i = s(\mathbf{x}_i, \mathbf{x}'_i) = p(y_i = y'_i | \mathbf{x}_i, \mathbf{x}'_i)$ denotes the probability that two data points share the same label. Then, an unbiased risk estimator for Sconf Learning is derived as follows:

$$\widehat{R}_{\text{Sconf}}(g) = \frac{1}{2n} \sum_{i=1}^n \left\{ \frac{(\pi_- - s_i)(\ell(g(\mathbf{x}_i), +1) + \ell(g(\mathbf{x}'_i), +1))}{\pi_- - \pi_+} + \frac{(\pi_+ - s_i)(\ell(g(\mathbf{x}_i), -1) + \ell(g(\mathbf{x}'_i), -1))}{\pi_+ - \pi_-} \right\}. \quad (3)$$

Here, the unlabeled data pair $(\mathbf{x}_i, \mathbf{x}'_i)$ is assumed to be drawn independently from a probability density $p(\mathbf{x}, \mathbf{x}') = p(\mathbf{x})p(\mathbf{x}')$.

2.3 Confidence-Difference (ConfDiff) Classification

In ConfDiff Classification [15], we are given unlabeled data pairs annotated with confidence-difference, $\mathcal{D}_n = \{(\mathbf{x}_i, \mathbf{x}'_i), c_i\}_{i=1}^n$, without ordinary class labels. Here, $c_i = c(\mathbf{x}_i, \mathbf{x}'_i) = p(y'_i = +1 | \mathbf{x}'_i) - p(y_i = +1 | \mathbf{x}_i)$ denotes the difference in the posterior probabilities between the unlabeled data pair. Then, an unbiased risk estimator for ConfDiff Classification is derived as follows:

$$\widehat{R}_{\text{CD}}(g) = \frac{1}{2n} \sum_{i=1}^n ((\pi_+ - c_i)\ell(g(\mathbf{x}_i), +1) + (\pi_- - c_i)\ell(g(\mathbf{x}'_i), -1) + (\pi_+ + c_i)\ell(g(\mathbf{x}'_i), +1) + (\pi_- + c_i)\ell(g(\mathbf{x}_i), -1)). \quad (4)$$

Here, similar to Sconf Learning, the unlabeled data pair $(\mathbf{x}_i, \mathbf{x}'_i)$ is assumed to be drawn independently from a probability density $p(\mathbf{x}, \mathbf{x}') = p(\mathbf{x})p(\mathbf{x}')$.

We remark that similarity-confidence and confidence-difference encode different aspects of the relationships between data points. In particular, they can be interpreted as capturing their relative positioning from distinct geometric perspectives, as illustrated in Appendix F, which offers additional intuition about the nature of these labels.

3 The Proposed Method and Theoretical Analysis

Under the above setting, we consider the problem of learning a binary classifier from unlabeled data pairs annotated with similarity-confidence and confidence-difference, $\mathcal{D}_n = \{(\mathbf{x}_i, \mathbf{x}'_i), s_i, c_i\}_{i=1}^n$. In this section, we formally define the proposed method and provide its theoretical guarantees. Furthermore, we analyze the impact of an inaccurate class prior probability and noisy similarity-confidence and confidence-difference labels, and introduce a risk correction approach to mitigate overfitting. Theoretical proofs are provided in the appendices.

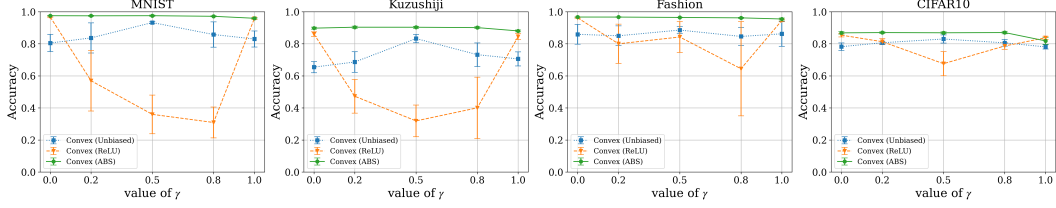


Figure 2: Experimental results for based on empirical risk minimization in Eq. (5). $\gamma = 0$ means ConfDiff Classification and $\gamma = 1$ means Sconf Learning.

3.1 Simple Convex Combination for Unbiased Risk Estimation

As previously discussed, unbiased risk estimators based solely on either similarity-confidence or confidence-difference can be expressed by Eq. (3) and Eq. (4), respectively. Given these prior results, it follows naturally that an unbiased estimator for the classification risk in Eq. (1) can be constructed as a convex combination of the two estimators. We formally present this result in the following theorem.

Theorem 1. *The following expression is an unbiased risk estimator:*

$$\widehat{R}_{\text{SCD}_{\text{convex}}}(g) = \gamma \widehat{R}_{\text{Sconf}}(g) + (1 - \gamma) \widehat{R}_{\text{CD}}(g), \quad (5)$$

where $\gamma \in [0, 1]$ is an arbitrary weight.

Figure 2 shows the classification performance based on empirical risk minimization as defined by Eq. (5), where the effects of applying the ReLU correction function and the absolute value correction function are compared. The absolute value correction retains the loss even when the estimated risk is negative, thus allowing the method to leverage both similarity-confidence and confidence-difference information. As a result, a simple convex combination using the absolute value correction achieves higher classification accuracy than the original unbiased estimator without correction. In contrast, the ReLU correction replaces negative risk values with zero, thereby inappropriately ignoring the corresponding losses. This may cause the loss associated with either s_i or c_i to be omitted for certain instances, thereby failing to account for the inherent correlation between the two signals, which are potentially complementary and may benefit from being used together. Consequently, we observe a degradation in classification performance when using the ReLU correction, as compared to using either similarity-confidence ($\gamma = 1.0$) or confidence-difference ($\gamma = 0.0$) alone. The theoretical analysis of the convex combination approach and the associated risk correction techniques is based on existing work and is provided in Appendix B.

Although the design of the risk correction function influences the estimation error, a more fundamental limitation lies in the structure of the estimator based on a simple convex combination. Specifically, the current approach computes the losses for similarity-confidence s_i and confidence-difference c_i independently for each data pair, and aggregates them without coherently utilizing both sources of information for individual instances. As a result, the estimator fails to fully exploit the combined effects of similarity-confidence and confidence-difference, which may structurally limit classification performance. To address this issue, we propose a novel unbiased risk estimator that directly incorporates both similarity-confidence and confidence-difference for each instance, rather than relying on a simple convex combination.

3.2 Unbiased Risk Estimator

In this section, we show that the classification risk in Eq. (1) can be expressed with Sconf and ConfDiff data.

Theorem 2. *The classification risk $R(g)$ in Eq. (1) can be equivalently expressed as*

$$R_{\text{SCD}}(g) = \mathbb{E}_{p(\mathbf{x}, \mathbf{x}')} \left[\frac{1}{2} (\mathcal{L}(\mathbf{x}, \mathbf{x}') + \mathcal{L}(\mathbf{x}', \mathbf{x})) \right], \quad (6)$$

where

$$\begin{aligned} \mathcal{L}(\mathbf{x}, \mathbf{x}') &= (2\pi_+(\pi_+ - c(\mathbf{x}, \mathbf{x}')) + \pi_- - s(\mathbf{x}, \mathbf{x}'))\ell(g(\mathbf{x}), +1) \\ &\quad + (2\pi_-(\pi_- - c(\mathbf{x}, \mathbf{x}')) + \pi_+ - s(\mathbf{x}, \mathbf{x}'))\ell(g(\mathbf{x}'), -1). \end{aligned}$$

Accordingly, we can derive an unbiased risk estimator for SconfConfDiff Classification:

$$\widehat{R}_{\text{SCD}}(g) = \frac{1}{2n} \sum_{i=1}^n (\mathcal{L}(\mathbf{x}_i, \mathbf{x}'_i) + \mathcal{L}(\mathbf{x}'_i, \mathbf{x}_i)). \quad (7)$$

3.3 Minimum-Variance Risk Estimator

Equation (7) is one of the candidates of the unbiased risk estimator. Actually, Eq. (8), which replaces the 1/2 in Eq. (7) with a weighted sum using $\lambda \in [0, 1]$, is also an unbiased risk estimator.

Lemma 1. *The following expression is also an unbiased risk estimator:*

$$\frac{1}{n} \sum_{i=1}^n (\lambda \mathcal{L}(\mathbf{x}_i, \mathbf{x}'_i) + (1 - \lambda) \mathcal{L}(\mathbf{x}'_i, \mathbf{x}_i)), \quad (8)$$

where $\lambda \in [0, 1]$ is an arbitrary weight.

Then, we introduce the following theorem, which characterizes the relationship between Eqs. (7) and (8).

Theorem 3. *The unbiased risk estimator in Eq. (7) has the minimum variance among all candidate unbiased risk estimators in the form of Eq. (8) w.r.t. $\lambda \in [0, 1]$.*

Based on the result of Theorem 3, we adopt the risk estimator in Eq. (7) in the following sections.

3.4 Estimation Error Bound

In this section, we discuss the convergence property of the proposed risk estimator $\widehat{R}_{\text{SCD}}(g)$ by providing an estimation error bound. As we will show, the bound exhibits non-trivial behavior, reflecting the interplay between similarity-confidence and confidence-difference information.

Let \mathcal{G} denote the model class. We assume that there exist some constant C_g such that $\sup_{g \in \mathcal{G}} \|g\|_\infty \leq C_g$ and some constant C_ℓ such that $\sup_{|z| \leq C_g} \ell(z, y) \leq C_\ell$. We also assume that the binary loss function $\ell(z, y)$ is Lipschitz continuous for z and y with a Lipschitz constant L_ℓ . Let $g^* = \arg \min_{g \in \mathcal{G}} R(g)$ denote the minimizer of the classification risk in Eq. (1) and $\hat{g}_{\text{SCD}} = \arg \min_{g \in \mathcal{G}} \widehat{R}_{\text{SCD}}(g)$ denote the minimizer of the unbiased risk estimator in Eq. (7). Then, the following theorem can be derived:

Theorem 4. *For any $\delta > 0$, the following inequality holds with probability at least $1 - \delta$:*

$$R(\hat{g}_{\text{SCD}}) - R(g^*) \leq 12L_\ell \mathfrak{R}_n(\mathcal{G}) + (2\pi_+^2 + 2\pi_-^2 + 5)C_\ell \sqrt{\frac{\log 2/\delta}{2n}}, \quad (9)$$

where $\mathfrak{R}_n(\mathcal{G})$ denotes the Rademacher complexity of \mathcal{G} for unlabeled data with size n .

From Theorem 4, we can observe that $R(\hat{g}_{\text{SCD}}) \rightarrow R(g^*)$ as $n \rightarrow \infty$, because $\mathfrak{R}_n(\mathcal{G}) = O(1/\sqrt{n}) \rightarrow 0$ as $n \rightarrow \infty$ for all parametric models with a bounded norm [1], such as deep neural networks trained with weight decay [17]. Furthermore, the estimation error bound converges in $\mathcal{O}_p(1/\sqrt{n})$, where \mathcal{O}_p denotes the order in probability. This rate is known to be typical for empirical risk minimization over a norm-bounded and finite-dimensional hypothesis class, and is considered optimal in the absence of additional smoothness or margin conditions [18].

3.5 Robustness of Risk Estimator

In the previous sections, it was assumed that the class prior probability is known in advance. Additionally, it was assumed that the ground-truth similarity-confidence and the ground-truth confidence-difference of each unlabeled data pair are accessible. However, these assumptions are not necessarily satisfied in real-world scenarios. In this section, we analyze the influence of an inaccurate class prior probability, noisy similarity-confidence, and noisy confidence-difference on learning performance.

Let $\bar{\mathcal{D}}_n = \{(\mathbf{x}_i, \mathbf{x}'_i), \bar{s}_i, \bar{c}_i\}_{i=1}^n$ denote n unlabeled data pairs with noisy similarity-confidence and noisy confidence-difference, where \bar{s}_i and \bar{c}_i are generated by adding noise to the ground-truth similarity-confidence s_i and the ground-truth confidence-difference c_i , respectively. Let $\bar{\pi}_+$ and $\bar{\pi}_-$ denote the inaccurate class prior probability accessible to the learning algorithm. Furthermore, let \bar{R}_{SCD} denote the empirical risk calculated based on the inaccurate class prior probability, noisy similarity-confidence, and noisy confidence-difference. Let $\bar{g}_{\text{SCD}} = \arg \min_{g \in \mathcal{G}} \bar{R}_{\text{SCD}}(g)$ denote the minimizer of \bar{R}_{SCD} . Then, the following theorem provides an estimation error bound:

Theorem 5. *Based on the assumption in Section 3.4, for any $\delta > 0$, the following inequality holds with probability at least $1 - \delta$:*

$$\begin{aligned} R(\tilde{g}_{\text{SCD}}) - R(g^*) &\leq 24L_\ell \mathfrak{R}_n(\mathcal{G}) + (4\pi_+^2 + 4\pi_-^2 + 10)C_\ell \sqrt{\frac{\log 2/\delta}{2n}} \\ &\quad + \frac{4C_\ell}{n} \sum_{i=1}^n (|\bar{\pi}_+ \bar{c}_i - \pi_+ c_i| + |\bar{\pi}_- \bar{c}_i - \pi_- c_i| + |\bar{s}_i - s_i|) \\ &\quad + 4C_\ell (|\bar{\pi}_+^2 - \pi_+^2| + |\bar{\pi}_-^2 - \pi_-^2| + |\bar{\pi}_+ - \pi_+|). \end{aligned} \quad (10)$$

Theorem 5 indicates the influence of an inaccurate class prior probability, noisy similarity-confidence, and noisy confidence-difference on the estimation error bound. From this inequality, while we observe that the estimation error bound is influenced by both the mean absolute error of the noisy labels and the absolute error in the class prior probability. If the total noise grows slower than linearly with respect to the sample size with high probability, and the class prior probability is estimated consistently, the risk estimator can be even consistent.

3.6 Risk Correction Approach

The risk estimator in Eq. (7) may take negative values, violating the non-negativity property of loss functions and potentially causing overfitting with complex models. To mitigate this, we apply simple correction functions, such as the rectified linear unit (ReLU) $f(z) = \max(0, z)$ and the absolute value function $f(z) = |z|$. The corrected risk estimator for SconfConfDiff Classification is then given by:

$$\tilde{R}_{\text{SCD}}(g) = f(\hat{A}(g)) + f(\hat{B}(g)) + f(\hat{C}(g)) + f(\hat{D}(g)), \quad (11)$$

where $\hat{A}(g) = \sum_{i=1}^n ((2\pi_+(\pi_+ - c_i) + \pi_- - s_i)\ell(g(\mathbf{x}_i), +1))/2n$, $\hat{B}(g) = \sum_{i=1}^n ((2\pi_-(\pi_- - c_i) + \pi_+ - s_i)\ell(g(\mathbf{x}'_i), -1))/2n$, $\hat{C}(g) = \sum_{i=1}^n ((2\pi_+(\pi_+ + c_i) + \pi_- - s_i)\ell(g(\mathbf{x}'_i), +1))/2n$, and $\hat{D}(g) = \sum_{i=1}^n ((2\pi_-(\pi_- + c_i) + \pi_+ - s_i)\ell(g(\mathbf{x}_i), -1))/2n$. We assume that the risk correction function $f(z)$ is Lipschitz continuous with Lipschitz constant L_f . From the proof of Theorem 2 in Appendix A, the values of $\mathbb{E}[\hat{A}(g)]$, $\mathbb{E}[\hat{B}(g)]$, $\mathbb{E}[\hat{C}(g)]$, and $\mathbb{E}[\hat{D}(g)]$ are non-negative. Therefore, we assume that there exist non-negative constants a, b, c, d such that $\mathbb{E}[\hat{A}(g)] \geq a$, $\mathbb{E}[\hat{B}(g)] \geq b$, $\mathbb{E}[\hat{C}(g)] \geq c$, and $\mathbb{E}[\hat{D}(g)] \geq d$. Moreover, let $\tilde{g}_{\text{SCD}} = \arg \min_{g \in \mathcal{G}} \tilde{R}_{\text{SCD}}(g)$ denote the minimizer of $\tilde{R}_{\text{SCD}}(g)$. Then, the following theorem provides the bias and consistency of $\tilde{R}_{\text{SCD}}(g)$.

Theorem 6. *Based on the assumptions above, the risk estimator $\tilde{R}_{\text{SCD}}(g)$ decays exponentially as $n \rightarrow \infty$:*

$$0 \leq \mathbb{E}[\tilde{R}_{\text{SCD}}(g)] - R(g) \leq 3(L_f + 1)C_\ell \Delta, \quad (12)$$

where $\Delta = \exp(-\frac{4a^2n}{(4\pi_+ + 1)^2 C_\ell^2}) + \exp(-\frac{4b^2n}{(4\pi_- + 1)^2 C_\ell^2}) + \exp(-\frac{4c^2n}{(4\pi_+ + 1)^2 C_\ell^2}) + \exp(-\frac{4d^2n}{(4\pi_- + 1)^2 C_\ell^2})$. Furthermore, the following inequality holds with probability at least $1 - \delta$:

$$|\tilde{R}_{\text{SCD}}(g) - R(g)| \leq 6L_f C_\ell \sqrt{\frac{\log 2/\delta}{2n}} + 3(L_f + 1)C_\ell \Delta. \quad (13)$$

Theorem 6 indicates that $\tilde{R}_{\text{SCD}}(g) \rightarrow R(g)$ in $\mathcal{O}_p(1/\sqrt{n})$, which means that $\tilde{R}_{\text{SCD}}(g)$ is biased yet consistent. The estimation error bound of \tilde{g}_{SCD} is analyzed in Theorem 7.

Theorem 7. *Based on the assumptions above, for any $\delta > 0$, the following inequality holds with probability at least $1 - \delta$:*

$$R(\tilde{g}_{\text{SCD}}) - R(g^*) \leq (12L_f + 2\pi_+^2 + 2\pi_-^2 + 5)C_\ell \sqrt{\frac{\log 4/\delta}{2n}} + 6(L_f + 1)C_\ell \Delta + 12L_\ell \mathfrak{R}_n(\mathcal{G}). \quad (14)$$

From Theorem 7, we can observe that $R(\tilde{g}_{\text{SCD}}) \rightarrow R(g^*)$ as $n \rightarrow \infty$, because $\mathfrak{R}_n(\mathcal{G}) = O(1/\sqrt{n}) \rightarrow 0$ as $n \rightarrow \infty$ for all parametric models with a bounded norm [1]. Furthermore, from Theorem 6, Δ associated with the risk correction approach decays exponentially as $n \rightarrow \infty$. Thus, as a whole, the estimation error bound converges in $\mathcal{O}_p(1/\sqrt{n})$, which is known to be the typical convergence rate achieved by empirical risk minimization over a norm-bounded, finite-dimensional hypothesis class, and is considered optimal in the absence of additional smoothness or margin assumptions [18].

4 Experiments

In this section, we verify the effectiveness of the proposed method experimentally.

4.1 Experimental Setup

Following the experimental setup of ConfDiff Classification [15], we conducted experiments on benchmark datasets, including MNIST [19], Kuzushiji-MNIST [20], Fashion-MNIST [21], and CIFAR-10 [22]. Additionally, we used four UCI datasets including Optdigits [23], Pendigits [24], Letter[25], and PMU-UD [26]. Since these datasets were originally designed for multi-class classification, we redesigned for binary classification. For CIFAR-10, we used ResNet34 [27] as the model architecture. For other datasets, we used a multilayer perceptron (MLP) with three hidden layers of width 300 equipped with the ReLU [28] activation function and batch normalization [29]. The logistic loss is used for the binary loss function ℓ .

To verify the effectiveness of our approaches under different class prior settings, we set $\pi_+ \in \{0.2, 0.5, 0.8\}$. Additionally, we assumed that the class prior π_+ was known for all the compared methods. We repeated the sampling-and-training procedure for five times and recorded both the mean accuracy and the standard deviation.

We adopted the following variants of the proposed approaches: 1) SconfConfDiff-Unbiased (the unbiased risk estimator based on Eq. (7)), 2) SconfConfDiff-ReLU (the corrected risk estimator with the ReLU function), 3) SconfConfDiff-ABS (the corrected risk estimator with the absolute value function). Similarly, we conducted experiments on convex combination approach (unbiased) in Eq. (5), the risk correction with the ReLU function, and the risk correction with the absolute value function. We compared the proposed approaches with Sconf Learning and ConfDiff Classification. Since SconfConfDiff-Convex and Sconf Learning cannot be executed when $\pi_+ = 0.5$, we compared only ConfDiff Classification in the case of $\pi_+ = 0.5$. Furthermore, we also recorded the experimental results of supervised learning methods with ground-truth hard labels. The details of the hyperparameter values and the data generation process can be found in Appendix D.

4.2 Experimental Results

Based on the experimental setting in Section 4.1, we verify the proposed method derived in Section 3. The experimental results demonstrated that the proposed method outperforms the comparison methods on many datasets, thereby validating its effectiveness. In the tables, SconfConfDiff-Convex is denoted as Convex($\gamma = \text{value}$), with varying values of γ .

Tables 1 and 3 report experimental results of classification accuracy for all the compared methods on four benchmark datasets. When $\pi_+ = 0.2$, the proposed approach, either SconfConfDiff-ABS or SconfConfDiff-Convex-ABS, achieves superior performance compared to other methods. In addition, SconfConfDiff-ABS has smaller variances than SconfConfDiff-Unbiased and SconfConfDiff-ReLU. This result demonstrates that the risk correction method can enhance the stability and robustness of SconfConfDiff Classification. In the case of $\pi_+ = 0.5$, ConfDiff-ABS achieves high accuracy on some datasets. This is likely because, when there is no difference in the class prior probability, the similarity-confidence information does not contribute significantly to the learning process.

Tables 2 and 4 report experimental results of classification accuracy for all the compared methods on four UCI datasets. We can observe that on all the UCI datasets under different class prior probability settings, the proposed approach, either SconfConfDiff-ABS or SconfConfDiff-Convex-ABS, achieves the best performance compared to other methods.

When $\pi_+ = 0.5$, the risk estimator assigned equal weight to the positive and negative class terms. This balance helped stabilize the overall estimate, making it less likely for the risk to take negative values. As a result, applying a risk correction function such as ReLU or the absolute value produced identical experimental results. Note that in Tables 1 through 4, only the absolute value correction results are shown for Sconf Learning, ConfDiff Classification, and SconfConfDiff-Convex. Detailed results, including those for the unbiased risk estimator and the corrected risk estimator with the ReLU function, as well as the results in the case of $\pi_+ = 0.8$, are provided in Appendix E.

Table 1: Classification accuracy (mean \pm std) of each method on benchmark datasets with $\pi_+ = 0.2$, where the best performance (excluding Supervised) is shown in bold.

Method	MNIST	Kuzushiji	Fashion	CIFAR-10
SconfConfDiff-Unbiased	0.894 \pm 0.043	0.706 \pm 0.016	0.851 \pm 0.085	0.865 \pm 0.006
SconfConfDiff-ReLU	0.975 \pm 0.002	0.890 \pm 0.010	0.965 \pm 0.002	0.871 \pm 0.012
SconfConfDiff-ABS	0.978 \pm 0.002	0.906 \pm 0.002	0.969 \pm 0.003	0.884 \pm 0.006
ConfDiff-ABS	0.975 \pm 0.001	0.898 \pm 0.006	0.967 \pm 0.001	0.868 \pm 0.007
Convex($\gamma = 0.2$)-ABS	0.975 \pm 0.003	0.904 \pm 0.007	0.967 \pm 0.002	0.870 \pm 0.005
Convex($\gamma = 0.5$)-ABS	0.976 \pm 0.004	0.903 \pm 0.006	0.965 \pm 0.002	0.869 \pm 0.006
Convex($\gamma = 0.8$)-ABS	0.972 \pm 0.003	0.901 \pm 0.005	0.962 \pm 0.004	0.870 \pm 0.008
Sconf-ABS	0.960 \pm 0.004	0.881 \pm 0.006	0.955 \pm 0.006	0.818 \pm 0.022
Supervised	0.990 \pm 0.000	0.936 \pm 0.003	0.979 \pm 0.002	0.895 \pm 0.003

Table 2: Classification accuracy (mean \pm std) of each method on UCI datasets with $\pi_+ = 0.2$, where the best performance (excluding Supervised) is shown in bold.

Method	Optdigits	Pendigits	Letter	PMU-UD
SconfConfDiff-Unbiased	0.917 \pm 0.067	0.954 \pm 0.041	0.746 \pm 0.044	0.841 \pm 0.058
SconfConfDiff-ReLU	0.955 \pm 0.023	0.987 \pm 0.003	0.934 \pm 0.007	0.966 \pm 0.007
SconfConfDiff-ABS	0.969 \pm 0.005	0.991 \pm 0.002	0.951 \pm 0.004	0.975 \pm 0.005
ConfDiff-ABS	0.964 \pm 0.010	0.988 \pm 0.005	0.945 \pm 0.004	0.978 \pm 0.008
Convex($\gamma = 0.2$)-ABS	0.969 \pm 0.009	0.987 \pm 0.004	0.947 \pm 0.005	0.979 \pm 0.006
Convex($\gamma = 0.5$)-ABS	0.969 \pm 0.005	0.987 \pm 0.004	0.946 \pm 0.004	0.979 \pm 0.008
Convex($\gamma = 0.8$)-ABS	0.966 \pm 0.006	0.986 \pm 0.004	0.941 \pm 0.004	0.976 \pm 0.004
Sconf-ABS	0.944 \pm 0.014	0.978 \pm 0.006	0.915 \pm 0.006	0.954 \pm 0.010
Supervised	0.989 \pm 0.003	0.997 \pm 0.001	0.978 \pm 0.004	0.994 \pm 0.003

Table 3: Classification accuracy (mean \pm std) of each method on benchmark datasets with $\pi_+ = 0.5$, where the best performance (excluding Supervised) is shown in bold.

Method	MNIST	Kuzushiji	Fashion	CIFAR-10
SconfConfDiff-Unbiased	0.977 \pm 0.004	0.901 \pm 0.005	0.963 \pm 0.002	0.837 \pm 0.004
SconfConfDiff-ReLU	0.977 \pm 0.004	0.901 \pm 0.005	0.963 \pm 0.002	0.837 \pm 0.004
SconfConfDiff-ABS	0.977 \pm 0.004	0.901 \pm 0.005	0.963 \pm 0.002	0.837 \pm 0.004
ConfDiff-ABS	0.965 \pm 0.001	0.866 \pm 0.004	0.968 \pm 0.001	0.842 \pm 0.002
Supervised	0.987 \pm 0.001	0.928 \pm 0.002	0.976 \pm 0.001	0.876 \pm 0.003

Table 4: Classification accuracy (mean \pm std) of each method on UCI datasets with $\pi_+ = 0.5$, where the best performance (excluding Supervised) is shown in bold.

Method	Optdigits	Pendigits	Letter	PMU-UD
SconfConfDiff-Unbiased	0.971 \pm 0.008	0.992 \pm 0.002	0.935 \pm 0.006	0.986 \pm 0.005
SconfConfDiff-ReLU	0.971 \pm 0.008	0.992 \pm 0.002	0.935 \pm 0.006	0.986 \pm 0.005
SconfConfDiff-ABS	0.971 \pm 0.008	0.992 \pm 0.002	0.935 \pm 0.006	0.986 \pm 0.005
ConfDiff-ABS	0.964 \pm 0.007	0.989 \pm 0.001	0.922 \pm 0.007	0.982 \pm 0.005
Supervised	0.991 \pm 0.003	0.996 \pm 0.002	0.976 \pm 0.002	0.993 \pm 0.002

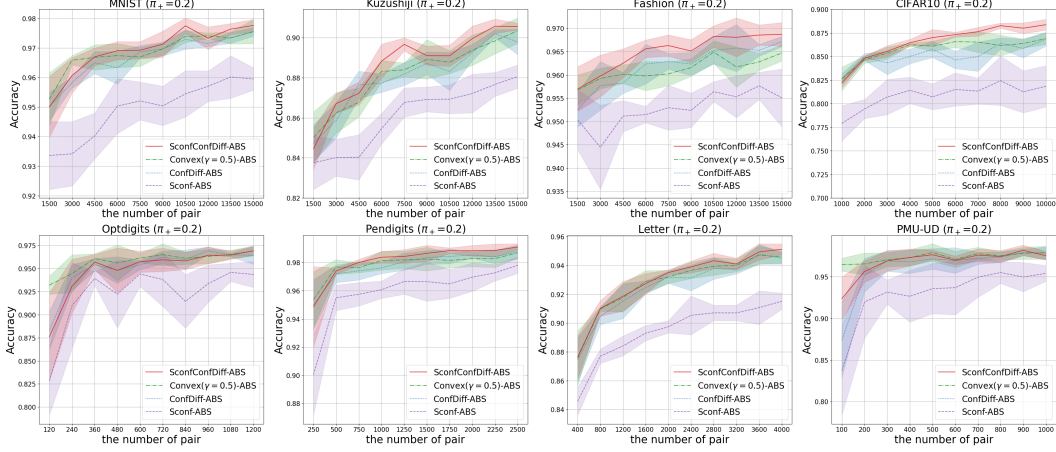


Figure 3: Classification performance of SconfConfDiff-ABS, SconfConfDiff-Convex($\gamma = 0.5$)-ABS, Sconf-ABS, and ConfDiff-ABS given a fraction of training data ($\pi_+ = 0.2$).

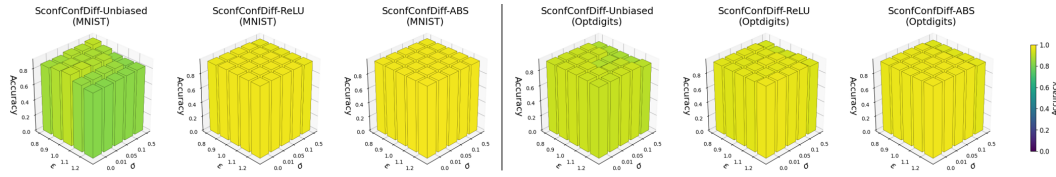


Figure 4: Classification performance on MNIST (left) and Optdigits (right) with $\pi_+ = 0.2$ given an inaccurate class prior probability, noisy similarity-confidence, and noisy confidence-difference. Both the height and color of the bars represent accuracy.

4.3 Experimental Results with Fewer Training Data

We conducted experiments by changing the fraction of training data for SconfConfDiff-ABS and SconfConfDiff-Convex-ABS. For comparison, we provide the results of Sconf Learning and ConfDiff Classification in Fig. 3. Figure. 3 shows the results for $\pi_+ = 0.2$, and more experimental results can be found in Appendix E. It can be observed that providing two types of weak supervision leads to improved classification performance.

4.4 Experimental Results of Robustness

In this section, we investigate the influence of an inaccurate class prior probability, noisy similarity-confidence, and noisy confidence-difference on the classification performance of the proposed approaches experimentally. Let $\bar{\pi}_+ = \epsilon\pi_+$ denote the corrupted class prior probability with ϵ being a real number around 1. Let $\bar{s}_i = \epsilon'_i s_i$ and $\bar{c}_i = \epsilon''_i c_i$ denote the noisy similarity-confidence and the noisy confidence-difference where ϵ'_i and ϵ''_i are sampled from a normal distribution $\mathcal{N}(1, \sigma^2)$. Figure. 4 shows the classification performance (only mean accuracy) of the proposed approaches on MNIST and Optdigits ($\pi_+ = 0.2$) with different ϵ and σ . From Fig. 4, it can be observed that the proposed method is robust to an inaccurate class prior probability, noisy similarity-confidence, and noisy confidence-difference. More experimental results (including the standard deviation of accuracy) can be found in Appendix E.

5 Conclusion

In this paper, we proposed a novel learning framework that integrates two types of weak supervision. Specifically, we considered a setting where unlabeled data pairs are annotated with both similarity-confidence and confidence-difference, and derived two unbiased risk estimators: SconfConfDiff-Convex Classification, which combines the risks from Sconf Learning and ConfDiff Classification via a convex formulation, and SconfConfDiff Classification, which integrates the two types of supervision

in a unified manner to reflect their interaction. To mitigate overfitting, we incorporate a risk correction approach that improves learning performance. Furthermore, we provided estimation error bounds for the classifier obtained by empirical risk minimization and proved its statistical consistency. Experimental results demonstrate that our method achieves performance comparable to or better than learning with a single weak supervision. Future directions include extending the proposed framework to handle other forms of weak supervision, scenarios with partially missing labels, and a learning framework that effectively leverages both ordinary supervised labels and weakly labels. Since our current method is limited to binary classification, extending it to multi-class problems is also a promising direction for future work.

Acknowledgment

This work was supported in part by the Japan Society for the Promotion of Science through Grants-in-Aid for Scientific Research (C) (23K11111).

References

- [1] Masashi Sugiyama, Han Bao, Takashi Ishida, Nan Lu, Taiji Sakai, and Gang Niu. *Machine Learning from Weak Supervision: An Empirical Risk Minimization Approach*. MIT Press, Cambridge, Massachusetts, USA, 2022.
- [2] Charles Elkan and Keith Noto. Learning classifiers from only positive and unlabeled data. In *Proceedings of the 14th ACM SIGKDD International Conference on Knowledge Discovery and Data Mining*, KDD '08, pages 213–220, New York, NY, USA, 2008. Association for Computing Machinery.
- [3] Marthinus C. du Plessis, Gang Niu, and Masashi Sugiyama. Analysis of learning from positive and unlabeled data. In *Proceedings of the 28th International Conference on Neural Information Processing Systems - Volume 1*, NIPS'14, pages 703–711, Cambridge, MA, USA, 2014. MIT Press.
- [4] Marthinus Du Plessis, Gang Niu, and Masashi Sugiyama. Convex formulation for learning from positive and unlabeled data. In Francis Bach and David Blei, editors, *Proceedings of the 32nd International Conference on Machine Learning*, volume 37 of *Proceedings of Machine Learning Research*, pages 1386–1394, Lille, France, 07–09 Jul 2015. PMLR.
- [5] Ryuichi Kiryo, Gang Niu, Marthinus C du Plessis, and Masashi Sugiyama. Positive-unlabeled learning with non-negative risk estimator. In I. Guyon, U. Von Luxburg, S. Bengio, H. Wallach, R. Fergus, S. Vishwanathan, and R. Garnett, editors, *Advances in Neural Information Processing Systems*, volume 30. Curran Associates, Inc., 2017.
- [6] Tomoya Sakai, Marthinus Christoffel du Plessis, Gang Niu, and Masashi Sugiyama. Semi-supervised classification based on classification from positive and unlabeled data. In Doina Precup and Yee Whye Teh, editors, *Proceedings of the 34th International Conference on Machine Learning*, volume 70 of *Proceedings of Machine Learning Research*, pages 2998–3006. PMLR, 06–11 Aug 2017.
- [7] Lei Feng, Jiaqi Lv, Bo Han, Miao Xu, Gang Niu, Xin Geng, Bo An, and Masashi Sugiyama. Provably consistent partial-label learning. In H. Larochelle, M. Ranzato, R. Hadsell, M.F. Balcan, and H. Lin, editors, *Advances in Neural Information Processing Systems*, volume 33, pages 10948–10960. Curran Associates, Inc., 2020.
- [8] Nan Lu, Gang Niu, Aditya K. Menon, and Masashi Sugiyama. On the minimal supervision for training any binary classifier from only unlabeled data. In *International Conference on Learning Representations*, 2019.
- [9] Takashi Ishida, Gang Niu, Weihua Hu, and Masashi Sugiyama. Learning from complementary labels. In I. Guyon, U. Von Luxburg, S. Bengio, H. Wallach, R. Fergus, S. Vishwanathan, and R. Garnett, editors, *Advances in Neural Information Processing Systems*, volume 30. Curran Associates, Inc., 2017.

- [10] Lei Feng, Takuo Kaneko, Bo Han, Gang Niu, Bo An, and Masashi Sugiyama. Learning with multiple complementary labels. In Hal Daumé III and Aarti Singh, editors, *Proceedings of the 37th International Conference on Machine Learning*, volume 119 of *Proceedings of Machine Learning Research*, pages 3072–3081. PMLR, 13–18 Jul 2020.
- [11] Han Bao, Gang Niu, and Masashi Sugiyama. Classification from pairwise similarity and unlabeled data. In Jennifer Dy and Andreas Krause, editors, *Proceedings of the 35th International Conference on Machine Learning*, volume 80 of *Proceedings of Machine Learning Research*, pages 452–461. PMLR, 10–15 Jul 2018.
- [12] Takuya Shimada, Han Bao, Issei Sato, and Masashi Sugiyama. Classification from pairwise similarities/dissimilarities and unlabeled data via empirical risk minimization. *Neural Computation*, 33(5):1234–1268, 2021.
- [13] Lei Feng, Senlin Shu, Nan Lu, Bo Han, Miao Xu, Gang Niu, Bo An, and Masashi Sugiyama. Pointwise binary classification with pairwise confidence comparisons. In Marina Meila and Tong Zhang, editors, *Proceedings of the 38th International Conference on Machine Learning*, volume 139 of *Proceedings of Machine Learning Research*, pages 3252–3262. PMLR, 18–24 Jul 2021.
- [14] Yuzhou Cao, Lei Feng, Yitian Xu, Bo An, Gang Niu, and Masashi Sugiyama. Learning from similarity-confidence data. In Marina Meila and Tong Zhang, editors, *Proceedings of the 38th International Conference on Machine Learning*, volume 139 of *Proceedings of Machine Learning Research*, pages 1272–1282. PMLR, 18–24 Jul 2021.
- [15] Wei Wang, Lei Feng, Yuchen Jiang, Gang Niu, Min-Ling Zhang, and Masashi Sugiyama. Binary classification with confidence difference. In *Thirty-seventh Conference on Neural Information Processing Systems*, 2023.
- [16] Mehryar Mohri, Afshin Rostamizadeh, and Ameet Talwalkar. *Foundations of Machine Learning*. The MIT Press, 2012.
- [17] Noah Golowich, Alexander Rakhlin, and Ohad Shamir. Size-independent sample complexity of neural networks. In Sébastien Bubeck, Vianney Perchet, and Philippe Rigollet, editors, *Proceedings of the 31st Conference On Learning Theory*, volume 75 of *Proceedings of Machine Learning Research*, pages 297–299. PMLR, 06–09 Jul 2018.
- [18] Shahar Mendelson. Lower bounds for the empirical minimization algorithm. *IEEE Transactions on Information Theory*, 54(8):3797–3803, 2008.
- [19] Y. Lecun, L. Bottou, Y. Bengio, and P. Haffner. Gradient-based learning applied to document recognition. *Proceedings of the IEEE*, 86(11):2278–2324, 1998.
- [20] Tarin Clanuwat, Mikel Bober-Irizar, Asanobu Kitamoto, Alex Lamb, Kazuaki Yamamoto, and David Ha. Deep learning for classical japanese literature. *CoRR*, abs/1812.01718, 2018.
- [21] Han Xiao, Kashif Rasul, and Roland Vollgraf. Fashion-mnist: a novel image dataset for benchmarking machine learning algorithms, 2017.
- [22] Alex Krizhevsky. Learning multiple layers of features from tiny images. 2009.
- [23] E. Alpaydin and C. Kaynak. Optical Recognition of Handwritten Digits. UCI Machine Learning Repository, 1998. DOI: <https://doi.org/10.24432/C50P49>.
- [24] E. Alpaydin and Fevzi. Alimoglu. Pen-Based Recognition of Handwritten Digits. UCI Machine Learning Repository, 1996. DOI: <https://doi.org/10.24432/C5MG6K>.
- [25] David Slate. Letter Recognition. UCI Machine Learning Repository, 1991. DOI: <https://doi.org/10.24432/C5ZP40>.
- [26] Ghazanfar Latif. PMU-UD. UCI Machine Learning Repository, 2018. DOI: <https://doi.org/10.24432/C5XG84>.

- [27] Kaiming He, Xiangyu Zhang, Shaoqing Ren, and Jian Sun. Deep residual learning for image recognition. In *2016 IEEE Conference on Computer Vision and Pattern Recognition (CVPR)*, pages 770–778, 2016.
- [28] Vinod Nair and Geoffrey E. Hinton. Rectified linear units improve restricted boltzmann machines. In *Proceedings of the 27th International Conference on International Conference on Machine Learning*, ICML’10, pages 807–814, Madison, WI, USA, 2010. Omnipress.
- [29] Sergey Ioffe and Christian Szegedy. Batch normalization: Accelerating deep network training by reducing internal covariate shift. In Francis Bach and David Blei, editors, *Proceedings of the 32nd International Conference on Machine Learning*, volume 37 of *Proceedings of Machine Learning Research*, pages 448–456, Lille, France, 07–09 Jul 2015. PMLR.
- [30] Adam Paszke, Sam Gross, Francisco Massa, Adam Lerer, James Bradbury, Gregory Chanan, Trevor Killeen, Zeming Lin, Natalia Gimelshein, Luca Antiga, Alban Desmaison, Andreas Kopf, Edward Yang, Zachary DeVito, Martin Raison, Alykhan Tejani, Sasank Chilamkurthy, Benoit Steiner, Lu Fang, Junjie Bai, and Soumith Chintala. Pytorch: An imperative style, high-performance deep learning library. In H. Wallach, H. Larochelle, A. Beygelzimer, F. d’Alché-Buc, E. Fox, and R. Garnett, editors, *Advances in Neural Information Processing Systems*, volume 32. Curran Associates, Inc., 2019.
- [31] Diederik P. Kingma and Jimmy Ba. Adam: A method for stochastic optimization. volume abs/1412.6980, 2014.

A Proof of Section 3

A.1 Proof of Theorem 2

Lemma 2 (cf. Lemma 3 in [15]). *The following equations hold:*

$$\mathbb{E}_{p(\mathbf{x}, \mathbf{x}')}[(\pi_+ - c(\mathbf{x}, \mathbf{x}'))\ell(g(\mathbf{x}), +1)] = \pi_+ \mathbb{E}_{p(\mathbf{x}|y=+1)}[\ell(g(\mathbf{x}), +1)], \quad (15)$$

$$\mathbb{E}_{p(\mathbf{x}, \mathbf{x}')}[(\pi_- + c(\mathbf{x}, \mathbf{x}'))\ell(g(\mathbf{x}), -1)] = \pi_- \mathbb{E}_{p(\mathbf{x}|y=-1)}[\ell(g(\mathbf{x}), -1)], \quad (16)$$

$$\mathbb{E}_{p(\mathbf{x}, \mathbf{x}')}[(\pi_+ + c(\mathbf{x}, \mathbf{x}'))\ell(g(\mathbf{x}'), +1)] = \pi_+ \mathbb{E}_{p(\mathbf{x}'|y=+1)}[\ell(g(\mathbf{x}'), +1)], \quad (17)$$

$$\mathbb{E}_{p(\mathbf{x}, \mathbf{x}')}[(\pi_- - c(\mathbf{x}, \mathbf{x}'))\ell(g(\mathbf{x}'), -1)] = \pi_- \mathbb{E}_{p(\mathbf{x}'|y=-1)}[\ell(g(\mathbf{x}'), -1)]. \quad (18)$$

Lemma 3 (cf. Lemma 2 in [14]). *The following equations hold:*

$$\begin{aligned} & \mathbb{E}_{p(\mathbf{x}, \mathbf{x}')} [s(\mathbf{x}, \mathbf{x}')\ell(g(\mathbf{x}), +1)] - \frac{\pi_-}{\pi_+} \mathbb{E}_{p(\mathbf{x}, \mathbf{x}')} [(1 - s(\mathbf{x}, \mathbf{x}'))\ell(g(\mathbf{x}), +1)] \\ &= (\pi_+ - \pi_-) \mathbb{E}_{p(\mathbf{x}|y=+1)} [\ell(g(\mathbf{x}), +1)]. \end{aligned} \quad (19)$$

Lemma 4. *The following equations hold:*

$$\pi_+ \mathbb{E}_{p(\mathbf{x}|y=+1)} [\ell(g(\mathbf{x}), +1)] = \mathbb{E}_{p(\mathbf{x}, \mathbf{x}')} [(2\pi_+(\pi_+ - c(\mathbf{x}, \mathbf{x}')) + \pi_- - s(\mathbf{x}, \mathbf{x}'))\ell(g(\mathbf{x}), +1)], \quad (20)$$

$$\pi_- \mathbb{E}_{p(\mathbf{x}|y=-1)} [\ell(g(\mathbf{x}), -1)] = \mathbb{E}_{p(\mathbf{x}, \mathbf{x}')} [(2\pi_-(\pi_- + c(\mathbf{x}, \mathbf{x}')) + \pi_+ - s(\mathbf{x}, \mathbf{x}'))\ell(g(\mathbf{x}), -1)], \quad (21)$$

$$\pi_+ \mathbb{E}_{p(\mathbf{x}'|y=+1)} [\ell(g(\mathbf{x}'), +1)] = \mathbb{E}_{p(\mathbf{x}, \mathbf{x}')} [(2\pi_+(\pi_+ + c(\mathbf{x}, \mathbf{x}')) + \pi_- - s(\mathbf{x}, \mathbf{x}'))\ell(g(\mathbf{x}'), +1)], \quad (22)$$

$$\pi_- \mathbb{E}_{p(\mathbf{x}'|y=-1)} [\ell(g(\mathbf{x}'), -1)] = \mathbb{E}_{p(\mathbf{x}, \mathbf{x}')} [(2\pi_-(\pi_- - c(\mathbf{x}, \mathbf{x}')) + \pi_+ - s(\mathbf{x}, \mathbf{x}'))\ell(g(\mathbf{x}'), -1)]. \quad (23)$$

Proof. Based on Lemma 3,

$$\begin{aligned} & \mathbb{E}_{p(\mathbf{x}, \mathbf{x}')} [s(\mathbf{x}, \mathbf{x}')\ell(g(\mathbf{x}), +1)] - \frac{\pi_-}{\pi_+} \mathbb{E}_{p(\mathbf{x}, \mathbf{x}')} [(1 - s(\mathbf{x}, \mathbf{x}'))\ell(g(\mathbf{x}), +1)] \\ &= 2\pi_+ \mathbb{E}_{p(\mathbf{x}|y=+1)} [\ell(g(\mathbf{x}), +1)] - \mathbb{E}_{p(\mathbf{x}|y=+1)} [\ell(g(\mathbf{x}), +1)] \\ &= 2\mathbb{E}_{p(\mathbf{x}, \mathbf{x}')} [(\pi_+ - c(\mathbf{x}, \mathbf{x}'))\ell(g(\mathbf{x}), +1)] - \mathbb{E}_{p(\mathbf{x}|y=+1)} [\ell(g(\mathbf{x}), +1)]. \end{aligned} \quad (24)$$

By multiplying both sides of Eq. (24) by π_+ and solving for $\pi_+ \mathbb{E}_{p(\mathbf{x}|y=+1)} [\ell(g(\mathbf{x}), +1)]$, we obtain

$$\begin{aligned} & \pi_+ \mathbb{E}_{p(\mathbf{x}|y=+1)} [\ell(g(\mathbf{x}), +1)] \\ &= 2\pi_+ \mathbb{E}_{p(\mathbf{x}, \mathbf{x}')} [(\pi_+ - c(\mathbf{x}, \mathbf{x}'))\ell(g(\mathbf{x}), +1)] - \pi_+ \mathbb{E}_{p(\mathbf{x}, \mathbf{x}')} [s(\mathbf{x}, \mathbf{x}')\ell(g(\mathbf{x}), +1)] \\ & \quad + \pi_- \mathbb{E}_{p(\mathbf{x}, \mathbf{x}')} [(1 - s(\mathbf{x}, \mathbf{x}'))\ell(g(\mathbf{x}), +1)] \\ &= \mathbb{E}_{p(\mathbf{x}, \mathbf{x}')} [2\pi_+(\pi_+ - c(\mathbf{x}, \mathbf{x}'))\ell(g(\mathbf{x}), +1) - \pi_+ s(\mathbf{x}, \mathbf{x}')\ell(g(\mathbf{x}), +1) \\ & \quad + \pi_-(1 - s(\mathbf{x}, \mathbf{x}'))\ell(g(\mathbf{x}), +1)] \\ &= \mathbb{E}_{p(\mathbf{x}, \mathbf{x}')} [(2\pi_+(\pi_+ - c(\mathbf{x}, \mathbf{x}')) + \pi_- - s(\mathbf{x}, \mathbf{x}'))\ell(g(\mathbf{x}), +1)]. \end{aligned}$$

Similarly,

$$\begin{aligned} & \mathbb{E}_{p(\mathbf{x}, \mathbf{x}')} [s(\mathbf{x}, \mathbf{x}')\ell(g(\mathbf{x}), -1)] - \frac{\pi_+}{\pi_-} \mathbb{E}_{p(\mathbf{x}, \mathbf{x}')} [(1 - s(\mathbf{x}, \mathbf{x}'))\ell(g(\mathbf{x}), -1)] \\ &= (\pi_- - \pi_+) \mathbb{E}_{p(\mathbf{x}|y=-1)} [\ell(g(\mathbf{x}), +1)] \\ &= 2\pi_- \mathbb{E}_{p(\mathbf{x}|y=-1)} [\ell(g(\mathbf{x}), -1)] - \mathbb{E}_{p(\mathbf{x}|y=-1)} [\ell(g(\mathbf{x}), -1)] \\ &= 2\mathbb{E}_{p(\mathbf{x}, \mathbf{x}')} [(\pi_- + c(\mathbf{x}, \mathbf{x}'))\ell(g(\mathbf{x}), -1)] - \mathbb{E}_{p(\mathbf{x}|y=-1)} [\ell(g(\mathbf{x}), -1)]. \end{aligned} \quad (25)$$

By multiplying both sides of Eq. (25) by π_- and solving for $\pi_- \mathbb{E}_{p(\mathbf{x}|y=-1)}[\ell(g(\mathbf{x}), -1)]$, we obtain

$$\begin{aligned}
& \pi_- \mathbb{E}_{p(\mathbf{x}|y=-1)}[\ell(g(\mathbf{x}), -1)] \\
&= 2\pi_- \mathbb{E}_{p(\mathbf{x}, \mathbf{x}')}[(\pi_- + c(\mathbf{x}, \mathbf{x}'))\ell(g(\mathbf{x}), -1)] - \pi_- \mathbb{E}_{p(\mathbf{x}, \mathbf{x}')}[s(\mathbf{x}, \mathbf{x}')\ell(g(\mathbf{x}), -1)] \\
&\quad + \pi_+ \mathbb{E}_{p(\mathbf{x}, \mathbf{x}')}[(1 - s(\mathbf{x}, \mathbf{x}'))\ell(g(\mathbf{x}), -1)] \\
&= \mathbb{E}_{p(\mathbf{x}, \mathbf{x}')}[2\pi_- (\pi_- + c(\mathbf{x}, \mathbf{x}'))\ell(g(\mathbf{x}), -1) - \pi_- s(\mathbf{x}, \mathbf{x}')\ell(g(\mathbf{x}), -1) \\
&\quad + \pi_+ (1 - s(\mathbf{x}, \mathbf{x}'))\ell(g(\mathbf{x}), -1)] \\
&= \mathbb{E}_{p(\mathbf{x}, \mathbf{x}')}[(2\pi_- (\pi_- + c(\mathbf{x}, \mathbf{x}')) + \pi_+ - s(\mathbf{x}, \mathbf{x}'))\ell(g(\mathbf{x}), -1)].
\end{aligned}$$

Similarly for \mathbf{x}' ,

$$\begin{aligned}
& \mathbb{E}_{p(\mathbf{x}, \mathbf{x}')}[s(\mathbf{x}, \mathbf{x}')\ell(g(\mathbf{x}'), +1)] - \frac{\pi_-}{\pi_+} \mathbb{E}_{p(\mathbf{x}, \mathbf{x}')}[(1 - s(\mathbf{x}, \mathbf{x}'))\ell(g(\mathbf{x}'), +1)] \\
&= (\pi_+ - \pi_-) \mathbb{E}_{p(\mathbf{x}'|y=+1)}[\ell(g(\mathbf{x}'), +1)] \\
&= 2\pi_+ \mathbb{E}_{p(\mathbf{x}'|y=+1)}[\ell(g(\mathbf{x}'), +1)] - \mathbb{E}_{p(\mathbf{x}'|y=+1)}[\ell(g(\mathbf{x}'), +1)] \\
&= 2\mathbb{E}_{p(\mathbf{x}, \mathbf{x}')}[(\pi_+ + c(\mathbf{x}, \mathbf{x}'))\ell(g(\mathbf{x}'), +1)] - \mathbb{E}_{p(\mathbf{x}'|y=+1)}[\ell(g(\mathbf{x}'), +1)]. \tag{26}
\end{aligned}$$

By multiplying both sides of Eq. (26) by π_+ and solving for $\pi_+ \mathbb{E}_{p(\mathbf{x}'|y=+1)}[\ell(g(\mathbf{x}'), +1)]$, we obtain

$$\begin{aligned}
& \pi_+ \mathbb{E}_{p(\mathbf{x}'|y=+1)}[\ell(g(\mathbf{x}'), +1)] \\
&= 2\pi_+ \mathbb{E}_{p(\mathbf{x}, \mathbf{x}')}[(\pi_+ + c(\mathbf{x}, \mathbf{x}'))\ell(g(\mathbf{x}'), +1)] - \pi_+ \mathbb{E}_{p(\mathbf{x}, \mathbf{x}')}[s(\mathbf{x}, \mathbf{x}')\ell(g(\mathbf{x}'), +1)] \\
&\quad + \pi_- \mathbb{E}_{p(\mathbf{x}, \mathbf{x}')}[(1 - s(\mathbf{x}, \mathbf{x}'))\ell(g(\mathbf{x}'), +1)] \\
&= \mathbb{E}_{p(\mathbf{x}, \mathbf{x}')}[2\pi_+ (\pi_+ + c(\mathbf{x}, \mathbf{x}'))\ell(g(\mathbf{x}'), +1) - \pi_+ s(\mathbf{x}, \mathbf{x}')\ell(g(\mathbf{x}'), +1) \\
&\quad + \pi_- (1 - s(\mathbf{x}, \mathbf{x}'))\ell(g(\mathbf{x}'), +1)] \\
&= \mathbb{E}_{p(\mathbf{x}, \mathbf{x}')}[(2\pi_+ (\pi_+ + c(\mathbf{x}, \mathbf{x}')) + \pi_- - s(\mathbf{x}, \mathbf{x}'))\ell(g(\mathbf{x}'), +1)].
\end{aligned}$$

Similarly,

$$\begin{aligned}
& \mathbb{E}_{p(\mathbf{x}, \mathbf{x}')}[s(\mathbf{x}, \mathbf{x}')\ell(g(\mathbf{x}'), -1)] - \frac{\pi_+}{\pi_-} \mathbb{E}_{p(\mathbf{x}, \mathbf{x}')}[(1 - s(\mathbf{x}, \mathbf{x}'))\ell(g(\mathbf{x}'), -1)] \\
&= (\pi_- - \pi_+) \mathbb{E}_{p(\mathbf{x}'|y=-1)}[\ell(g(\mathbf{x}'), -1)] \\
&= 2\pi_- \mathbb{E}_{p(\mathbf{x}'|y=-1)}[\ell(g(\mathbf{x}'), -1)] - \mathbb{E}_{p(\mathbf{x}'|y=-1)}[\ell(g(\mathbf{x}'), -1)] \\
&= 2\mathbb{E}_{p(\mathbf{x}, \mathbf{x}')}[(\pi_- - c(\mathbf{x}, \mathbf{x}'))\ell(g(\mathbf{x}'), -1)] - \mathbb{E}_{p(\mathbf{x}'|y=-1)}[\ell(g(\mathbf{x}'), -1)]. \tag{27}
\end{aligned}$$

By multiplying both sides of Eq. (27) by π_- and solving for $\pi_- \mathbb{E}_{p(\mathbf{x}'|y=-1)}[\ell(g(\mathbf{x}'), -1)]$, we obtain

$$\begin{aligned}
& \pi_- \mathbb{E}_{p(\mathbf{x}'|y=-1)}[\ell(g(\mathbf{x}'), -1)] \\
&= 2\pi_- \mathbb{E}_{p(\mathbf{x}, \mathbf{x}')}[(\pi_- - c(\mathbf{x}, \mathbf{x}'))\ell(g(\mathbf{x}'), -1)] - \pi_- \mathbb{E}_{p(\mathbf{x}, \mathbf{x}')}[s(\mathbf{x}, \mathbf{x}')\ell(g(\mathbf{x}'), -1)] \\
&\quad + \pi_+ \mathbb{E}_{p(\mathbf{x}, \mathbf{x}')}[(1 - s(\mathbf{x}, \mathbf{x}'))\ell(g(\mathbf{x}'), -1)] \\
&= \mathbb{E}_{p(\mathbf{x}, \mathbf{x}')}[2\pi_- (\pi_- - c(\mathbf{x}, \mathbf{x}'))\ell(g(\mathbf{x}'), -1) - \pi_- s(\mathbf{x}, \mathbf{x}')\ell(g(\mathbf{x}'), -1) \\
&\quad + \pi_+ (1 - s(\mathbf{x}, \mathbf{x}'))\ell(g(\mathbf{x}'), -1)] \\
&= \mathbb{E}_{p(\mathbf{x}, \mathbf{x}')}[(2\pi_- (\pi_- - c(\mathbf{x}, \mathbf{x}')) + \pi_+ - s(\mathbf{x}, \mathbf{x}'))\ell(g(\mathbf{x}'), -1)].
\end{aligned}$$

□

Then, we provide the proof of Theorem 2.

Proof. Firstly, it can be noticed that

$$\begin{aligned}
\mathbb{E}_{p(\mathbf{x}|y=+1)}[\ell(g(\mathbf{x}), +1)] &= \mathbb{E}_{p(\mathbf{x}'|y=+1)}[\ell(g(\mathbf{x}'), +1)], \\
\mathbb{E}_{p(\mathbf{x}|y=-1)}[\ell(g(\mathbf{x}), -1)] &= \mathbb{E}_{p(\mathbf{x}'|y=-1)}[\ell(g(\mathbf{x}'), -1)].
\end{aligned}$$

Based on Lemma 4,

$$\begin{aligned}
& \mathbb{E}_{p(\mathbf{x}, \mathbf{x}')} [(2\pi_+ (\pi_+ - c(\mathbf{x}, \mathbf{x}')) + \pi_- - s(\mathbf{x}, \mathbf{x}')) \ell(g(\mathbf{x}), +1) \\
& \quad + (2\pi_- (\pi_- + c(\mathbf{x}, \mathbf{x}')) + \pi_+ - s(\mathbf{x}, \mathbf{x}')) \ell(g(\mathbf{x}), -1) \\
& \quad + (2\pi_+ (\pi_+ + c(\mathbf{x}, \mathbf{x}')) + \pi_- - s(\mathbf{x}, \mathbf{x}')) \ell(g(\mathbf{x}'), +1) \\
& \quad + (2\pi_- (\pi_- - c(\mathbf{x}, \mathbf{x}')) + \pi_+ - s(\mathbf{x}, \mathbf{x}')) \ell(g(\mathbf{x}'), -1)] \\
& = 2\pi_+ \mathbb{E}_{p(\mathbf{x}|y=+1)} [\ell(g(\mathbf{x}), +1)] + 2\pi_- \mathbb{E}_{p(\mathbf{x}|y=-1)} [\ell(g(\mathbf{x}), -1)] \\
& = 2R(g).
\end{aligned}$$

After dividing each side of the equation above by 2, we can obtain Theorem 2. \square

A.2 Proof of Theorem 3

Firstly, we begin with the proof of Lemma 1:

Proof. Based on Lemma 4, the following equations hold:

$$\begin{aligned}
& \mathbb{E}_{p(\mathbf{x}, \mathbf{x}')} [\mathcal{L}(\mathbf{x}, \mathbf{x}')] \\
& = \mathbb{E}_{p(\mathbf{x}, \mathbf{x}')} [(2\pi_+ (\pi_+ - c(\mathbf{x}, \mathbf{x}')) + \pi_- - s(\mathbf{x}, \mathbf{x}')) \ell(g(\mathbf{x}), +1) \\
& \quad + (2\pi_- (\pi_- - c(\mathbf{x}, \mathbf{x}')) + \pi_+ - s(\mathbf{x}, \mathbf{x}')) \ell(g(\mathbf{x}'), -1)] \\
& = \pi_+ \mathbb{E}_{p(\mathbf{x}|y=+1)} [\ell(g(\mathbf{x}), +1)] + \pi_- \mathbb{E}_{p(\mathbf{x}'|y=-1)} [\ell(g(\mathbf{x}'), -1)] \\
& = \pi_+ \mathbb{E}_{p(\mathbf{x}|y=+1)} [\ell(g(\mathbf{x}), +1)] + \pi_- \mathbb{E}_{p(\mathbf{x}|y=-1)} [\ell(g(\mathbf{x}), -1)] \\
& = R(g),
\end{aligned}$$

and

$$\begin{aligned}
& \mathbb{E}_{p(\mathbf{x}, \mathbf{x}')} [\mathcal{L}(\mathbf{x}', \mathbf{x})] \\
& = \mathbb{E}_{p(\mathbf{x}, \mathbf{x}')} [(2\pi_+ (\pi_+ + c(\mathbf{x}, \mathbf{x}')) + \pi_- - s(\mathbf{x}, \mathbf{x}')) \ell(g(\mathbf{x}'), +1) \\
& \quad + (2\pi_- (\pi_- + c(\mathbf{x}, \mathbf{x}')) + \pi_+ - s(\mathbf{x}, \mathbf{x}')) \ell(g(\mathbf{x}), -1)] \\
& = \pi_+ \mathbb{E}_{p(\mathbf{x}'|y=+1)} [\ell(g(\mathbf{x}'), +1)] + \pi_- \mathbb{E}_{p(\mathbf{x}|y=-1)} [\ell(g(\mathbf{x}), -1)] \\
& = \pi_+ \mathbb{E}_{p(\mathbf{x}|y=+1)} [\ell(g(\mathbf{x}), +1)] + \pi_- \mathbb{E}_{p(\mathbf{x}|y=-1)} [\ell(g(\mathbf{x}), -1)] \\
& = R(g).
\end{aligned}$$

Therefore, for an arbitrary weight $\lambda \in [0, 1]$,

$$\begin{aligned}
R(g) & = \lambda R(g) + (1 - \lambda) R(g) \\
& = \lambda \mathbb{E}_{p(\mathbf{x}, \mathbf{x}')} [\mathcal{L}(\mathbf{x}, \mathbf{x}')] + (1 - \lambda) \mathbb{E}_{p(\mathbf{x}, \mathbf{x}')} [\mathcal{L}(\mathbf{x}', \mathbf{x})].
\end{aligned}$$

This indicates that

$$\frac{1}{n} \sum_{i=1}^n (\lambda \mathcal{L}(\mathbf{x}_i, \mathbf{x}'_i) + (1 - \lambda) \mathcal{L}(\mathbf{x}'_i, \mathbf{x}_i))$$

is also an unbiased risk estimator and concludes the proof. \square

We now prove Theorem 3. We introduce the following notations:

$$\begin{aligned}
S(g; \lambda) & = \frac{1}{n} \sum_{i=1}^n (\lambda \mathcal{L}(\mathbf{x}_i, \mathbf{x}'_i) + (1 - \lambda) \mathcal{L}(\mathbf{x}'_i, \mathbf{x}_i)), \\
\mu_1 & \triangleq \mathbb{E}_{p(\mathbf{x}, \mathbf{x}')} \left[\left(\frac{1}{n} \sum_{i=1}^n \mathcal{L}(\mathbf{x}_i, \mathbf{x}'_i) \right)^2 \right] = \mathbb{E}_{p(\mathbf{x}, \mathbf{x}')} \left[\left(\frac{1}{n} \sum_{i=1}^n \mathcal{L}(\mathbf{x}'_i, \mathbf{x}_i) \right)^2 \right], \\
\mu_2 & \triangleq \mathbb{E}_{p(\mathbf{x}, \mathbf{x}')} \left[\frac{1}{n^2} \sum_{i=1}^n \mathcal{L}(\mathbf{x}_i, \mathbf{x}'_i) \sum_{i=1}^n \mathcal{L}(\mathbf{x}'_i, \mathbf{x}_i) \right].
\end{aligned}$$

Based on Lemma 1,

$$\mathbb{E}_{p(\mathbf{x}, \mathbf{x}')} [S(g; \lambda)] = R(g).$$

Proof.

$$\begin{aligned}
\text{Var}(S(g; \lambda)) &= \mathbb{E}_{p(\mathbf{x}, \mathbf{x}')} [(S(g; \lambda) - R(g))^2] \\
&= \mathbb{E}_{p(\mathbf{x}, \mathbf{x}')} [S(g; \lambda)^2] - R(g)^2 \\
&= \lambda^2 \mathbb{E}_{p(\mathbf{x}, \mathbf{x}')} \left[\left(\frac{1}{n} \sum_{i=1}^n \mathcal{L}(\mathbf{x}_i, \mathbf{x}'_i) \right)^2 \right] + (1 - \lambda)^2 \mathbb{E}_{p(\mathbf{x}, \mathbf{x}')} \left[\left(\frac{1}{n} \sum_{i=1}^n \mathcal{L}(\mathbf{x}'_i, \mathbf{x}_i) \right)^2 \right] \\
&\quad + 2\lambda(1 - \lambda) \mathbb{E}_{p(\mathbf{x}, \mathbf{x}')} \left[\frac{1}{n^2} \sum_{i=1}^n \mathcal{L}(\mathbf{x}_i, \mathbf{x}'_i) \sum_{i=1}^n \mathcal{L}(\mathbf{x}'_i, \mathbf{x}_i) \right] - R(g)^2 \\
&= \mu_1 \lambda^2 + \mu_1 (1 - \lambda)^2 + 2\mu_2 \lambda(1 - \lambda) - R(g)^2 \\
&= (2\mu_1 - 2\mu_2) \lambda^2 - (2\mu_1 - 2\mu_2) \lambda + \mu_1 - R(g)^2 \\
&= (2\mu_1 - 2\mu_2) \left(\lambda - \frac{1}{2} \right)^2 + \frac{1}{2} (\mu_1 + \mu_2) - R(g)^2.
\end{aligned}$$

Besides, it can be observed that

$$\begin{aligned}
2\mu_1 - 2\mu_2 &= \mathbb{E}_{p(\mathbf{x}, \mathbf{x}')} \left[\left(\frac{1}{n} \sum_{i=1}^n \mathcal{L}(\mathbf{x}_i, \mathbf{x}'_i) \right)^2 \right] + \mathbb{E}_{p(\mathbf{x}, \mathbf{x}')} \left[\left(\frac{1}{n} \sum_{i=1}^n \mathcal{L}(\mathbf{x}'_i, \mathbf{x}_i) \right)^2 \right] \\
&\quad - 2 \mathbb{E}_{p(\mathbf{x}, \mathbf{x}')} \left[\frac{1}{n^2} \sum_{i=1}^n \mathcal{L}(\mathbf{x}_i, \mathbf{x}'_i) \sum_{i=1}^n \mathcal{L}(\mathbf{x}'_i, \mathbf{x}_i) \right] \\
&= \mathbb{E}_{p(\mathbf{x}, \mathbf{x}')} \left[\left(\frac{1}{n} \sum_{i=1}^n (\mathcal{L}(\mathbf{x}_i, \mathbf{x}'_i) - \mathcal{L}(\mathbf{x}'_i, \mathbf{x}_i)) \right)^2 \right] \geq 0.
\end{aligned}$$

Therefore, $\text{Var}(S(g; \lambda))$ achieves the minimum value when $\lambda = 1/2$, which concludes the proof. \square

A.3 Proof of Theorem 4

For convenience, we make the following notation:

$$\begin{aligned}
\mathcal{L}_{\text{SCD}}(g; \mathbf{x}_i, \mathbf{x}'_i) &= \frac{1}{2} \{ (2\pi_+ (\pi_+ - c(\mathbf{x}_i, \mathbf{x}'_i)) + \pi_- - s(\mathbf{x}_i, \mathbf{x}'_i)) \ell(g(\mathbf{x}_i), +1) \\
&\quad + (2\pi_- (\pi_- - c(\mathbf{x}_i, \mathbf{x}'_i)) + \pi_+ - s(\mathbf{x}_i, \mathbf{x}'_i)) \ell(g(\mathbf{x}'_i), -1) \\
&\quad + (2\pi_+ (\pi_+ + c(\mathbf{x}_i, \mathbf{x}'_i)) + \pi_- - s(\mathbf{x}_i, \mathbf{x}'_i)) \ell(g(\mathbf{x}'_i), +1) \\
&\quad + (2\pi_- (\pi_- + c(\mathbf{x}_i, \mathbf{x}'_i)) + \pi_+ - s(\mathbf{x}_i, \mathbf{x}'_i)) \ell(g(\mathbf{x}_i), -1) \}.
\end{aligned}$$

Definition 1 (Rademacher complexity). *Let $\mathcal{X}_n = \{\mathbf{x}_1, \dots, \mathbf{x}_n\}$ denote n i.i.d. random variables drawn from a probability distribution with density $p(\mathbf{x})$, $\mathcal{G} = \{g : \mathcal{X} \rightarrow \mathbb{R}\}$ denote a class of measurable functions, and $\boldsymbol{\sigma} = (\sigma_1, \dots, \sigma_n)$ denote Rademacher variables taking values from $\{-1, +1\}$ uniformly. Then, the (expected) Rademacher complexity of \mathcal{G} is defined as*

$$\mathfrak{R}(\mathcal{G}) = \mathbb{E}_{\mathbf{x}_1, \dots, \mathbf{x}_n} \mathbb{E}_{\boldsymbol{\sigma}} \left[\sup_{g \in \mathcal{G}} \frac{1}{n} \sum_{i=1}^n \sigma_i g(\mathbf{x}_i) \right]. \quad (28)$$

Lemma 5.

$$\bar{\mathfrak{R}}_n(\mathcal{L}_{\text{SCD}} \circ \mathcal{G}) \leq 3L_\ell \mathfrak{R}_n(\mathcal{G}),$$

where $\mathcal{L}_{\text{SCD}} \circ \mathcal{G} = \{\mathcal{L}_{\text{SCD}} \circ g\}$ and $\bar{\mathfrak{R}}_n(\cdot)$ is the Rademacher complexity over SconfConfDiff data pairs \mathcal{D}_n of size n .

Proof.

$$\begin{aligned}
\bar{\mathfrak{R}}_n(\mathcal{L}_{\text{SCD}} \circ \mathcal{G}) &= \mathbb{E}_{\mathcal{D}_n} \mathbb{E}_{\boldsymbol{\sigma}} \left[\sup_{g \in \mathcal{G}} \frac{1}{n} \sum_{i=1}^n \sigma_i \mathcal{L}_{\text{SCD}}(g; \mathbf{x}_i, \mathbf{x}'_i) \right] \\
&= \mathbb{E}_{\mathcal{D}_n} \mathbb{E}_{\boldsymbol{\sigma}} \left[\sup_{g \in \mathcal{G}} \frac{1}{2n} \sum_{i=1}^n \left\{ (2\pi_+(\pi_+ - c(\mathbf{x}_i, \mathbf{x}'_i)) + \pi_- - s(\mathbf{x}_i, \mathbf{x}'_i)) \ell(g(\mathbf{x}_i), +1) \right. \right. \\
&\quad \left. \left. + (2\pi_-(\pi_- - c(\mathbf{x}_i, \mathbf{x}'_i)) + \pi_+ - s(\mathbf{x}_i, \mathbf{x}'_i)) \ell(g(\mathbf{x}'_i), -1) \right. \right. \\
&\quad \left. \left. + (2\pi_+(\pi_+ + c(\mathbf{x}_i, \mathbf{x}'_i)) + \pi_- - s(\mathbf{x}_i, \mathbf{x}'_i)) \ell(g(\mathbf{x}'_i), +1) \right. \right. \\
&\quad \left. \left. + (2\pi_-(\pi_- + c(\mathbf{x}_i, \mathbf{x}'_i)) + \pi_+ - s(\mathbf{x}_i, \mathbf{x}'_i)) \ell(g(\mathbf{x}_i), -1) \right\} \right].
\end{aligned}$$

Then, we can induce that

$$\begin{aligned}
&\|\nabla \mathcal{L}_{\text{SCD}}(g; \mathbf{x}, \mathbf{x}')\|_2 \\
&= \left\| \nabla \left(\frac{(2\pi_+(\pi_+ - c(\mathbf{x}, \mathbf{x}')) + \pi_- - s(\mathbf{x}, \mathbf{x}')) \ell(g(\mathbf{x}), +1)}{2} \right. \right. \\
&\quad \left. \left. + \frac{(2\pi_-(\pi_- - c(\mathbf{x}, \mathbf{x}')) + \pi_+ - s(\mathbf{x}, \mathbf{x}')) \ell(g(\mathbf{x}'), -1)}{2} \right. \right. \\
&\quad \left. \left. + \frac{(2\pi_+(\pi_+ + c(\mathbf{x}, \mathbf{x}')) + \pi_- - s(\mathbf{x}, \mathbf{x}')) \ell(g(\mathbf{x}'), +1)}{2} \right. \right. \\
&\quad \left. \left. + \frac{(2\pi_-(\pi_- + c(\mathbf{x}, \mathbf{x}')) + \pi_+ - s(\mathbf{x}, \mathbf{x}')) \ell(g(\mathbf{x}), -1)}{2} \right) \right\|_2 \\
&\leq \left\| \nabla \left(\frac{(2\pi_+(\pi_+ - c(\mathbf{x}, \mathbf{x}')) + \pi_- - s(\mathbf{x}, \mathbf{x}')) \ell(g(\mathbf{x}), +1)}{2} \right) \right\|_2 \\
&\quad + \left\| \nabla \left(\frac{(2\pi_-(\pi_- - c(\mathbf{x}, \mathbf{x}')) + \pi_+ - s(\mathbf{x}, \mathbf{x}')) \ell(g(\mathbf{x}'), -1)}{2} \right) \right\|_2 \\
&\quad + \left\| \nabla \left(\frac{(2\pi_+(\pi_+ + c(\mathbf{x}, \mathbf{x}')) + \pi_- - s(\mathbf{x}, \mathbf{x}')) \ell(g(\mathbf{x}'), +1)}{2} \right) \right\|_2 \\
&\quad + \left\| \nabla \left(\frac{(2\pi_-(\pi_- + c(\mathbf{x}, \mathbf{x}')) + \pi_+ - s(\mathbf{x}, \mathbf{x}')) \ell(g(\mathbf{x}), -1)}{2} \right) \right\|_2 \\
&\leq \frac{|2\pi_+(\pi_+ - c(\mathbf{x}, \mathbf{x}')) + \pi_- - s(\mathbf{x}, \mathbf{x}')| L_\ell}{2} + \frac{|2\pi_-(\pi_- - c(\mathbf{x}, \mathbf{x}')) + \pi_+ - s(\mathbf{x}, \mathbf{x}')| L_\ell}{2} \\
&\quad + \frac{|2\pi_+(\pi_+ + c(\mathbf{x}, \mathbf{x}')) + \pi_- - s(\mathbf{x}, \mathbf{x}')| L_\ell}{2} + \frac{|2\pi_-(\pi_- + c(\mathbf{x}, \mathbf{x}')) + \pi_+ - s(\mathbf{x}, \mathbf{x}')| L_\ell}{2} \\
&\leq \left(\frac{|2\pi_+(\pi_+ - c(\mathbf{x}, \mathbf{x}'))| + |\pi_- - s(\mathbf{x}, \mathbf{x}')|}{2} + \frac{|2\pi_-(\pi_- - c(\mathbf{x}, \mathbf{x}'))| + |\pi_+ - s(\mathbf{x}, \mathbf{x}')|}{2} \right. \\
&\quad \left. + \frac{|2\pi_+(\pi_+ + c(\mathbf{x}, \mathbf{x}'))| + |\pi_- - s(\mathbf{x}, \mathbf{x}')|}{2} + \frac{|2\pi_-(\pi_- + c(\mathbf{x}, \mathbf{x}'))| + |\pi_+ - s(\mathbf{x}, \mathbf{x}')|}{2} \right) L_\ell.
\end{aligned}$$

Suppose $\pi_+ \geq \pi_-$.

(i) When $c(\mathbf{x}, \mathbf{x}') \in [-1, -\pi_+)$,

$$\begin{aligned}
\frac{|2\pi_+(\pi_+ - c(\mathbf{x}, \mathbf{x}'))| + |\pi_- - s(\mathbf{x}, \mathbf{x}')|}{2} &= \begin{cases} \frac{2\pi_+(\pi_+ - c(\mathbf{x}, \mathbf{x}')) + \pi_- - s(\mathbf{x}, \mathbf{x}')}{2}, & s(\mathbf{x}, \mathbf{x}') \in [0, \pi_-) \\ \frac{2\pi_+(\pi_+ - c(\mathbf{x}, \mathbf{x}')) + s(\mathbf{x}, \mathbf{x}') - \pi_-}{2}, & s(\mathbf{x}, \mathbf{x}') \in [\pi_-, \pi_+) \\ \frac{2\pi_+(\pi_+ - c(\mathbf{x}, \mathbf{x}')) + s(\mathbf{x}, \mathbf{x}') - \pi_-}{2}, & s(\mathbf{x}, \mathbf{x}') \in [\pi_+, 1] \end{cases} \\
\frac{|2\pi_-(\pi_- - c(\mathbf{x}, \mathbf{x}'))| + |\pi_+ - s(\mathbf{x}, \mathbf{x}')|}{2} &= \begin{cases} \frac{2\pi_-(\pi_- - c(\mathbf{x}, \mathbf{x}')) + \pi_+ - s(\mathbf{x}, \mathbf{x}')}{2}, & s(\mathbf{x}, \mathbf{x}') \in [0, \pi_-) \\ \frac{2\pi_-(\pi_- - c(\mathbf{x}, \mathbf{x}')) + \pi_+ - s(\mathbf{x}, \mathbf{x}')}{2}, & s(\mathbf{x}, \mathbf{x}') \in [\pi_-, \pi_+) \\ \frac{2\pi_-(\pi_- - c(\mathbf{x}, \mathbf{x}')) + s(\mathbf{x}, \mathbf{x}') - \pi_+}{2}, & s(\mathbf{x}, \mathbf{x}') \in [\pi_+, 1] \end{cases}
\end{aligned}$$

Therefore,

$$\|\nabla \mathcal{L}_{\text{SCD}}(g; \mathbf{x}, \mathbf{x}')\|_2 \leq \begin{cases} (2(\pi_+^2 + \pi_-^2) + 1 - 2s(\mathbf{x}, \mathbf{x}'))L_\ell, & s(\mathbf{x}, \mathbf{x}') \in [0, \pi_-) \\ (2(\pi_+^2 + \pi_-^2) + \pi_+ - \pi_-)L_\ell, & s(\mathbf{x}, \mathbf{x}') \in [\pi_-, \pi_+) \\ (2(\pi_+^2 + \pi_-^2) + 2s(\mathbf{x}, \mathbf{x}') - 1)L_\ell, & s(\mathbf{x}, \mathbf{x}') \in [\pi_+, 1] \end{cases}$$

(iv) When $c(\mathbf{x}, \mathbf{x}') \in [\pi_-, \pi_+)$,

$$\begin{aligned} \frac{|2\pi_+(\pi_+ - c(\mathbf{x}, \mathbf{x}'))| + |\pi_- - s(\mathbf{x}, \mathbf{x}')|}{2} &= \begin{cases} \frac{2\pi_+(\pi_+ - c(\mathbf{x}, \mathbf{x}')) + \pi_- - s(\mathbf{x}, \mathbf{x}')}{2}, & s(\mathbf{x}, \mathbf{x}') \in [0, \pi_-) \\ \frac{2\pi_+(\pi_+ - c(\mathbf{x}, \mathbf{x}')) + s(\mathbf{x}, \mathbf{x}') - \pi_-}{2}, & s(\mathbf{x}, \mathbf{x}') \in [\pi_-, \pi_+) \\ \frac{2\pi_+(\pi_+ - c(\mathbf{x}, \mathbf{x}')) + s(\mathbf{x}, \mathbf{x}') - \pi_-}{2}, & s(\mathbf{x}, \mathbf{x}') \in [\pi_+, 1] \end{cases} \\ \frac{|2\pi_-(\pi_- - c(\mathbf{x}, \mathbf{x}'))| + |\pi_+ - s(\mathbf{x}, \mathbf{x}')|}{2} &= \begin{cases} \frac{-2\pi_-(\pi_- - c(\mathbf{x}, \mathbf{x}')) + \pi_+ - s(\mathbf{x}, \mathbf{x}')}{2}, & s(\mathbf{x}, \mathbf{x}') \in [0, \pi_-) \\ \frac{-2\pi_-(\pi_- - c(\mathbf{x}, \mathbf{x}')) + \pi_+ - s(\mathbf{x}, \mathbf{x}')}{2}, & s(\mathbf{x}, \mathbf{x}') \in [\pi_-, \pi_+) \\ \frac{-2\pi_-(\pi_- - c(\mathbf{x}, \mathbf{x}')) + s(\mathbf{x}, \mathbf{x}') - \pi_+}{2}, & s(\mathbf{x}, \mathbf{x}') \in [\pi_+, 1] \end{cases} \\ \frac{|2\pi_+(\pi_+ + c(\mathbf{x}, \mathbf{x}'))| + |\pi_- - s(\mathbf{x}, \mathbf{x}')|}{2} &= \begin{cases} \frac{2\pi_+(\pi_+ + c(\mathbf{x}, \mathbf{x}')) + \pi_- - s(\mathbf{x}, \mathbf{x}')}{2}, & s(\mathbf{x}, \mathbf{x}') \in [0, \pi_-) \\ \frac{2\pi_+(\pi_+ + c(\mathbf{x}, \mathbf{x}')) + s(\mathbf{x}, \mathbf{x}') - \pi_-}{2}, & s(\mathbf{x}, \mathbf{x}') \in [\pi_-, \pi_+) \\ \frac{2\pi_+(\pi_+ + c(\mathbf{x}, \mathbf{x}')) + s(\mathbf{x}, \mathbf{x}') - \pi_-}{2}, & s(\mathbf{x}, \mathbf{x}') \in [\pi_+, 1] \end{cases} \\ \frac{|2\pi_-(\pi_- + c(\mathbf{x}, \mathbf{x}'))| + |\pi_+ - s(\mathbf{x}, \mathbf{x}')|}{2} &= \begin{cases} \frac{2\pi_-(\pi_- + c(\mathbf{x}, \mathbf{x}')) + \pi_+ - s(\mathbf{x}, \mathbf{x}')}{2}, & s(\mathbf{x}, \mathbf{x}') \in [0, \pi_-) \\ \frac{2\pi_-(\pi_- + c(\mathbf{x}, \mathbf{x}')) + \pi_+ - s(\mathbf{x}, \mathbf{x}')}{2}, & s(\mathbf{x}, \mathbf{x}') \in [\pi_-, \pi_+) \\ \frac{2\pi_-(\pi_- + c(\mathbf{x}, \mathbf{x}')) + s(\mathbf{x}, \mathbf{x}') - \pi_+}{2}, & s(\mathbf{x}, \mathbf{x}') \in [\pi_+, 1] \end{cases} \end{aligned}$$

Therefore,

$$\|\nabla \mathcal{L}_{\text{SCD}}(g; \mathbf{x}, \mathbf{x}')\|_2 \leq \begin{cases} (2\pi_+^2 + 1 - 2(s(\mathbf{x}, \mathbf{x}') - \pi_- c(\mathbf{x}, \mathbf{x}'))L_\ell, & s(\mathbf{x}, \mathbf{x}') \in [0, \pi_-) \\ (2(\pi_+^2 + \pi_- c(\mathbf{x}, \mathbf{x}')) + \pi_+ - \pi_-)L_\ell, & s(\mathbf{x}, \mathbf{x}') \in [\pi_-, \pi_+) \\ (2\pi_+^2 - 1 + 2(s(\mathbf{x}, \mathbf{x}') + \pi_- c(\mathbf{x}, \mathbf{x}'))L_\ell, & s(\mathbf{x}, \mathbf{x}') \in [\pi_+, 1] \end{cases}$$

(v) When $c(\mathbf{x}, \mathbf{x}') \in [\pi_+, 1]$,

$$\begin{aligned} \frac{|2\pi_+(\pi_+ - c(\mathbf{x}, \mathbf{x}'))| + |\pi_- - s(\mathbf{x}, \mathbf{x}')|}{2} &= \begin{cases} \frac{-2\pi_+(\pi_+ - c(\mathbf{x}, \mathbf{x}')) + \pi_- - s(\mathbf{x}, \mathbf{x}')}{2}, & s(\mathbf{x}, \mathbf{x}') \in [0, \pi_-) \\ \frac{-2\pi_+(\pi_+ - c(\mathbf{x}, \mathbf{x}')) + s(\mathbf{x}, \mathbf{x}') - \pi_-}{2}, & s(\mathbf{x}, \mathbf{x}') \in [\pi_-, \pi_+) \\ \frac{-2\pi_+(\pi_+ - c(\mathbf{x}, \mathbf{x}')) + s(\mathbf{x}, \mathbf{x}') - \pi_-}{2}, & s(\mathbf{x}, \mathbf{x}') \in [\pi_+, 1] \end{cases} \\ \frac{|2\pi_-(\pi_- - c(\mathbf{x}, \mathbf{x}'))| + |\pi_+ - s(\mathbf{x}, \mathbf{x}')|}{2} &= \begin{cases} \frac{-2\pi_-(\pi_- - c(\mathbf{x}, \mathbf{x}')) + \pi_+ - s(\mathbf{x}, \mathbf{x}')}{2}, & s(\mathbf{x}, \mathbf{x}') \in [0, \pi_-) \\ \frac{-2\pi_-(\pi_- - c(\mathbf{x}, \mathbf{x}')) + \pi_+ - s(\mathbf{x}, \mathbf{x}')}{2}, & s(\mathbf{x}, \mathbf{x}') \in [\pi_-, \pi_+) \\ \frac{-2\pi_-(\pi_- - c(\mathbf{x}, \mathbf{x}')) + s(\mathbf{x}, \mathbf{x}') - \pi_+}{2}, & s(\mathbf{x}, \mathbf{x}') \in [\pi_+, 1] \end{cases} \\ \frac{|2\pi_+(\pi_+ + c(\mathbf{x}, \mathbf{x}'))| + |\pi_- - s(\mathbf{x}, \mathbf{x}')|}{2} &= \begin{cases} \frac{2\pi_+(\pi_+ + c(\mathbf{x}, \mathbf{x}')) + \pi_- - s(\mathbf{x}, \mathbf{x}')}{2}, & s(\mathbf{x}, \mathbf{x}') \in [0, \pi_-) \\ \frac{2\pi_+(\pi_+ + c(\mathbf{x}, \mathbf{x}')) + s(\mathbf{x}, \mathbf{x}') - \pi_-}{2}, & s(\mathbf{x}, \mathbf{x}') \in [\pi_-, \pi_+) \\ \frac{2\pi_+(\pi_+ + c(\mathbf{x}, \mathbf{x}')) + s(\mathbf{x}, \mathbf{x}') - \pi_-}{2}, & s(\mathbf{x}, \mathbf{x}') \in [\pi_+, 1] \end{cases} \\ \frac{|2\pi_-(\pi_- + c(\mathbf{x}, \mathbf{x}'))| + |\pi_+ - s(\mathbf{x}, \mathbf{x}')|}{2} &= \begin{cases} \frac{2\pi_-(\pi_- + c(\mathbf{x}, \mathbf{x}')) + \pi_+ - s(\mathbf{x}, \mathbf{x}')}{2}, & s(\mathbf{x}, \mathbf{x}') \in [0, \pi_-) \\ \frac{2\pi_-(\pi_- + c(\mathbf{x}, \mathbf{x}')) + \pi_+ - s(\mathbf{x}, \mathbf{x}')}{2}, & s(\mathbf{x}, \mathbf{x}') \in [\pi_-, \pi_+) \\ \frac{2\pi_-(\pi_- + c(\mathbf{x}, \mathbf{x}')) + s(\mathbf{x}, \mathbf{x}') - \pi_+}{2}, & s(\mathbf{x}, \mathbf{x}') \in [\pi_+, 1] \end{cases} \end{aligned}$$

Therefore,

$$\|\nabla \mathcal{L}_{\text{SCD}}(g; \mathbf{x}, \mathbf{x}')\|_2 \leq \begin{cases} (1 - 2(s(\mathbf{x}, \mathbf{x}') - c(\mathbf{x}, \mathbf{x}'))L_\ell, & s(\mathbf{x}, \mathbf{x}') \in [0, \pi_-) \\ (2c(\mathbf{x}, \mathbf{x}') + \pi_+ - \pi_-)L_\ell, & s(\mathbf{x}, \mathbf{x}') \in [\pi_-, \pi_+) \\ (2(s(\mathbf{x}, \mathbf{x}') + c(\mathbf{x}, \mathbf{x}')) - 1)L_\ell, & s(\mathbf{x}, \mathbf{x}') \in [\pi_+, 1] \end{cases}$$

As a result,

$$\|\nabla \mathcal{L}_{\text{SCD}}(g; \mathbf{x}, \mathbf{x}')\|_2 \leq 3L_\ell, \quad (29)$$

and consequently,

$$\begin{aligned} \bar{\mathfrak{R}}_n(\mathcal{L}_{\text{SCD}} \circ \mathcal{G}) &\leq 3L_\ell \mathbb{E}_{\mathcal{D}_n} \mathbb{E}_\sigma \left[\sup_{g \in \mathcal{G}} \frac{1}{n} \sum_{i=1}^n \sigma_i g(\mathbf{x}_i) \right] \\ &= 3L_\ell \mathfrak{R}_n(\mathcal{G}). \end{aligned}$$

□

Lemma 6. *The following inequality holds with probability at least $1 - \delta$:*

$$\sup_{g \in \mathcal{G}} |R(g) - \widehat{R}_{\text{SCD}}(g)| \leq 6L_\ell \mathfrak{R}_n(\mathcal{G}) + \left(\pi_+^2 + \pi_-^2 + \frac{5}{2} \right) C_\ell \sqrt{\frac{\log 2/\delta}{2n}}$$

Proof. The following inequalities hold for \mathcal{L}_{SCD} .

$$\begin{aligned} \mathcal{L}_{\text{SCD}}(g; \mathbf{x}, \mathbf{x}') &\leq \frac{1}{2n} ((2\pi_+^2 - 2\pi_+ c_i + \pi_-) C_\ell + (2\pi_-^2 - 2\pi_- c_i + \pi_+) C_\ell \\ &\quad + (2\pi_+^2 + 2\pi_+ c_i + \pi_-) C_\ell + (2\pi_-^2 + 2\pi_- c_i + \pi_+) C_\ell) \\ &= \frac{1}{2n} (4(\pi_+^2 + \pi_-^2) + 2) C_\ell \\ &= \frac{1}{n} (2\pi_+^2 + 2\pi_-^2 + 1) C_\ell, \end{aligned}$$

and

$$\begin{aligned} \mathcal{L}_{\text{SCD}}(g; \mathbf{x}, \mathbf{x}') &> \frac{1}{2n} \leq (2\pi_+^2 - 2\pi_+ c_i + \pi_- - 1 + 2\pi_-^2 - 2\pi_- c_i + \pi_+ - 1) C_\ell \\ &= \frac{1}{2n} (2(\pi_+^2 + \pi_-^2) - 2c_i - 1) C_\ell \\ &= \frac{1}{n} \left(\pi_+^2 + \pi_-^2 - \frac{3}{2} \right). \end{aligned}$$

Thus, the following inequality holds:

$$\frac{1}{n} \left(\pi_+^2 + \pi_-^2 - \frac{3}{2} \right) < \mathcal{L}_{\text{SCD}}(g; \mathbf{x}, \mathbf{x}') \leq \frac{1}{n} (2\pi_+^2 + 2\pi_-^2 + 1) C_\ell$$

Here, we introduce $\Phi = \sup_{g \in \mathcal{G}} (R(g) - \widehat{R}_{\text{SCD}}(g))$, $\dot{\Phi} = \sup_{g \in \mathcal{G}} (R(g) - \widehat{\dot{R}}_{\text{SCD}}(g))$, where $\widehat{R}_{\text{SCD}}(g)$ and $\widehat{\dot{R}}_{\text{SCD}}(g)$ denote the empirical risk over two sets of training examples with exactly one different point $\{(\mathbf{x}_i, \mathbf{x}'_i), s_i, c_i\}$ and $\{(\dot{\mathbf{x}}_i, \dot{\mathbf{x}}'_i), \dot{s}_i, \dot{c}_i\}$. Then, based on uniform law of large numbers,

$$\begin{aligned} \dot{\Phi} - \Phi &\leq \sup_{g \in \mathcal{G}} (\widehat{\dot{R}}_{\text{SCD}}(g) - \widehat{R}_{\text{SCD}}(g)) \\ &\leq \sup_{g \in \mathcal{G}} \left(\frac{\mathcal{L}_{\text{SCD}}(g; \mathbf{x}_i, \mathbf{x}'_i) - \mathcal{L}_{\text{SCD}}(g; \dot{\mathbf{x}}_i, \dot{\mathbf{x}}'_i)}{n} \right) \\ &\leq \frac{(\pi_+^2 + \pi_-^2 + \frac{5}{2}) C_\ell}{n}. \end{aligned}$$

The following inequality holds with probability at least $1 - \delta/2$ by applying McDiarmid's inequality:

$$\sup_{g \in \mathcal{G}} (R(g) - \widehat{R}_{\text{SCD}}(g)) \leq \mathbb{E}_{\mathcal{D}_n} [\sup_{g \in \mathcal{G}} (R(g) - \widehat{R}_{\text{SCD}}(g))] + \left(\pi_+^2 + \pi_-^2 + \frac{5}{2} \right) C_\ell \sqrt{\frac{\log 2/\delta}{2n}}.$$

Furthermore, we can bound $\mathbb{E}_{\mathcal{D}_n} [\sup_{g \in \mathcal{G}} (R(g) - \widehat{R}_{\text{SCD}}(g))]$ with Rademacher complexity.

$$\mathbb{E}_{\mathcal{D}_n} [\sup_{g \in \mathcal{G}} (R(g) - \widehat{R}_{\text{SCD}}(g))] \leq 2\bar{\mathfrak{R}}_n(\mathcal{L}_{\text{SCD}} \circ \mathcal{G}) \leq 6L_\ell \mathfrak{R}_n(\mathcal{G}).$$

As a result, The following inequality holds with probability at least $1 - \delta$:

$$\sup_{g \in \mathcal{G}} |R(g) - \widehat{R}_{\text{SCD}}(g)| \leq 6L_\ell \mathfrak{R}_n(\mathcal{G}) + \left(\pi_+^2 + \pi_-^2 + \frac{5}{2} \right) C_\ell \sqrt{\frac{\log 2/\delta}{2n}}.$$

□

Finally, the proof of Theorem 4 is provided.

Proof.

$$\begin{aligned}
R(\hat{g}_{\text{SCD}}) - R(g^*) &= (R(\hat{g}_{\text{SCD}}) - \widehat{R}(\hat{g}_{\text{SCD}})) + (\widehat{R}(\hat{g}_{\text{SCD}}) - \widehat{R}_{\text{SCD}}(g^*)) + (\widehat{R}_{\text{SCD}}(g^*) - R(g^*)) \\
&\leq (R(\hat{g}_{\text{SCD}}) - \widehat{R}(\hat{g}_{\text{SCD}})) + (\widehat{R}_{\text{SCD}}(g^*) - R(g^*)) \\
&\leq |R(\hat{g}_{\text{SCD}}) - \widehat{R}(\hat{g}_{\text{SCD}})| + |\widehat{R}_{\text{SCD}}(g^*) - R(g^*)| \\
&\leq 2 \sup_{g \in \mathcal{G}} |R(g) - \widehat{R}_{\text{SCD}}(g)| \\
&\leq 12L_\ell \mathfrak{R}_n(\mathcal{G}) + (2\pi_+^2 + 2\pi_-^2 + 5)C_\ell \sqrt{\frac{\log 2/\delta}{2n}}.
\end{aligned}$$

The first inequality is deduced because \hat{g}_{SCD} is the minimizer of $\widehat{R}_{\text{SCD}}(g)$. \square

A.4 Proof of Theorem 5

Proof.

$$\begin{aligned}
&|\bar{R}_{\text{SCD}}(g) - \widehat{R}_{\text{SCD}}(g)| \\
&= \frac{1}{2n} \left| \sum_{i=1}^n ((2(\bar{\pi}_+^2 - \pi_+^2) - 2(\bar{\pi}_+ \bar{c}_i - \pi_+ c_i) + (\bar{\pi}_- - \pi_-) - (\bar{s}_i - s_i))\ell(g(\mathbf{x}_i), +1) \right. \\
&\quad + (2(\bar{\pi}_-^2 - \pi_-^2) - 2(\bar{\pi}_- \bar{c}_i - \pi_- c_i) + (\bar{\pi}_+ - \pi_+) - (\bar{s}_i - s_i))\ell(g(\mathbf{x}'_i), -1) \\
&\quad + (2(\bar{\pi}_+^2 - \pi_+^2) + 2(\bar{\pi}_+ \bar{c}_i - \pi_+ c_i) + (\bar{\pi}_- - \pi_-) - (\bar{s}_i - s_i))\ell(g(\mathbf{x}'_i), +1) \\
&\quad \left. + (2(\bar{\pi}_-^2 - \pi_-^2) + 2(\bar{\pi}_- \bar{c}_i - \pi_- c_i) + (\bar{\pi}_+ - \pi_+) - (\bar{s}_i - s_i))\ell(g(\mathbf{x}_i), -1) \right| \\
&\leq \frac{C_\ell}{2n} \sum_{i=1}^n (4|\bar{\pi}_+^2 - \pi_+^2| + 4|\bar{\pi}_-^2 - \pi_-^2| + 4|\bar{\pi}_+ \bar{c}_i - \pi_+ c_i| \\
&\quad + 4|\bar{\pi}_- \bar{c}_i - \pi_- c_i| + 4|\bar{\pi}_+ - \pi_+| + 4|\bar{s}_i - s_i|) \\
&= \frac{2C_\ell}{n} \sum_{i=1}^n (|\bar{\pi}_+ \bar{c}_i - \pi_+ c_i| + |\bar{\pi}_- \bar{c}_i - \pi_- c_i| + |\bar{s}_i - s_i|) \\
&\quad + 2C_\ell (|\bar{\pi}_+^2 - \pi_+^2| + |\bar{\pi}_-^2 - \pi_-^2| + |\bar{\pi}_+ - \pi_+|).
\end{aligned}$$

Then, the following inequality can be derived.

$$\begin{aligned}
&R(\bar{g}_{\text{SCD}}) - R(g^*) \\
&= (R(\bar{g}_{\text{SCD}}) - \widehat{R}_{\text{SCD}}(\bar{g}_{\text{SCD}})) + (\widehat{R}_{\text{SCD}}(\bar{g}_{\text{SCD}}) - \bar{R}_{\text{SCD}}(\bar{g}_{\text{SCD}})) + (\bar{R}_{\text{SCD}}(\bar{g}_{\text{SCD}}) - \bar{R}_{\text{SCD}}(\hat{g}_{\text{SCD}})) \\
&\quad + (\bar{R}_{\text{SCD}}(\hat{g}_{\text{SCD}}) - \widehat{R}_{\text{SCD}}(\hat{g}_{\text{SCD}})) + (\widehat{R}_{\text{SCD}}(\hat{g}_{\text{SCD}}) - R_{\text{SCD}}(\hat{g}_{\text{SCD}})) + (R_{\text{SCD}}(\hat{g}_{\text{SCD}}) - R(g^*)) \\
&\leq 2 \sup_{g \in \mathcal{G}} |R(g) - \widehat{R}_{\text{SCD}}(g)| + 2 \sup_{g \in \mathcal{G}} |\bar{R}_{\text{SCD}}(g) - \widehat{R}_{\text{SCD}}(g)| + (R_{\text{SCD}}(\hat{g}_{\text{SCD}}) - R(g^*)) \\
&\leq 4 \sup_{g \in \mathcal{G}} |R(g) - \widehat{R}_{\text{SCD}}(g)| + 2 \sup_{g \in \mathcal{G}} |\bar{R}_{\text{SCD}}(g) - \widehat{R}_{\text{SCD}}(g)| \\
&\leq 24L_\ell \mathfrak{R}_n(\mathcal{G}) + (4\pi_+^2 + 4\pi_-^2 + 10)C_\ell \sqrt{\frac{\log 2/\delta}{2n}} \\
&\quad + \frac{4C_\ell}{n} \sum_{i=1}^n (|\bar{\pi}_+ \bar{c}_i - \pi_+ c_i| + |\bar{\pi}_- \bar{c}_i - \pi_- c_i| + |\bar{s}_i - s_i|) \\
&\quad + 4C_\ell (|\bar{\pi}_+^2 - \pi_+^2| + |\bar{\pi}_-^2 - \pi_-^2| + |\bar{\pi}_+ - \pi_+|).
\end{aligned}$$

The second inequality is derived based on the proof of Theorem 4. \square

A.5 Proof of Theorem 6

To begin with, let $\mathfrak{D}_n^+(g) = \{\mathcal{D}_n | \widehat{A}(g) \geq 0 \cap \widehat{B}(g) \geq 0 \cap \widehat{C}(g) \geq 0 \cap \widehat{D}(g) \geq 0\}$, $\mathfrak{D}_n^-(g) = \{\mathcal{D}_n | \widehat{A}(g) \leq 0 \cup \widehat{B}(g) \leq 0 \cup \widehat{C}(g) \leq 0 \cup \widehat{D}(g) \leq 0\}$. Before giving the proof of Theorem 6, we give the following lemma.

Lemma 7. *The probability measure of $\mathfrak{D}_n^-(g)$ can be bounded as follows:*

$$\begin{aligned} \mathbb{P}(\mathfrak{D}_n^-(g)) &\leq \exp\left(-\frac{4a^2n}{(4\pi_+ + 1)^2C_\ell^2}\right) + \exp\left(-\frac{4b^2n}{(4\pi_- + 1)^2C_\ell^2}\right) \\ &\quad + \exp\left(-\frac{4c^2n}{(4\pi_+ + 1)^2C_\ell^2}\right) + \exp\left(-\frac{4d^2n}{(4\pi_- + 1)^2C_\ell^2}\right). \end{aligned} \quad (30)$$

Proof. It can be observed that

$$\begin{aligned} p(\mathcal{D}_n) &= p(\mathbf{x}_1, \mathbf{x}'_1) \cdots p(\mathbf{x}_n, \mathbf{x}'_n) \\ &= p(\mathbf{x}_1) \cdots p(\mathbf{x}_n) p(\mathbf{x}'_1) \cdots p(\mathbf{x}'_n). \end{aligned}$$

Therefore, the probability measure of $\mathfrak{D}_n^-(g)$ can be defined as follows:

$$\begin{aligned} \mathbb{P}(\mathfrak{D}_n^-(g)) &= \int_{\mathcal{D}_n \in \mathfrak{D}_n^-(g)} p(\mathcal{D}_n) \, d\mathcal{D}_n \\ &= \int_{\mathcal{D}_n \in \mathfrak{D}_n^-(g)} p(\mathcal{D}_n) \, d\mathbf{x}_1 \cdots d\mathbf{x}_n d\mathbf{x}'_1 \cdots d\mathbf{x}'_n. \end{aligned}$$

When exactly one SconfConfDiff data pair in \mathcal{D}_n is replaced, the changes in $\widehat{A}(g)$ and $\widehat{C}(g)$ are no more than $(4\pi_+ + 1)C_\ell/2n$, and the changes in $\widehat{B}(g)$ and $\widehat{D}(g)$ are no more than $(4\pi_- + 1)C_\ell/2n$. By applying McDiarmid's inequality, the following inequalities hold.

$$\begin{aligned} \mathbb{P}(\mathbb{E}[\widehat{A}(g)] - \widehat{A}(g) \geq a) &\leq \exp\left(-\frac{4a^2n}{(4\pi_+ + 1)^2C_\ell^2}\right), \\ \mathbb{P}(\mathbb{E}[\widehat{B}(g)] - \widehat{B}(g) \geq b) &\leq \exp\left(-\frac{4b^2n}{(4\pi_- + 1)^2C_\ell^2}\right), \\ \mathbb{P}(\mathbb{E}[\widehat{C}(g)] - \widehat{C}(g) \geq c) &\leq \exp\left(-\frac{4c^2n}{(4\pi_+ + 1)^2C_\ell^2}\right), \\ \mathbb{P}(\mathbb{E}[\widehat{D}(g)] - \widehat{D}(g) \geq d) &\leq \exp\left(-\frac{4d^2n}{(4\pi_- + 1)^2C_\ell^2}\right). \end{aligned}$$

Furthermore,

$$\begin{aligned} \mathbb{P}(\mathfrak{D}_n^-(g)) &\leq \mathbb{P}(\widehat{A}(g) \leq 0) + \mathbb{P}(\widehat{B}(g) \leq 0) + \mathbb{P}(\widehat{C}(g) \leq 0) + \mathbb{P}(\widehat{D}(g) \leq 0) \\ &\leq \mathbb{P}(\widehat{A}(g) \leq \mathbb{E}[\widehat{A}(g)] - a) + \mathbb{P}(\widehat{B}(g) \leq \mathbb{E}[\widehat{B}(g)] - b) \\ &\quad + \mathbb{P}(\widehat{C}(g) \leq \mathbb{E}[\widehat{C}(g)] - c) + \mathbb{P}(\widehat{D}(g) \leq \mathbb{E}[\widehat{D}(g)] - d) \\ &= \mathbb{P}(\mathbb{E}[\widehat{A}(g)] - \widehat{A}(g) \geq a) + \mathbb{P}(\mathbb{E}[\widehat{B}(g)] - \widehat{B}(g) \geq b) \\ &\quad + \mathbb{P}(\mathbb{E}[\widehat{C}(g)] - \widehat{C}(g) \geq c) + \mathbb{P}(\mathbb{E}[\widehat{D}(g)] - \widehat{D}(g) \geq d) \\ &\leq \exp\left(-\frac{4a^2n}{(4\pi_+ + 1)^2C_\ell^2}\right) + \exp\left(-\frac{4b^2n}{(4\pi_- + 1)^2C_\ell^2}\right) \\ &\quad + \exp\left(-\frac{4c^2n}{(4\pi_+ + 1)^2C_\ell^2}\right) + \exp\left(-\frac{4d^2n}{(4\pi_- + 1)^2C_\ell^2}\right), \end{aligned}$$

which concludes the proof. \square

Then, the proof of Theorem 6 is given.

Proof.

$$\begin{aligned} &\mathbb{E}[\widetilde{R}_{\text{SCD}}(g)] - R(g) \\ &= \mathbb{E}[\widetilde{R}_{\text{SCD}}(g) - \widehat{R}_{\text{SCD}}(g)] \\ &= \int_{\mathcal{D}_n \in \mathfrak{D}_n^+(g)} (\widetilde{R}_{\text{SCD}}(g) - \widehat{R}_{\text{SCD}}(g)) p(\mathcal{D}_n) \, d\mathcal{D}_n + \int_{\mathcal{D}_n \in \mathfrak{D}_n^-(g)} (\widetilde{R}_{\text{SCD}}(g) - \widehat{R}_{\text{SCD}}(g)) p(\mathcal{D}_n) \, d\mathcal{D}_n \\ &= \int_{\mathcal{D}_n \in \mathfrak{D}_n^-(g)} (\widetilde{R}_{\text{SCD}}(g) - \widehat{R}_{\text{SCD}}(g)) p(\mathcal{D}_n) \, d\mathcal{D}_n \geq 0. \end{aligned}$$

In addition,

$$\begin{aligned}
& \mathbb{E}[\tilde{R}_{\text{SCD}}(g)] - R(g) \\
&= \int_{\mathcal{D}_n \in \mathfrak{D}_n^-(g)} (\tilde{R}_{\text{SCD}}(g) - \hat{R}_{\text{SCD}}(g)) p(\mathcal{D}_n) d\mathcal{D}_n \\
&\leq \sup_{\mathcal{D}_n \in \mathfrak{D}_n^-(g)} (\tilde{R}_{\text{SCD}}(g) - \hat{R}_{\text{SCD}}(g)) \int_{\mathcal{D}_n \in \mathfrak{D}_n^-(g)} p(\mathcal{D}_n) d\mathcal{D}_n \\
&= \sup_{\mathcal{D}_n \in \mathfrak{D}_n^-(g)} (\tilde{R}_{\text{SCD}}(g) - \hat{R}_{\text{SCD}}(g)) \mathbb{P}(\mathfrak{D}_n^-(g)) \\
&= \sup_{\mathcal{D}_n \in \mathfrak{D}_n^-(g)} (f(\hat{A}(g)) + f(\hat{B}(g)) + f(\hat{C}(g)) + f(\hat{D}(g)) \\
&\quad - \hat{A}(g) - \hat{B}(g) - \hat{C}(g) - \hat{D}(g)) \mathbb{P}(\mathfrak{D}_n^-(g)) \\
&\leq \sup_{\mathcal{D}_n \in \mathfrak{D}_n^-(g)} (L_f |\hat{A}(g)| + L_f |\hat{B}(g)| + L_f |\hat{C}(g)| + L_f |\hat{D}(g)| \\
&\quad + |\hat{A}(g)| + |\hat{B}(g)| + |\hat{C}(g)| + |\hat{D}(g)|) \mathbb{P}(\mathfrak{D}_n^-(g)) \\
&= \sup_{\mathcal{D}_n \in \mathfrak{D}_n^-(g)} \frac{L_f + 1}{2n} \left\{ \left| \sum_{i=1}^n (2\pi_+(\pi_+ - c_i) + \pi_- - s_i) \ell(g(\mathbf{x}_i), +1) \right| \right. \\
&\quad + \left| \sum_{i=1}^n (2\pi_-(\pi_- - c_i) + \pi_+ - s_i) \ell(g(\mathbf{x}'_i), -1) \right| \\
&\quad + \left| \sum_{i=1}^n (2\pi_+(\pi_+ + c_i) + \pi_- - s_i) \ell(g(\mathbf{x}'_i), +1) \right| \\
&\quad \left. + \left| \sum_{i=1}^n (2\pi_-(\pi_- + c_i) + \pi_+ - s_i) \ell(g(\mathbf{x}_i), -1) \right| \right\} \mathbb{P}(\mathfrak{D}_n^-(g)) \\
&\leq \sup_{\mathcal{D}_n \in \mathfrak{D}_n^-(g)} \frac{L_f + 1}{2n} \left\{ \sum_{i=1}^n |(2\pi_+(\pi_+ - c_i) + \pi_- - s_i) \ell(g(\mathbf{x}_i), +1)| \right. \\
&\quad + \sum_{i=1}^n |(2\pi_-(\pi_- - c_i) + \pi_+ - s_i) \ell(g(\mathbf{x}'_i), -1)| \\
&\quad + \sum_{i=1}^n |(2\pi_+(\pi_+ + c_i) + \pi_- - s_i) \ell(g(\mathbf{x}'_i), +1)| \\
&\quad \left. + \sum_{i=1}^n |(2\pi_-(\pi_- + c_i) + \pi_+ - s_i) \ell(g(\mathbf{x}_i), -1)| \right\} \mathbb{P}(\mathfrak{D}_n^-(g)) \\
&= \sup_{\mathcal{D}_n \in \mathfrak{D}_n^-(g)} \frac{L_f + 1}{2n} \left\{ \sum_{i=1}^n |((2\pi_+(\pi_+ - c_i)) + \pi_- - s_i) \ell(g(\mathbf{x}_i), +1)| \right. \\
&\quad + |((2\pi_-(\pi_- - c_i)) + \pi_+ - s_i) \ell(g(\mathbf{x}'_i), -1)| \\
&\quad + |(2\pi_+(\pi_+ + c_i) + \pi_- - s_i) \ell(g(\mathbf{x}'_i), +1)| \\
&\quad \left. + |(2\pi_-(\pi_- + c_i) + \pi_+ - s_i) \ell(g(\mathbf{x}_i), -1)| \right\} \mathbb{P}(\mathfrak{D}_n^-(g)) \\
&\leq \sup_{\mathcal{D}_n \in \mathfrak{D}_n^-(g)} \frac{(L_f + 1)C_\ell}{2n} \left\{ \sum_{i=1}^n |2\pi_+(\pi_+ - c_i) + \pi_- - s_i| + |2\pi_-(\pi_- - c_i) + \pi_+ - s_i| \right. \\
&\quad \left. + |2\pi_+(\pi_+ + c_i) + \pi_- - s_i| + |2\pi_-(\pi_- + c_i) + \pi_+ - s_i| \right\} \mathbb{P}(\mathfrak{D}_n^-(g)).
\end{aligned}$$

Then, based on the derivation of Eq. 29, the following inequality holds:

$$\begin{aligned} & |2\pi_+(\pi_+ - c_i) + \pi_- - s_i| + |2\pi_-(\pi_- - c_i) + \pi_+ - s_i| \\ & + |2\pi_+(\pi_+ + c_i) + \pi_- - s_i| + |2\pi_-(\pi_- + c_i) + \pi_+ - s_i| \leq 6. \end{aligned}$$

Thus, we have

$$\mathbb{E}[\tilde{R}_{\text{SCD}}(g)] - R(g) \leq 3(L_f + 1)C_\ell\Delta.$$

We now derive the upper bound of $|\tilde{R}_{\text{SCD}}(g) - \mathbb{E}[\tilde{R}_{\text{SCD}}(g)]|$. Let

$$\tilde{R}_{\text{SCD}}(g) = f(\hat{A}(g)) + f(\hat{B}(g)) + f(\hat{C}(g)) + f(\hat{D}(g)),$$

$$\tilde{\tilde{R}}_{\text{SCD}}(g) = f(\hat{\hat{A}}(g)) + f(\hat{\hat{B}}(g)) + f(\hat{\hat{C}}(g)) + f(\hat{\hat{D}}(g))$$

denote the empirical risks when exactly one SconfConfDiff data pair in \mathcal{D}_n is replaced. Then, the following inequality holds.

$$\begin{aligned} & |\tilde{R}_{\text{SCD}}(g) - \tilde{\tilde{R}}_{\text{SCD}}(g)| \\ & = |f(\hat{A}(g)) - f(\hat{\hat{A}}(g)) + f(\hat{B}(g)) - f(\hat{\hat{B}}(g)) \\ & \quad + f(\hat{C}(g)) - f(\hat{\hat{C}}(g)) + f(\hat{D}(g)) - f(\hat{\hat{D}}(g))| \\ & \leq |f(\hat{A}(g)) - f(\hat{\hat{A}}(g))| + |f(\hat{B}(g)) - f(\hat{\hat{B}}(g))| \\ & \quad + |f(\hat{C}(g)) - f(\hat{\hat{C}}(g))| + |f(\hat{D}(g)) - f(\hat{\hat{D}}(g))| \\ & \leq L_f|\hat{A}(g) - \hat{\hat{A}}(g)| + L_f|\hat{B}(g) - \hat{\hat{B}}(g)| + L_f|\hat{C}(g) - \hat{\hat{C}}(g)| + L_f|\hat{D}(g) - \hat{\hat{D}}(g)| \\ & \leq L_f \left\{ \frac{(4\pi_+ + 1)C_\ell}{2n} + \frac{(4\pi_- + 1)C_\ell}{2n} + \frac{(4\pi_+ + 1)C_\ell}{2n} + \frac{(4\pi_- + 1)C_\ell}{2n} \right\} \\ & \leq \frac{6L_fC_\ell}{n}, \end{aligned}$$

where the second inequality is derived based on the Lipschitz continuity of the risk correction function. From this inequality, the change of $\tilde{R}_{\text{SCD}}(g)$ is no more than $6L_fC_\ell/n$. By applying McDiarmid's inequality, the following inequalities hold at least $1 - \delta/2$.

$$\tilde{R}_{\text{SCD}}(g) - \mathbb{E}[\tilde{R}_{\text{SCD}}(g)] \leq 6L_fC_\ell\sqrt{\frac{\log 2/\delta}{2n}},$$

$$\mathbb{E}[\tilde{R}_{\text{SCD}}(g)] - \tilde{R}_{\text{SCD}}(g) \leq 6L_fC_\ell\sqrt{\frac{\log 2/\delta}{2n}}.$$

Therefore, with probability at least $1 - \delta$, we have

$$|\tilde{R}_{\text{SCD}}(g) - \mathbb{E}[\tilde{R}_{\text{SCD}}(g)]| \leq 6L_fC_\ell\sqrt{\frac{\log 2/\delta}{2n}}.$$

Finally, we have

$$\begin{aligned} |\tilde{R}_{\text{SCD}}(g) - R(g)| & = |\tilde{R}_{\text{SCD}}(g) - \mathbb{E}[\tilde{R}_{\text{SCD}}(g)] + \mathbb{E}[\tilde{R}_{\text{SCD}}(g)] - R(g)| \\ & \leq |\tilde{R}_{\text{SCD}}(g) - \mathbb{E}[\tilde{R}_{\text{SCD}}(g)]| + |\mathbb{E}[\tilde{R}_{\text{SCD}}(g)] - R(g)| \\ & = |\tilde{R}_{\text{SCD}}(g) - \mathbb{E}[\tilde{R}_{\text{SCD}}(g)]| + \mathbb{E}[\tilde{R}_{\text{SCD}}(g)] - R(g) \\ & \leq 6L_fC_\ell\sqrt{\frac{\log 2/\delta}{2n}} + 3(L_f + 1)C_\ell\Delta, \end{aligned}$$

with probability at least $1 - \delta$, which concludes the proof. \square

A.6 Proof of Theorem 7

Proof. By combining the probabilistic inequalities established in Theorem 6 and Theorem 4, each of which holds with probability at least $1 - \delta/2$, we obtain the following inequality, which holds with probability at least $1 - \delta$.

$$\begin{aligned}
R(\tilde{g}_{\text{SCD}}) - R(g^*) &= (R(\tilde{g}_{\text{SCD}}) - \tilde{R}_{\text{SCD}}(\tilde{g}_{\text{SCD}})) + (\tilde{R}_{\text{SCD}}(\tilde{g}_{\text{SCD}}) - \tilde{R}_{\text{SCD}}(\hat{g}_{\text{SCD}})) \\
&\quad + (\tilde{R}_{\text{SCD}}(\hat{g}_{\text{SCD}}) - R(\hat{g}_{\text{SCD}})) + (R(\hat{g}_{\text{SCD}}) - R(g^*)) \\
&\leq |R(\tilde{g}_{\text{SCD}}) - \tilde{R}_{\text{SCD}}(\tilde{g}_{\text{SCD}})| + |\tilde{R}_{\text{SCD}}(\hat{g}_{\text{SCD}}) - R(\hat{g}_{\text{SCD}})| \\
&\quad + (R(\hat{g}_{\text{SCD}}) - R(g^*)) \\
&\leq (12L_f + 2\pi_+^2 + 2\pi_-^2 + 5)C_\ell \sqrt{\frac{\log 4/\delta}{2n}} + 6(L_f + 1)C_\ell \Delta + 12L_\ell \mathfrak{R}_n(\mathcal{G})
\end{aligned}$$

The first inequality is deduced because \tilde{g}_{SCD} is the minimizer of $\tilde{R}_{\text{SCD}}(g)$, and the proof is completed. \square

B Analysis of Risk Estimator by Convex Combination

B.1 Estimation Error Bound

We make the same assumptions as in Section 3.4, and let $\hat{g}_{\text{SCD}_{\text{convex}}} = \arg \min_{g \in \mathcal{G}} \hat{R}_{\text{SCD}_{\text{convex}}}(g)$ denote the minimizer of the classification risk in Eq. 5. Then, the following theorem can be derived.

Theorem 8. *For any $\delta > 0$, the following inequality holds with probability at least $1 - \delta$:*

$$\begin{aligned}
&R(\hat{g}_{\text{SCD}_{\text{convex}}}) - R(g^*) \\
&\leq \frac{4\gamma + 8(1 - \gamma)|\pi_+ - \pi_-|}{|\pi_+ - \pi_-|} L_\ell \mathfrak{R}_n(\mathcal{G}) + \frac{2\gamma + 4(1 - \gamma)|\pi_+ - \pi_-|}{|\pi_+ - \pi_-|} C_\ell \sqrt{\frac{\log 4/\delta}{2n}}, \quad (31)
\end{aligned}$$

where $\gamma \in [0, 1]$ is an arbitrary weight.

Then, the proof of Theorem 8 is given. For convenience, we make the following notation:

$$\begin{aligned}
\mathcal{L}_{\text{Sconf}}(g; \mathbf{x}_i, \mathbf{x}'_i) &= \frac{(s(\mathbf{x}, \mathbf{x}') - \pi_-)(\ell(g(\mathbf{x}), +1) + \ell(g(\mathbf{x}'), +1))}{2(\pi_+ - \pi_-)} \\
&\quad + \frac{(\pi_+ - s(\mathbf{x}, \mathbf{x}'))(\ell(g(\mathbf{x}), -1) + \ell(g(\mathbf{x}'), -1))}{2(\pi_+ - \pi_-)},
\end{aligned}$$

$$\begin{aligned}
\mathcal{L}_{\text{CD}}(g; \mathbf{x}_i, \mathbf{x}'_i) &= \frac{(\pi_+ - c_i)\ell(g(\mathbf{x}_i), +1)}{2} + \frac{(\pi_- - c_i)\ell(g(\mathbf{x}'_i), -1)}{2} \\
&\quad + \frac{(\pi_+ + c_i)\ell(g(\mathbf{x}'_i), +1)}{2} + \frac{(\pi_- + c_i)\ell(g(\mathbf{x}_i), -1)}{2}.
\end{aligned}$$

Lemma 8. *The following inequality holds with probability at least $1 - \delta$:*

$$\begin{aligned}
&\sup_{g \in \mathcal{G}} |R(g) - \hat{R}_{\text{SCD}_{\text{convex}}}(g)| \\
&\leq \frac{2\gamma + 4(1 - \gamma)|\pi_+ - \pi_-|}{|\pi_+ - \pi_-|} L_\ell \mathfrak{R}_n(\mathcal{G}) + \frac{\gamma + 2(1 - \gamma)|\pi_+ - \pi_-|}{|\pi_+ - \pi_-|} C_\ell \sqrt{\frac{\log 4/\delta}{2n}}.
\end{aligned}$$

Proof. With probability at least $1 - \delta$, the following inequality holds (cf. Lemma 7 in [14], Lemma 5 in [15]).

$$\begin{aligned}
|R(g) - \widehat{R}_{\text{SCD}_{\text{convex}}}(g)| &= |\gamma(R(g) - \widehat{R}_{\text{Sconf}}(g)) + (1 - \gamma)(R(g) - \widehat{R}_{\text{CD}}(g))| \\
&\leq \gamma |R(g) - \widehat{R}_{\text{Sconf}}(g)| + (1 - \gamma) |R(g) - \widehat{R}_{\text{CD}}(g)| \\
&\leq \frac{2\gamma L_\ell}{|\pi_+ - \pi_-|} \mathfrak{R}_n(\mathcal{G}) + \frac{\gamma C_\ell}{|\pi_+ - \pi_-|} \sqrt{\frac{\log 4/\delta}{2n}} \\
&\quad + 4(1 - \gamma) L_\ell \mathfrak{R}_n(\mathcal{G}) + 2(1 - \gamma) C_\ell \sqrt{\frac{\log 4/\delta}{2n}} \\
&\leq \frac{2\gamma + 4(1 - \gamma)|\pi_+ - \pi_-|}{|\pi_+ - \pi_-|} L_\ell \mathfrak{R}_n(\mathcal{G}) \\
&\quad + \frac{\gamma + 2(1 - \gamma)|\pi_+ - \pi_-|}{|\pi_+ - \pi_-|} C_\ell \sqrt{\frac{\log 4/\delta}{2n}}.
\end{aligned}$$

The second inequality is based on the fact that the probabilistic bounds on the estimation errors of $\widehat{R}_{\text{Sconf}}(g)$ and $\widehat{R}_{\text{CD}}(g)$ each hold with probability at least $1 - \delta/2$. \square

Then, the proof of Theorem 8 is provided as follows.

Proof. With probability at least $1 - \delta$, the following inequality holds.

$$\begin{aligned}
&R(\widehat{g}_{\text{SCD}_{\text{convex}}}) - R(g^*) \\
&= (R(\widehat{g}_{\text{SCD}_{\text{convex}}}) - \widehat{R}(\widehat{g}_{\text{SCD}_{\text{convex}}})) + (\widehat{R}(\widehat{g}_{\text{SCD}_{\text{convex}}}) - \widehat{R}_{\text{SCD}_{\text{convex}}}(g^*)) \\
&\quad + (\widehat{R}_{\text{SCD}_{\text{convex}}}(g^*) - R(g^*)) \\
&\leq (R(\widehat{g}_{\text{SCD}_{\text{convex}}}) - \widehat{R}(\widehat{g}_{\text{SCD}_{\text{convex}}})) + (\widehat{R}_{\text{SCD}_{\text{convex}}}(g^*) - R(g^*)) \\
&\leq |R(\widehat{g}_{\text{SCD}_{\text{convex}}}) - \widehat{R}(\widehat{g}_{\text{SCD}_{\text{convex}}})| + |\widehat{R}_{\text{SCD}_{\text{convex}}}(g^*) - R(g^*)| \\
&\leq 2 \sup_{g \in \mathcal{G}} |R(g) - \widehat{R}_{\text{SCD}_{\text{convex}}}(g)| \\
&\leq \frac{4\gamma + 8(1 - \gamma)|\pi_+ - \pi_-|}{|\pi_+ - \pi_-|} L_\ell \mathfrak{R}_n(\mathcal{G}) + \frac{2\gamma + 4(1 - \gamma)|\pi_+ - \pi_-|}{|\pi_+ - \pi_-|} C_\ell \sqrt{\frac{\log 4/\delta}{2n}}.
\end{aligned}$$

The first inequality is deduced because $\widehat{g}_{\text{SCD}_{\text{convex}}}$ is the minimizer of $\widehat{R}_{\text{SCD}_{\text{convex}}}(g)$. \square

B.2 Robustness of The Risk Estimator

In the previous sections, it was assumed that the ground-truth similarity-confidence and the ground-truth confidence-difference of each unlabeled data pair are accessible. However, these assumptions are not necessarily satisfied in real-world scenarios. In this section, we analyze the influence of noisy similarity-confidence and noisy confidence-difference on the learning procedure. While the robustness of convex combinations has not been analyzed under the inaccurate class prior probability in the empirical risk of Sconf Learning, and such analysis tends to be intractable, we limit our analysis here to the impact of label noise.

Let $\bar{R}_{\text{SCD}_{\text{convex}}}$ denote the empirical risk calculated from $\bar{\mathcal{D}}_n = \{(\mathbf{x}_i, \mathbf{x}'_i), \bar{s}_i, \bar{c}_i\}_{i=1}^n$, and let $\bar{g}_{\text{SCD}_{\text{convex}}} = \arg \min_{g \in \mathcal{G}} \bar{R}_{\text{SCD}_{\text{convex}}}(g)$ denote the minimizer of $\bar{R}_{\text{SCD}_{\text{convex}}}$. Then the following theorem gives an estimation error bound:

Theorem 9. *Based on the assumption above, for any $\delta > 0$, the following inequality holds with probability at least $1 - \delta$:*

$$\begin{aligned}
&R(\bar{g}_{\text{SCD}_{\text{convex}}}) - R(g^*) \\
&\leq \frac{8\gamma + 16(1 - \gamma)|\pi_+ - \pi_-|}{|\pi_+ - \pi_-|} L_\ell \mathfrak{R}_n(\mathcal{G}) + \frac{4\gamma + 8(1 - \gamma)|\pi_+ - \pi_-|}{|\pi_+ - \pi_-|} C_\ell \sqrt{\frac{\log 4/\delta}{2n}} \\
&\quad + \frac{2\gamma C_\ell \sum_{i=1}^n |\bar{s}_i - s_i|}{n|\pi_+ - \pi_-|} + \frac{4(1 - \gamma) C_\ell \sum_{i=1}^n |\bar{c}_i - c_i|}{n}.
\end{aligned} \tag{32}$$

Then, the proof of Theorem 9 is given (cf. Theorem 6 in [14], Theorem 4 in [15]).

Proof. The following inequality holds:

$$\begin{aligned} |\bar{R}_{\text{SCD}_{\text{convex}}}(g) - \hat{R}_{\text{SCD}_{\text{convex}}}(g)| &= |\gamma(\bar{R}_{\text{Sconf}}(g) - \hat{R}_{\text{Sconf}}(g)) + (1 - \gamma)(\bar{R}_{\text{CD}}(g) - \hat{R}_{\text{CD}}(g))| \\ &\leq \gamma|\bar{R}_{\text{Sconf}}(g) - \hat{R}_{\text{Sconf}}(g)| + (1 - \gamma)|\bar{R}_{\text{CD}}(g) - \hat{R}_{\text{CD}}(g)| \\ &\leq \frac{\gamma C_\ell \sum_{i=1}^n |\bar{s}_i - s_i|}{n|\pi_+ - \pi_-|} + \frac{2(1 - \gamma)C_\ell \sum_{i=1}^n |\bar{c}_i - c_i|}{n}. \end{aligned}$$

Thus, with probability at least $1 - \delta$, the following inequality can be derived.

$$\begin{aligned} &R(\bar{g}_{\text{SCD}_{\text{convex}}}) - R(g^*) \\ &= (R(\bar{g}_{\text{SCD}_{\text{convex}}}) - \hat{R}_{\text{SCD}_{\text{convex}}}(\bar{g}_{\text{SCD}_{\text{convex}}})) \\ &\quad + (\hat{R}_{\text{SCD}_{\text{convex}}}(\bar{g}_{\text{SCD}_{\text{convex}}}) - \bar{R}_{\text{SCD}_{\text{convex}}}(\bar{g}_{\text{SCD}_{\text{convex}}})) \\ &\quad + (\bar{R}_{\text{SCD}_{\text{convex}}}(\bar{g}_{\text{SCD}_{\text{convex}}}) - \bar{R}_{\text{SCD}_{\text{convex}}}(\hat{g}_{\text{SCD}_{\text{convex}}})) \\ &\quad + (\bar{R}_{\text{SCD}_{\text{convex}}}(\hat{g}_{\text{SCD}_{\text{convex}}}) - \hat{R}_{\text{SCD}_{\text{convex}}}(\hat{g}_{\text{SCD}_{\text{convex}}})) \\ &\quad + (\hat{R}_{\text{SCD}_{\text{convex}}}(\hat{g}_{\text{SCD}_{\text{convex}}}) - R_{\text{SCD}_{\text{convex}}}(\hat{g}_{\text{SCD}_{\text{convex}}})) \\ &\quad + (R_{\text{SCD}_{\text{convex}}}(\hat{g}_{\text{SCD}_{\text{convex}}}) - R(g^*)) \\ &\leq 2\sup_{g \in \mathcal{G}} |R(g) - \hat{R}_{\text{SCD}_{\text{convex}}}(g)| + 2\sup_{g \in \mathcal{G}} |\bar{R}_{\text{SCD}_{\text{convex}}}(g) - \hat{R}_{\text{SCD}_{\text{convex}}}(g)| \\ &\quad + (R_{\text{SCD}_{\text{convex}}}(\hat{g}_{\text{SCD}_{\text{convex}}}) - R(g^*)) \\ &\leq 4\sup_{g \in \mathcal{G}} |R(g) - \hat{R}_{\text{SCD}_{\text{convex}}}(g)| + 2\sup_{g \in \mathcal{G}} |\bar{R}_{\text{SCD}_{\text{convex}}}(g) - \hat{R}_{\text{SCD}_{\text{convex}}}(g)| \\ &\leq \frac{8\gamma + 16(1 - \gamma)|\pi_+ - \pi_-|}{|\pi_+ - \pi_-|} L_\ell \mathfrak{R}_n(\mathcal{G}) + \frac{4\gamma + 8(1 - \gamma)|\pi_+ - \pi_-|}{|\pi_+ - \pi_-|} C_\ell \sqrt{\frac{\log 4/\delta}{2n}} \\ &\quad + \frac{2\gamma C_\ell \sum_{i=1}^n |\bar{s}_i - s_i|}{n|\pi_+ - \pi_-|} + \frac{4(1 - \gamma)C_\ell \sum_{i=1}^n |\bar{c}_i - c_i|}{n}. \end{aligned}$$

The second and third inequalities are based on the proof of Theorem 8. \square

B.3 The Correction of The Risk Estimator

Similarly to Section 3.6, the risk estimator in Eq. (5) may take negative values and therefore does not satisfy the non-negative property of loss functions. To overcome this difficulty, risk correction approach with risk correction functions is proposed, such as the rectified linear unit (ReLU) function $f(z) = \max(0, z)$ and the absolute value function $f(z) = |z|$. In this way, the corrected risk estimator for SconfConfDiff Classification by convex combination can be expressed as follows:

$$\tilde{R}_{\text{SCD}_{\text{convex}}}(g) = \gamma \tilde{R}_{\text{Sconf}}(g) + (1 - \gamma) \tilde{R}_{\text{CD}}(g), \quad (33)$$

where

$$\begin{aligned} \tilde{R}_{\text{Sconf}}(g) &= f\left(\sum_{i=1}^n \frac{(s_i - \pi_-)(\ell(g(\mathbf{x}_i), +1) + \ell(g(\mathbf{x}'_i), +1))}{2n(\pi_+ - \pi_-)}\right) \\ &\quad + f\left(\sum_{i=1}^n \frac{(\pi_+ - s_i)(\ell(g(\mathbf{x}_i), -1) + \ell(g(\mathbf{x}'_i), -1))}{2n(\pi_+ - \pi_-)}\right), \\ \tilde{R}_{\text{CD}}(g) &= \frac{1}{2n} \left\{ f\left(\sum_{i=1}^n (\pi_+ - c_i) \ell(g(\mathbf{x}_i), +1)\right) + f\left(\sum_{i=1}^n (\pi_- - c_i) \ell(g(\mathbf{x}'_i), -1)\right) \right. \\ &\quad \left. + f\left(\sum_{i=1}^n (\pi_+ + c_i) \ell(g(\mathbf{x}'_i), +1)\right) + f\left(\sum_{i=1}^n (\pi_- + c_i) \ell(g(\mathbf{x}_i), -1)\right) \right\}. \end{aligned}$$

Here, it is assumed that

$$\begin{aligned} \mathbb{E} \left[\sum_{i=1}^n \frac{(s_i - \pi_-)(\ell(g(\mathbf{x}_i), +1) + \ell(g(\mathbf{x}'_i), +1))}{2n(\pi_+ - \pi_-)} \right] &\geq \alpha, \\ \mathbb{E} \left[\sum_{i=1}^n \frac{(\pi_+ - s_i)(\ell(g(\mathbf{x}_i), -1) + \ell(g(\mathbf{x}'_i), -1))}{2n(\pi_+ - \pi_-)} \right] &\geq \beta, \\ \mathbb{E} \left[\sum_{i=1}^n \frac{(\pi_+ - c_i)\ell(g(\mathbf{x}_i), +1)}{2n} \right] &\geq a, \quad \mathbb{E} \left[\sum_{i=1}^n \frac{(\pi_- - c_i)\ell(g(\mathbf{x}'_i), -1)}{2n} \right] \geq b, \\ \mathbb{E} \left[\sum_{i=1}^n \frac{(\pi_+ + c_i)\ell(g(\mathbf{x}'_i), +1)}{2n} \right] &\geq c, \quad \mathbb{E} \left[\sum_{i=1}^n \frac{(\pi_- + c_i)\ell(g(\mathbf{x}_i), -1)}{2n} \right] \geq d. \end{aligned}$$

Let $\tilde{g}_{\text{SCD}_{\text{convex}}} = \arg \min_{g \in \mathcal{G}} \tilde{R}_{\text{SCD}_{\text{convex}}}(g)$ denote the minimizer of the classification risk in Eq. (33).

Theorem 10. *Based on the assumption above, for any $\delta > 0$, the following inequality holds with probability at least $1 - \delta$:*

$$\begin{aligned} &R(\tilde{g}_{\text{SCD}_{\text{convex}}}) - R(g^*) \\ &\leq \frac{2\gamma + 4(1 - \gamma)|\pi_+ - \pi_-|}{|\pi_+ - \pi_-|} (L_f + 1) C_\ell \sqrt{\frac{\log 8/\delta}{2n}} \\ &\quad + \frac{2\gamma \Delta_{\text{Sconf}} + 4(1 - \gamma) \Delta_{\text{CD}} |\pi_+ - \pi_-|}{|\pi_+ - \pi_-|} (L_f + 1) C_\ell + \frac{4\gamma + 8(1 - \gamma)|\pi_+ - \pi_-|}{|\pi_+ - \pi_-|} L_\ell \mathfrak{R}_n(\mathcal{G}), \end{aligned} \tag{34}$$

where

$$\begin{aligned} \Delta_{\text{Sconf}} &= \exp\left(-\frac{(\pi_+ - \pi_-)^2 n}{2C_\ell^2}\right) (\exp(\alpha^2) + \exp(\beta^2)), \\ \Delta_{\text{CD}} &= \exp\left(-\frac{2a^2 n}{C_\ell^2}\right) + \exp\left(-\frac{2b^2 n}{C_\ell^2}\right) + \exp\left(-\frac{2c^2 n}{C_\ell^2}\right) + \exp\left(-\frac{2d^2 n}{C_\ell^2}\right). \end{aligned}$$

Then, the proof of Theorem 10 is given (cf. Theorem 7 in [14], Theorem 5 in [15]).

Proof. The following inequality holds with the probability at least $1 - \delta/2$.

$$\begin{aligned} &|\tilde{R}_{\text{SCD}_{\text{convex}}}(g) - R(g)| \\ &= |\gamma(\tilde{R}_{\text{Sconf}}(g) - R(g)) + (1 - \gamma)(\tilde{R}_{\text{CD}}(g) - R(g))| \\ &\leq \gamma |\tilde{R}_{\text{Sconf}}(g) - R(g)| + (1 - \gamma) |\tilde{R}_{\text{CD}}(g) - R(g)| \\ &\leq \gamma \left(\frac{L_f C_\ell}{|\pi_+ - \pi_-|} \sqrt{\frac{\log 8/\delta}{2n}} + \frac{(L_f + 1) C_\ell}{|\pi_+ - \pi_-|} \Delta_{\text{Sconf}} \right) \\ &\quad + (1 - \gamma) \left(2C_\ell L_f \sqrt{\frac{\log 8/\delta}{2n}} + 2(L_f + 1) C_\ell \Delta_{\text{CD}} \right) \\ &= \frac{\gamma L_f + 2(1 - \gamma) L_f |\pi_+ - \pi_-|}{|\pi_+ - \pi_-|} C_\ell \sqrt{\frac{\log 8/\delta}{2n}} + \frac{\gamma \Delta_{\text{Sconf}} + 2(1 - \gamma) \Delta_{\text{CD}}}{|\pi_+ - \pi_-|} (L_f + 1) C_\ell. \end{aligned} \tag{35}$$

The second inequality is based on the fact that the probabilistic bounds on the estimation errors of $\tilde{R}_{\text{Sconf}}(g)$ and $\tilde{R}_{\text{CD}}(g)$ each hold with probability at least $1 - \delta/2$.

Therefore, if the probabilistic bounds in Eq. (31) and Eq. (35) respectively hold with probability at least $1 - \delta/2$, then the following inequality holds with probability at least $1 - \delta$.

$$\begin{aligned}
& R(\tilde{g}_{\text{SCD}_{\text{convex}}}) - R(g^*) \\
&= (R(\tilde{g}_{\text{SCD}_{\text{convex}}}) - \tilde{R}_{\text{SCD}_{\text{convex}}}(\tilde{g}_{\text{SCD}_{\text{convex}}})) \\
&\quad + (\tilde{R}_{\text{SCD}_{\text{convex}}}(\tilde{g}_{\text{SCD}_{\text{convex}}}) - \tilde{R}_{\text{SCD}_{\text{convex}}}(\hat{g}_{\text{SCD}_{\text{convex}}})) \\
&\quad + (\tilde{R}_{\text{SCD}_{\text{convex}}}(\hat{g}_{\text{SCD}_{\text{convex}}}) - R(\hat{g}_{\text{SCD}_{\text{convex}}})) + (R(\hat{g}_{\text{SCD}_{\text{convex}}}) - R(g^*)) \\
&\leq |R(\tilde{g}_{\text{SCD}_{\text{convex}}}) - \tilde{R}_{\text{SCD}_{\text{convex}}}(\tilde{g}_{\text{SCD}_{\text{convex}}})| + |\tilde{R}_{\text{SCD}_{\text{convex}}}(\hat{g}_{\text{SCD}_{\text{convex}}}) - R(\hat{g}_{\text{SCD}_{\text{convex}}})| \\
&\quad + (R(\hat{g}_{\text{SCD}_{\text{convex}}}) - R(g^*)) \\
&\leq \frac{2\gamma + 4(1-\gamma)|\pi_+ - \pi_-|}{|\pi_+ - \pi_-|} (L_f + 1) C_\ell \sqrt{\frac{\log 8/\delta}{2n}} \\
&\quad + \frac{2\gamma\Delta_{\text{Sconf}} + 4(1-\gamma)\Delta_{\text{CD}}|\pi_+ - \pi_-|}{|\pi_+ - \pi_-|} (L_f + 1) C_\ell + \frac{4\gamma + 8(1-\gamma)|\pi_+ - \pi_-|}{|\pi_+ - \pi_-|} L_\ell \mathfrak{R}_n(\mathcal{G}).
\end{aligned}$$

The first inequality is deduced because $\tilde{g}_{\text{SCD}_{\text{convex}}}$ is the minimizer of $\tilde{R}_{\text{SCD}_{\text{convex}}}(g)$. \square

C Limitations and Potential Negative Social Impacts

C.1 Limitations

This study focuses on binary classification problems and is not readily extendable to multi-class classification. To handle multi-class tasks, both similarity-confidence and confidence-difference must be redefined to accommodate multiclass settings. Furthermore, while this work utilizes two weak supervision: similarity-confidence and confidence-difference, it is important future work to explore a unified learning framework that can incorporate a broader variety of weak labels. Our current formulation assumes that each data pair is annotated with both similarity-confidence and confidence-difference. However, the proposed method does not simply extend to cases where either label is missing. Developing a robust learning framework for such incomplete settings is an important direction for future work. This paper derives two methods, SconfConfDiff-Convex Classification and SconfConfDiff Classification, but at this stage, there is no clear criterion to determine which method is more appropriate depending on the situation. For practical implementation in the future, it is necessary to clarify the conditions under which each method should be applied and the differences in their effectiveness, and to establish guidelines for selecting the appropriate method.

C.2 Potential Negative Social Impacts

The proposed method improves model accuracy by effectively integrating multiple sources of information. However, this enhancement may raise privacy concerns, as combining such information could potentially enable the inference of sensitive attributes. This reflects an inherent trade-off between performance gains and privacy risks. We acknowledge this tension and emphasize the importance of applying our method in contexts where appropriate safeguards and ethical considerations are in place.

D Additional Information about Experiments

In this section, the details of experimental datasets and hyperparameters are provided. We implemented the proposed method based on the original code for ConfDiff Classification which is available at <https://github.com/wwangwitsel/ConfDiff>.

D.1 Generation of Similarity-Confidence and Confidence-Difference

Similarity-confidence and confidence-difference are given by labelers in real-world applications, while it was generated synthetically in this paper to facilitate comprehensive experimental analysis. We firstly trained a probabilistic classifier via logistic regression with ordinarily labeled data and the same neural network architecture. Then, we sampled unlabeled data in pairs at random, and generated the class posterior probabilities by inputting them into the probabilistic classifier. After

Table 5: Characteristics of experimental datasets.

Dataset	# Train	# Test	# Features	# Class Labels	Model
MNIST	60,000	10,000	784	10	MLP
Kuzushiji	60,000	10,000	784	10	MLP
Fashion	60,000	10,000	784	10	MLP
CIFAR-10	50,000	10,000	3,072	10	ResNet-34
Optdigits	4,495	1,125	62	10	MLP
Pendigits	8,793	2,199	16	10	MLP
Letter	16,000	4,000	16	10	MLP
PMU-UD	4,144	1,036	784	26	MLP

that, we generated similarity-confidence and confidence-difference for each pair of sampled data according to the definition in Section 2.2 and Section 2.3.

D.2 Details of Experimental Datasets

The detailed statistics and corresponding model architectures are summarized in Table 5. The basic information of datasets, sources and data split details are elaborated as follows.

- MNIST [19]: a grayscale handwritten digit classification dataset consisting of 60,000 training samples and 10,000 test samples. The original feature dimension is 28×28 , and the label space comprises digits from 0 to 9. To formulate a binary classification task, we treated even digits as positive class and odd digits as negative class. We sampled 15,000 unlabeled data pairs from the training set for use in our experiments. The dataset is available at <http://yann.lecun.com/exdb/mnist/>.
- Kuzushiji-MNIST [20]: a grayscale handwritten Japanese character classification dataset, consisting of 60,000 training samples and 10,000 test samples. The original feature dimension is 28×28 , and the label space is ‘o’, ‘su’, ‘na’, ‘ma’, ‘re’, ‘ki’, ‘tsu’, ‘ha’, ‘ya’, ‘wo’. To formulate a binary classification task, we assigned the characters ‘o’, ‘su’, ‘na’, ‘ma’, ‘re’ to the positive class and ‘ki’, ‘tsu’, ‘ha’, ‘ya’, ‘wo’ to the negative class. We sampled 15,000 unlabeled data pairs from the training set for use in our experiments. The dataset is available at <https://github.com/rois-codh/kmnist>.
- Fashion-MNIST [21]: a grayscale image dataset for fashion item classification, consisting of 60,000 training samples and 10,000 test samples. The original feature dimension is 28×28 , and the label space is ‘T-shirt’, ‘trouser’, ‘pullover’, ‘dress’, ‘sandal’, ‘coat’, ‘shirt’, ‘sneaker’, ‘bag’, ‘ankle boot’. To formulate a binary classification task, we assigned ‘T-shirt’, ‘pullover’, ‘coat’, ‘shirt’, ‘bag’ to the positive class and ‘trouser’, ‘dress’, ‘sandal’, ‘sneaker’, ‘ankle boot’ to the negative class. We sampled 15,000 unlabeled data pairs from the training set for use in our experiments. The dataset is available at <https://github.com/zalando-research/fashion-mnist>.
- CIFAR-10 [22]: a color image dataset for object classification, consisting of 50,000 training samples and 10,000 test samples. The original feature dimension is $32 \times 32 \times 3$, and the label space is ‘airplane’, ‘bird’, ‘automobile’, ‘cat’, ‘deer’, ‘dog’, ‘frog’, ‘horse’, ‘ship’, ‘truck’. To formulate a binary classification task, we assigned ‘bird’, ‘deer’, ‘dog’, ‘frog’, ‘cat’, ‘horse’ to the positive class and ‘airplane’, ‘automobile’, ‘ship’, ‘truck’ to the negative class. We sampled 10,000 unlabeled data pairs from the training set for use in our experiments. The dataset is available at <https://www.cs.toronto.edu/~kriz/cifar.html>.
- Optdigits [23], Pendigits [24], and PMU-UD [26] are UCI datasets for handwritten digit recognition. The train-test splits are summarized in Table 5. The feature dimensions are 62, 16, and 784, respectively. For PMU-UD, which consists of image data, we resized each image to 28×28 grayscale before training. The label space consists of digits from 0 to 9. To formulate a binary classification task, we treated even digits as the positive class and odd digits as the negative class. We sampled 1,200, 2,500, and 1,000 unlabeled data pairs from the training sets of Optdigits, Pendigits, and PMU-UD, respectively. The dataset is available at
 - <https://archive.ics.uci.edu/dataset/80/optical+recognition+of+handwritten+digits>
 - <https://archive.ics.uci.edu/dataset/81/pen+based+recognition+of+handwritten+digits>
 - <https://archive.ics.uci.edu/dataset/469/pmu+ud>

- Letter [25] is a UCI dataset for letter recognition, consisting of 16,000 training samples and 4,000 test samples. The feature dimension is 16, and the label space consists of 26 capital letters in the English alphabet. To formulate a binary classification task, we assigned the first 13 characters to the positive class and the remaining 13 characters to the negative class. We sampled 4,000 unlabeled data pairs from the training set for use in our experiments. The dataset is available at <https://archive.ics.uci.edu/dataset/59/letter+recognition>.

D.3 Details of Hyperparameters

The number of training epoches was set to 200 and we obtained the testing accuracy by averaging the results in the last 10 epoches. All the methods were implemented in PyTorch [30]. We used the Adam optimizer [31]. To ensure fair comparisons, we set the same hyperparameter values for all the compared approaches.

For MNIST, Kuzushiji-MNIST, and Fashion-MNIST, we set the learning rate to $1e-3$, weight decay to $1e-5$, and the batch size to 256 pairs. For training the probabilistic classifier to generate confidence, we used a batch size of 256 and trained for 10 epochs.

For CIFAR-10, we set the learning rate to $5e-4$, weight decay to $1e-5$, and the batch size to 128 pairs. For training the probabilistic classifier to generate confidence, we used a batch size of 128 and trained for 10 epochs.

For UCI datasets, we set the learning rate to $1e-3$, weight decay to $1e-5$, and the batch size to 128 pairs. For training the probabilistic classifier to generate confidence, we used a batch size of 128 and trained for 10 epochs.

D.4 Computational Resources

The experiments were conducted on a machine with the following specifications:

- **CPU:** Intel(R) Xeon(R) Gold 6312U (24 cores, 48 threads, 2.40 GHz)
- **RAM:** 1.0 TB
- **GPU:** NVIDIA RTX A6000 (48 GB VRAM)
- **Storage:** 1 TB SSD
- **OS:** Rocky Linux 9.2
- **Software:** Python 3.12.2, numpy 1.26.4, torch 2.3.0, torchvision 0.18.0, CUDA 11.8

E Additional Results of Experiments

In this section, we provide the details of the experimental results.

Table 6: Overall classification accuracy (mean \pm std) of each method on benchmark datasets with $\pi_+ = 0.2$, where the best performance (excluding Supervised) is shown in bold.

Method	MNIST	Kuzushiji	Fashion	CIFAR-10
SconfConfDiff-Unbiased	0.894 \pm 0.043	0.706 \pm 0.016	0.851 \pm 0.085	0.865 \pm 0.006
SconfConfDiff-ReLU	0.975 \pm 0.002	0.890 \pm 0.010	0.965 \pm 0.002	0.871 \pm 0.012
SconfConfDiff-ABS	0.978 \pm 0.002	0.906 \pm 0.002	0.969 \pm 0.003	0.884 \pm 0.006
ConfDiff-Unbiased	0.805 \pm 0.054	0.655 \pm 0.035	0.859 \pm 0.061	0.782 \pm 0.024
Convex(0.2)-Unbiased	0.837 \pm 0.094	0.687 \pm 0.064	0.850 \pm 0.062	0.807 \pm 0.009
Convex(0.5)-Unbiased	0.933 \pm 0.007	0.833 \pm 0.026	0.886 \pm 0.021	0.830 \pm 0.025
Convex(0.8)-Unbiased	0.858 \pm 0.079	0.732 \pm 0.074	0.846 \pm 0.056	0.806 \pm 0.021
Sconf-Unbiased	0.830 \pm 0.050	0.706 \pm 0.044	0.862 \pm 0.078	0.781 \pm 0.014
ConfDiff-ReLU	0.967 \pm 0.005	0.861 \pm 0.014	0.962 \pm 0.003	0.854 \pm 0.011
Convex($\gamma = 0.2$)-ReLU	0.569 \pm 0.189	0.473 \pm 0.105	0.800 \pm 0.122	0.813 \pm 0.019
Convex($\gamma = 0.5$)-ReLU	0.360 \pm 0.121	0.319 \pm 0.099	0.843 \pm 0.097	0.676 \pm 0.075
Convex($\gamma = 0.8$)-ReLU	0.309 \pm 0.096	0.400 \pm 0.192	0.644 \pm 0.294	0.787 \pm 0.021
Sconf-ReLU	0.959 \pm 0.006	0.845 \pm 0.019	0.946 \pm 0.008	0.838 \pm 0.010
ConfDiff-ABS	0.975 \pm 0.001	0.898 \pm 0.006	0.967 \pm 0.001	0.868 \pm 0.007
Convex($\gamma = 0.2$)-ABS	0.975 \pm 0.003	0.904 \pm 0.007	0.967 \pm 0.002	0.870 \pm 0.005
Convex($\gamma = 0.5$)-ABS	0.976 \pm 0.004	0.903 \pm 0.006	0.965 \pm 0.002	0.869 \pm 0.006
Convex($\gamma = 0.8$)-ABS	0.972 \pm 0.003	0.901 \pm 0.005	0.962 \pm 0.004	0.870 \pm 0.008
Sconf-ABS	0.960 \pm 0.004	0.881 \pm 0.006	0.955 \pm 0.006	0.818 \pm 0.022
Supervised	0.990 \pm 0.000	0.936 \pm 0.003	0.979 \pm 0.002	0.895 \pm 0.003

Table 7: Overall classification accuracy (mean \pm std) of each method on UCI datasets with $\pi_+ = 0.2$, where the best performance (excluding Supervised) is shown in bold.

Method	Optdigits	Pendigits	Letter	PMU-UD
SconfConfDiff-Unbiased	0.917 \pm 0.067	0.954 \pm 0.041	0.746 \pm 0.044	0.841 \pm 0.058
SconfConfDiff-ReLU	0.955 \pm 0.023	0.987 \pm 0.003	0.934 \pm 0.007	0.966 \pm 0.007
SconfConfDiff-ABS	0.969 \pm 0.005	0.991 \pm 0.002	0.951 \pm 0.004	0.975 \pm 0.005
ConfDiff-Unbiased	0.883 \pm 0.053	0.940 \pm 0.050	0.765 \pm 0.051	0.822 \pm 0.057
Convex(0.2)-Unbiased	0.949 \pm 0.015	0.963 \pm 0.028	0.736 \pm 0.099	0.867 \pm 0.062
Convex(0.5)-Unbiased	0.952 \pm 0.015	0.971 \pm 0.008	0.736 \pm 0.100	0.918 \pm 0.047
Convex(0.8)-Unbiased	0.884 \pm 0.076	0.938 \pm 0.066	0.781 \pm 0.027	0.857 \pm 0.070
Sconf-Unbiased	0.874 \pm 0.056	0.931 \pm 0.052	0.754 \pm 0.027	0.853 \pm 0.052
ConfDiff-ReLU	0.958 \pm 0.011	0.982 \pm 0.004	0.930 \pm 0.005	0.977 \pm 0.010
Convex($\gamma = 0.2$)-ReLU	0.723 \pm 0.069	0.982 \pm 0.004	0.890 \pm 0.015	0.776 \pm 0.188
Convex($\gamma = 0.5$)-ReLU	0.605 \pm 0.356	0.959 \pm 0.041	0.853 \pm 0.019	0.242 \pm 0.080
Convex($\gamma = 0.8$)-ReLU	0.688 \pm 0.321	0.945 \pm 0.053	0.838 \pm 0.047	0.475 \pm 0.306
Sconf-ReLU	0.931 \pm 0.016	0.968 \pm 0.011	0.897 \pm 0.007	0.900 \pm 0.053
ConfDiff-ABS	0.964 \pm 0.010	0.988 \pm 0.005	0.945 \pm 0.004	0.978 \pm 0.008
Convex($\gamma = 0.2$)-ABS	0.969 \pm 0.009	0.987 \pm 0.004	0.947 \pm 0.005	0.979 \pm 0.006
Convex($\gamma = 0.5$)-ABS	0.969 \pm 0.005	0.987 \pm 0.004	0.946 \pm 0.004	0.979 \pm 0.008
Convex($\gamma = 0.8$)-ABS	0.966 \pm 0.006	0.986 \pm 0.004	0.941 \pm 0.004	0.976 \pm 0.004
Sconf-ABS	0.944 \pm 0.014	0.978 \pm 0.006	0.915 \pm 0.006	0.954 \pm 0.010
Supervised	0.989 \pm 0.003	0.997 \pm 0.001	0.978 \pm 0.004	0.994 \pm 0.003

Table 8: Overall classification accuracy (mean \pm std) of each method on benchmark datasets with $\pi_+ = 0.5$, where the best performance (excluding Supervised) is shown in bold.

Method	MNIST	Kuzushiji	Fashion	CIFAR-10
SconfConfDiff-Unbiased	0.977 \pm 0.004	0.901 \pm 0.005	0.963 \pm 0.002	0.837 \pm 0.004
SconfConfDiff-ReLU	0.977 \pm 0.004	0.901 \pm 0.005	0.963 \pm 0.002	0.837 \pm 0.004
SconfConfDiff-ABS	0.977 \pm 0.004	0.901 \pm 0.005	0.963 \pm 0.002	0.837 \pm 0.004
ConfDiff-Unbiased	0.931 \pm 0.030	0.795 \pm 0.041	0.867 \pm 0.090	0.738 \pm 0.019
ConfDiff-ReLU	0.946 \pm 0.008	0.805 \pm 0.012	0.960 \pm 0.002	0.837 \pm 0.003
ConfDiff-ABS	0.965 \pm 0.001	0.866 \pm 0.004	0.968 \pm 0.001	0.842 \pm 0.002
Supervised	0.987 \pm 0.001	0.928 \pm 0.002	0.976 \pm 0.001	0.876 \pm 0.003

Table 9: Overall classification accuracy (mean \pm std) of each method on benchmark datasets with $\pi_+ = 0.8$, where the best performance (excluding Supervised) is shown in bold.

Method	MNIST	Kuzushiji	Fashion	CIFAR-10
SconfConfDiff-Unbiased	0.801 \pm 0.064	0.796 \pm 0.047	0.854 \pm 0.071	0.872 \pm 0.008
SconfConfDiff-ReLU	0.975 \pm 0.003	0.887 \pm 0.012	0.969 \pm 0.003	0.850 \pm 0.009
SconfConfDiff-ABS	0.985 \pm 0.002	0.920 \pm 0.004	0.976 \pm 0.001	0.858 \pm 0.061
ConfDiff-Unbiased	0.778 \pm 0.019	0.719 \pm 0.083	0.867 \pm 0.031	0.793 \pm 0.012
Convex(0.2)-Unbiased	0.834 \pm 0.080	0.849 \pm 0.036	0.832 \pm 0.031	0.813 \pm 0.014
Convex(0.5)-Unbiased	0.942 \pm 0.024	0.829 \pm 0.038	0.879 \pm 0.064	0.848 \pm 0.031
Convex(0.8)-Unbiased	0.826 \pm 0.086	0.774 \pm 0.063	0.874 \pm 0.055	0.815 \pm 0.016
Sconf-Unbiased	0.804 \pm 0.051	0.766 \pm 0.038	0.867 \pm 0.101	0.796 \pm 0.017
ConfDiff-ReLU	0.972 \pm 0.003	0.879 \pm 0.006	0.970 \pm 0.001	0.854 \pm 0.003
Convex($\gamma = 0.2$)-ReLU	0.739 \pm 0.257	0.455 \pm 0.132	0.916 \pm 0.028	0.795 \pm 0.032
Convex($\gamma = 0.5$)-ReLU	0.397 \pm 0.147	0.266 \pm 0.064	0.802 \pm 0.135	0.697 \pm 0.030
Convex($\gamma = 0.8$)-ReLU	0.558 \pm 0.277	0.299 \pm 0.051	0.857 \pm 0.111	0.795 \pm 0.028
Sconf-ReLU	0.957 \pm 0.019	0.846 \pm 0.014	0.950 \pm 0.010	0.836 \pm 0.009
ConfDiff-ABS	0.983 \pm 0.001	0.916 \pm 0.005	0.973 \pm 0.001	0.860 \pm 0.007
Convex($\gamma = 0.2$)-ABS	0.983 \pm 0.001	0.918 \pm 0.004	0.973 \pm 0.001	0.880 \pm 0.005
Convex($\gamma = 0.5$)-ABS	0.983 \pm 0.001	0.917 \pm 0.005	0.971 \pm 0.001	0.878 \pm 0.008
Convex($\gamma = 0.8$)-ABS	0.982 \pm 0.003	0.914 \pm 0.005	0.971 \pm 0.002	0.874 \pm 0.007
Sconf-ABS	0.973 \pm 0.001	0.889 \pm 0.004	0.966 \pm 0.003	0.839 \pm 0.018
Supervised	0.992 \pm 0.000	0.942 \pm 0.003	0.980 \pm 0.001	0.898 \pm 0.003

Table 10: Overall classification accuracy (mean \pm std) of each method on UCI datasets with $\pi_+ = 0.5$, where the best performance (excluding Supervised) is shown in bold.

Method	Optdigits	Pendigits	Letter	PMU-UD
SconfConfDiff-Unbiased	0.971 \pm 0.008	0.992 \pm 0.002	0.935 \pm 0.006	0.986 \pm 0.005
SconfConfDiff-ReLU	0.971 \pm 0.008	0.992 \pm 0.002	0.935 \pm 0.006	0.986 \pm 0.005
SconfConfDiff-ABS	0.971 \pm 0.008	0.992 \pm 0.002	0.935 \pm 0.006	0.986 \pm 0.005
ConfDiff-Unbiased	0.924 \pm 0.014	0.945 \pm 0.024	0.701 \pm 0.079	0.913 \pm 0.060
ConfDiff-ReLU	0.922 \pm 0.007	0.977 \pm 0.004	0.899 \pm 0.008	0.952 \pm 0.014
ConfDiff-ABS	0.964 \pm 0.007	0.989 \pm 0.001	0.922 \pm 0.007	0.982 \pm 0.005
Supervised	0.991 \pm 0.003	0.996 \pm 0.002	0.976 \pm 0.002	0.993 \pm 0.002

Table 11: Overall classification accuracy (mean \pm std) of each method on UCI datasets with $\pi_+ = 0.8$, where the best performance (excluding Supervised) is shown in bold.

Method	Optdigits	Pendigits	Letter	PMU-UD
SconfConfDiff-Unbiased	0.894 \pm 0.059	0.927 \pm 0.044	0.789 \pm 0.027	0.818 \pm 0.050
SconfConfDiff-ReLU	0.957 \pm 0.012	0.985 \pm 0.004	0.935 \pm 0.004	0.951 \pm 0.025
SconfConfDiff-ABS	0.963 \pm 0.008	0.987 \pm 0.005	0.948 \pm 0.004	0.975 \pm 0.005
ConfDiff-Unbiased	0.867 \pm 0.050	0.881 \pm 0.097	0.726 \pm 0.044	0.785 \pm 0.050
Convex($\gamma = 0.2$)-Unbiased	0.912 \pm 0.058	0.958 \pm 0.029	0.743 \pm 0.037	0.824 \pm 0.077
Convex($\gamma = 0.5$)-Unbiased	0.946 \pm 0.010	0.966 \pm 0.017	0.765 \pm 0.029	0.857 \pm 0.078
Convex($\gamma = 0.8$)-Unbiased	0.912 \pm 0.022	0.913 \pm 0.043	0.813 \pm 0.017	0.823 \pm 0.025
Sconf-Unbiased	0.876 \pm 0.047	0.898 \pm 0.063	0.784 \pm 0.035	0.827 \pm 0.032
ConfDiff-ReLU	0.961 \pm 0.011	0.980 \pm 0.007	0.926 \pm 0.006	0.971 \pm 0.007
Convex($\gamma = 0.2$)-ReLU	0.602 \pm 0.177	0.981 \pm 0.004	0.878 \pm 0.032	0.577 \pm 0.319
Convex($\gamma = 0.5$)-ReLU	0.541 \pm 0.352	0.976 \pm 0.007	0.847 \pm 0.035	0.346 \pm 0.249
Convex($\gamma = 0.8$)-ReLU	0.494 \pm 0.333	0.972 \pm 0.008	0.792 \pm 0.101	0.329 \pm 0.206
Sconf-ReLU	0.902 \pm 0.021	0.966 \pm 0.005	0.896 \pm 0.011	0.896 \pm 0.058
ConfDiff-ABS	0.963 \pm 0.005	0.983 \pm 0.004	0.943 \pm 0.004	0.972 \pm 0.002
Convex($\gamma = 0.2$)-ABS	0.967 \pm 0.004	0.982 \pm 0.005	0.945 \pm 0.001	0.973 \pm 0.004
Convex($\gamma = 0.5$)-ABS	0.969 \pm 0.009	0.980 \pm 0.005	0.942 \pm 0.002	0.976 \pm 0.005
Convex($\gamma = 0.8$)-ABS	0.966 \pm 0.007	0.977 \pm 0.007	0.937 \pm 0.004	0.974 \pm 0.005
Sconf-ABS	0.948 \pm 0.012	0.966 \pm 0.013	0.915 \pm 0.004	0.940 \pm 0.034
Supervised	0.990 \pm 0.004	0.997 \pm 0.001	0.977 \pm 0.004	0.995 \pm 0.002

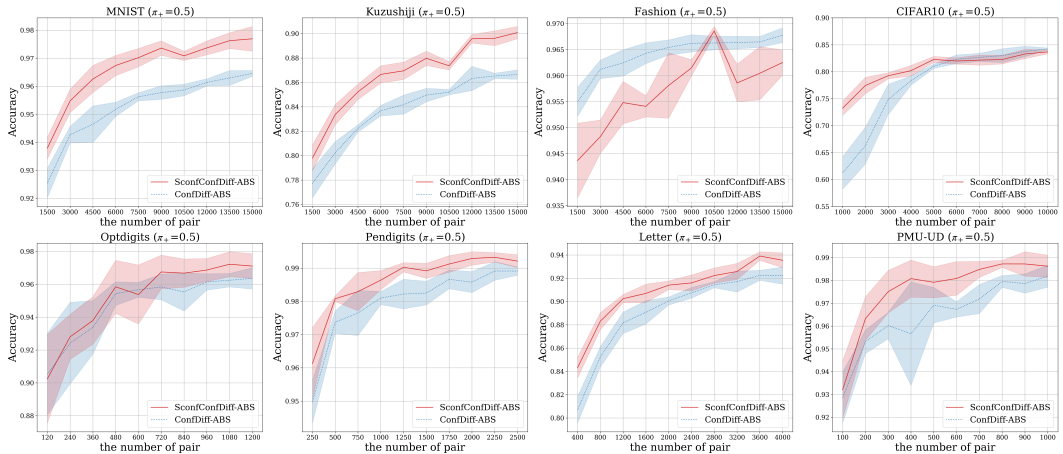


Figure 5: Classification performance of SconfConfDiff-ABS, SconfConfDiff-Convex($\gamma = 0.5$)-ABS, Sconf-ABS, and ConfDiff-ABS given a fraction of training data ($\pi_+ = 0.5$).

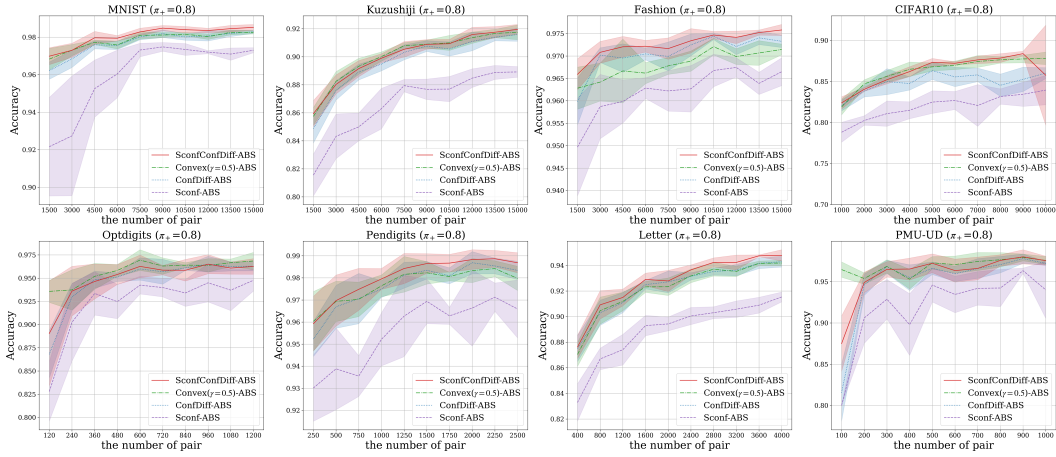


Figure 6: Classification performance of SconfConfDiff-ABS, SconfConfDiff-Convex($\gamma = 0.5$)-ABS, Sconf-ABS, and ConfDiff-ABS given a fraction of training data ($\pi_+ = 0.8$).

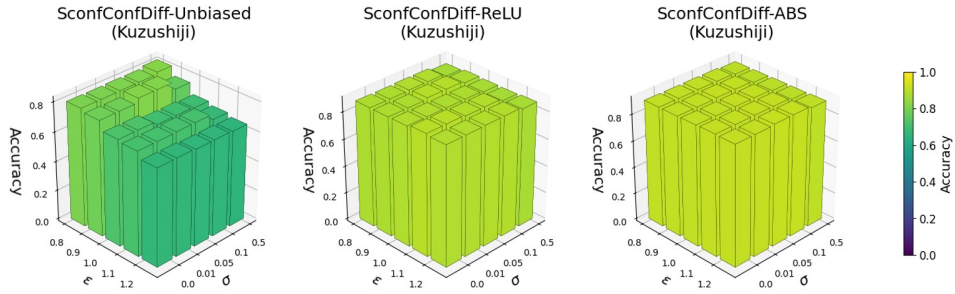


Figure 7: Classification performance on Kuzushiji-MNIST with $\pi_+ = 0.2$ given an inaccurate class prior probability, noisy similarity-confidence, and noisy confidence-difference. Both the height and color of the bars represent accuracy.

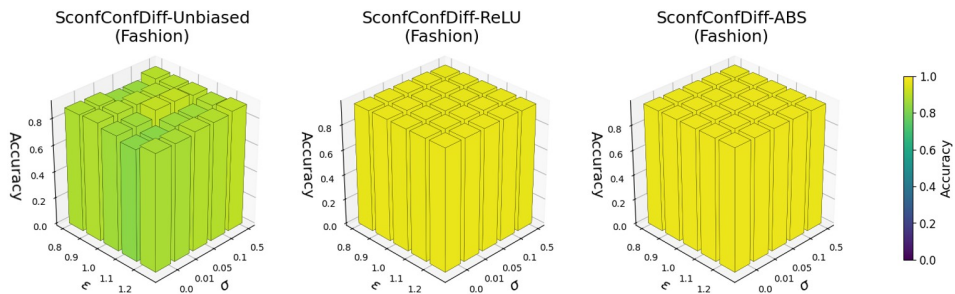


Figure 8: Classification performance on Fashion-MNIST with $\pi_+ = 0.2$ given an inaccurate class prior probability, noisy similarity-confidence, and noisy confidence-difference. Both the height and color of the bars represent accuracy.

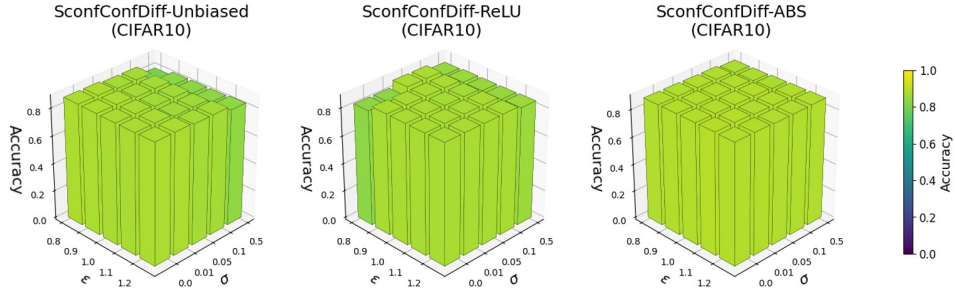


Figure 9: Classification performance on CIFAR-10 with $\pi_+ = 0.2$ given an inaccurate class prior probability, noisy similarity-confidence, and noisy confidence-difference. Both the height and color of the bars represent accuracy.

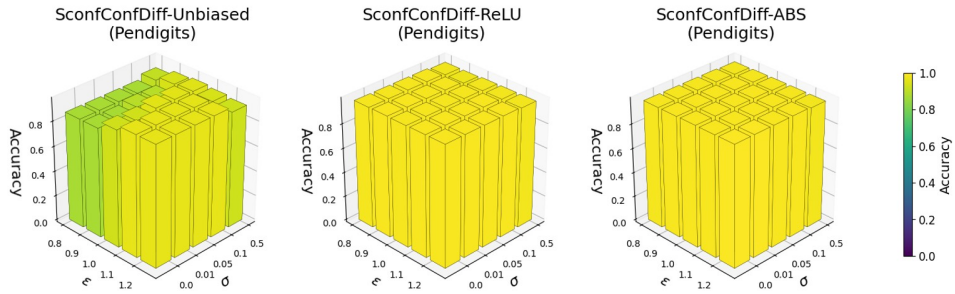


Figure 10: Classification performance on Pendigits with $\pi_+ = 0.2$ given an inaccurate class prior probability, noisy similarity-confidence, and noisy confidence-difference. Both the height and color of the bars represent accuracy.

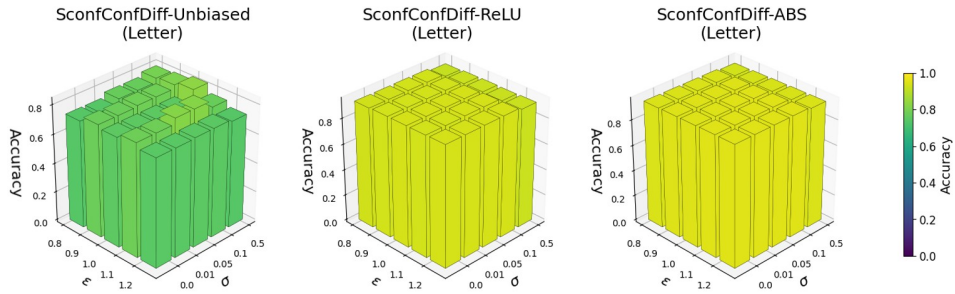


Figure 11: Classification performance on Letter with $\pi_+ = 0.2$ given an inaccurate class prior probability, noisy similarity-confidence, and noisy confidence-difference. Both the height and color of the bars represent accuracy.

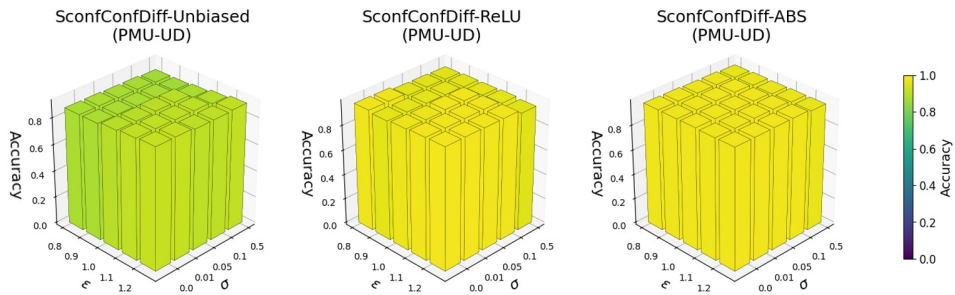


Figure 12: Classification performance on PMU-UD with $\pi_+ = 0.2$ given an inaccurate class prior probability, noisy similarity-confidence, and noisy confidence-difference. Both the height and color of the bars represent accuracy.

Table 12: The detail of accuracy (mean \pm std) on MNIST in Fig 4.

Dataset	(ϵ, σ)	Unbiased	ReLU	ABS
MNIST	(0.8,0.0)	0.857 \pm 0.041	0.966 \pm 0.011	0.974 \pm 0.003
	(0.8,0.01)	0.857 \pm 0.041	0.966 \pm 0.011	0.974 \pm 0.003
	(0.8,0.05)	0.880 \pm 0.034	0.970 \pm 0.004	0.974 \pm 0.002
	(0.8,0.1)	0.880 \pm 0.034	0.970 \pm 0.004	0.974 \pm 0.002
	(0.8,0.5)	0.899 \pm 0.028	0.959 \pm 0.011	0.971 \pm 0.003
	(0.9,0.0)	0.883 \pm 0.028	0.975 \pm 0.005	0.976 \pm 0.003
	(0.9,0.01)	0.883 \pm 0.028	0.975 \pm 0.005	0.976 \pm 0.003
	(0.9,0.05)	0.873 \pm 0.051	0.969 \pm 0.004	0.975 \pm 0.004
	(0.9,0.1)	0.873 \pm 0.051	0.969 \pm 0.004	0.975 \pm 0.004
	(0.9,0.5)	0.865 \pm 0.083	0.961 \pm 0.010	0.971 \pm 0.001
	(1.0,0.0)	0.900 \pm 0.035	0.975 \pm 0.004	0.978 \pm 0.003
	(1.0,0.01)	0.900 \pm 0.035	0.975 \pm 0.004	0.978 \pm 0.003
	(1.0,0.05)	0.881 \pm 0.050	0.973 \pm 0.002	0.978 \pm 0.002
	(1.0,0.1)	0.881 \pm 0.050	0.973 \pm 0.002	0.978 \pm 0.002
	(1.0,0.5)	0.830 \pm 0.048	0.963 \pm 0.007	0.974 \pm 0.002
	(1.1,0.0)	0.842 \pm 0.031	0.974 \pm 0.006	0.981 \pm 0.003
	(1.1,0.01)	0.842 \pm 0.031	0.974 \pm 0.006	0.981 \pm 0.003
	(1.1,0.05)	0.849 \pm 0.043	0.974 \pm 0.003	0.979 \pm 0.003
	(1.1,0.1)	0.849 \pm 0.043	0.974 \pm 0.003	0.979 \pm 0.003
	(1.1,0.5)	0.822 \pm 0.048	0.962 \pm 0.008	0.975 \pm 0.004
(1.2,0.0)	0.819 \pm 0.030	0.975 \pm 0.003	0.982 \pm 0.001	
(1.2,0.01)	0.819 \pm 0.030	0.975 \pm 0.003	0.982 \pm 0.001	
(1.2,0.05)	0.825 \pm 0.038	0.974 \pm 0.002	0.980 \pm 0.002	
(1.2,0.1)	0.825 \pm 0.038	0.974 \pm 0.002	0.980 \pm 0.002	
(1.2,0.5)	0.829 \pm 0.027	0.965 \pm 0.003	0.977 \pm 0.003	

Table 13: The detail of accuracy (mean \pm std) in Fig 7.

Dataset	(ϵ, σ)	Unbiased	ReLU	ABS
KMNIIST	(0.8,0.0)	0.803 \pm 0.032	0.879 \pm 0.011	0.903 \pm 0.005
	(0.8,0.01)	0.803 \pm 0.032	0.879 \pm 0.011	0.903 \pm 0.005
	(0.8,0.05)	0.805 \pm 0.062	0.882 \pm 0.010	0.905 \pm 0.006
	(0.8,0.1)	0.805 \pm 0.062	0.882 \pm 0.010	0.905 \pm 0.006
	(0.8,0.5)	0.819 \pm 0.020	0.864 \pm 0.007	0.898 \pm 0.009
	(0.9,0.0)	0.784 \pm 0.050	0.878 \pm 0.007	0.903 \pm 0.006
	(0.9,0.01)	0.784 \pm 0.050	0.878 \pm 0.007	0.903 \pm 0.006
	(0.9,0.05)	0.813 \pm 0.011	0.888 \pm 0.007	0.908 \pm 0.004
	(0.9,0.1)	0.813 \pm 0.011	0.888 \pm 0.007	0.908 \pm 0.004
	(0.9,0.5)	0.760 \pm 0.062	0.873 \pm 0.014	0.897 \pm 0.005
	(1.0,0.0)	0.720 \pm 0.028	0.879 \pm 0.009	0.906 \pm 0.004
	(1.0,0.01)	0.720 \pm 0.028	0.879 \pm 0.009	0.906 \pm 0.004
	(1.0,0.05)	0.698 \pm 0.024	0.878 \pm 0.013	0.908 \pm 0.006
	(1.0,0.1)	0.698 \pm 0.024	0.878 \pm 0.013	0.908 \pm 0.006
	(1.0,0.5)	0.690 \pm 0.065	0.869 \pm 0.014	0.898 \pm 0.009
	(1.1,0.0)	0.707 \pm 0.076	0.892 \pm 0.009	0.909 \pm 0.003
	(1.1,0.01)	0.707 \pm 0.076	0.892 \pm 0.009	0.909 \pm 0.003
	(1.1,0.05)	0.709 \pm 0.048	0.884 \pm 0.005	0.910 \pm 0.008
	(1.1,0.1)	0.709 \pm 0.048	0.884 \pm 0.005	0.910 \pm 0.008
	(1.1,0.5)	0.672 \pm 0.044	0.867 \pm 0.008	0.897 \pm 0.009
(1.2,0.0)	0.663 \pm 0.063	0.882 \pm 0.013	0.906 \pm 0.005	
(1.2,0.01)	0.663 \pm 0.063	0.882 \pm 0.013	0.906 \pm 0.005	
(1.2,0.05)	0.657 \pm 0.031	0.884 \pm 0.009	0.913 \pm 0.007	
(1.2,0.1)	0.657 \pm 0.031	0.884 \pm 0.009	0.913 \pm 0.007	
(1.2,0.5)	0.652 \pm 0.030	0.871 \pm 0.008	0.899 \pm 0.010	

Table 14: The detail of accuracy (mean \pm std) in Fig 8.

Dataset	(ϵ, σ)	Unbiased	ReLU	ABS
Fashion	(0.8,0.0)	0.877 \pm 0.017	0.964 \pm 0.004	0.967 \pm 0.002
	(0.8,0.01)	0.877 \pm 0.017	0.964 \pm 0.004	0.967 \pm 0.002
	(0.8,0.05)	0.844 \pm 0.044	0.965 \pm 0.005	0.967 \pm 0.002
	(0.8,0.1)	0.844 \pm 0.044	0.965 \pm 0.005	0.967 \pm 0.002
	(0.8,0.5)	0.890 \pm 0.037	0.958 \pm 0.008	0.964 \pm 0.004
	(0.9,0.0)	0.883 \pm 0.010	0.965 \pm 0.001	0.969 \pm 0.003
	(0.9,0.01)	0.883 \pm 0.010	0.965 \pm 0.001	0.969 \pm 0.003
	(0.9,0.05)	0.886 \pm 0.043	0.963 \pm 0.004	0.969 \pm 0.003
	(0.9,0.1)	0.886 \pm 0.043	0.963 \pm 0.004	0.969 \pm 0.003
	(0.9,0.5)	0.887 \pm 0.040	0.960 \pm 0.002	0.966 \pm 0.005
	(1.0,0.0)	0.857 \pm 0.042	0.963 \pm 0.002	0.969 \pm 0.002
	(1.0,0.01)	0.857 \pm 0.042	0.963 \pm 0.002	0.969 \pm 0.002
	(1.0,0.05)	0.910 \pm 0.029	0.962 \pm 0.004	0.970 \pm 0.003
	(1.0,0.1)	0.910 \pm 0.029	0.962 \pm 0.004	0.970 \pm 0.003
	(1.0,0.5)	0.891 \pm 0.054	0.960 \pm 0.003	0.968 \pm 0.003
	(1.1,0.0)	0.827 \pm 0.063	0.964 \pm 0.003	0.971 \pm 0.002
	(1.1,0.01)	0.827 \pm 0.063	0.964 \pm 0.003	0.971 \pm 0.002
	(1.1,0.05)	0.857 \pm 0.035	0.966 \pm 0.003	0.971 \pm 0.001
	(1.1,0.1)	0.857 \pm 0.035	0.966 \pm 0.003	0.971 \pm 0.001
	(1.1,0.5)	0.881 \pm 0.034	0.962 \pm 0.003	0.967 \pm 0.002
(1.2,0.0)	0.869 \pm 0.029	0.966 \pm 0.002	0.972 \pm 0.001	
(1.2,0.01)	0.869 \pm 0.029	0.966 \pm 0.002	0.972 \pm 0.001	
(1.2,0.05)	0.886 \pm 0.011	0.967 \pm 0.002	0.972 \pm 0.003	
(1.2,0.1)	0.886 \pm 0.011	0.967 \pm 0.002	0.972 \pm 0.003	
(1.2,0.5)	0.902 \pm 0.019	0.962 \pm 0.003	0.969 \pm 0.002	

Table 15: The detail of accuracy (mean \pm std) in Fig 9.

Dataset	(ϵ, σ)	Unbiased	ReLU	ABS
CIFAR10	(0.8,0.0)	0.875 \pm 0.003	0.829 \pm 0.040	0.883 \pm 0.005
	(0.8,0.01)	0.875 \pm 0.003	0.829 \pm 0.040	0.883 \pm 0.005
	(0.8,0.05)	0.865 \pm 0.008	0.874 \pm 0.014	0.882 \pm 0.007
	(0.8,0.1)	0.865 \pm 0.008	0.874 \pm 0.014	0.882 \pm 0.007
	(0.8,0.5)	0.801 \pm 0.038	0.843 \pm 0.007	0.871 \pm 0.004
	(0.9,0.0)	0.873 \pm 0.007	0.869 \pm 0.012	0.884 \pm 0.005
	(0.9,0.01)	0.873 \pm 0.007	0.869 \pm 0.012	0.884 \pm 0.005
	(0.9,0.05)	0.864 \pm 0.008	0.869 \pm 0.013	0.882 \pm 0.004
	(0.9,0.1)	0.864 \pm 0.008	0.869 \pm 0.013	0.882 \pm 0.004
	(0.9,0.5)	0.829 \pm 0.014	0.848 \pm 0.006	0.872 \pm 0.003
	(1.0,0.0)	0.871 \pm 0.007	0.869 \pm 0.010	0.885 \pm 0.004
	(1.0,0.01)	0.871 \pm 0.007	0.869 \pm 0.010	0.885 \pm 0.004
	(1.0,0.05)	0.862 \pm 0.009	0.866 \pm 0.010	0.883 \pm 0.005
	(1.0,0.1)	0.862 \pm 0.009	0.866 \pm 0.010	0.883 \pm 0.005
	(1.0,0.5)	0.829 \pm 0.008	0.847 \pm 0.007	0.876 \pm 0.004
	(1.1,0.0)	0.871 \pm 0.009	0.868 \pm 0.007	0.887 \pm 0.004
	(1.1,0.01)	0.871 \pm 0.009	0.868 \pm 0.007	0.887 \pm 0.004
	(1.1,0.05)	0.856 \pm 0.015	0.869 \pm 0.009	0.880 \pm 0.001
	(1.1,0.1)	0.856 \pm 0.015	0.869 \pm 0.009	0.880 \pm 0.001
	(1.1,0.5)	0.829 \pm 0.016	0.847 \pm 0.011	0.879 \pm 0.002
(1.2,0.0)	0.873 \pm 0.010	0.870 \pm 0.010	0.884 \pm 0.004	
(1.2,0.01)	0.873 \pm 0.010	0.870 \pm 0.010	0.884 \pm 0.004	
(1.2,0.05)	0.864 \pm 0.005	0.868 \pm 0.010	0.880 \pm 0.002	
(1.2,0.1)	0.864 \pm 0.005	0.868 \pm 0.010	0.880 \pm 0.002	
(1.2,0.5)	0.835 \pm 0.006	0.850 \pm 0.005	0.882 \pm 0.004	

Table 16: The detail of accuracy (mean \pm std) Optdigits in Fig 4.

Dataset	(ϵ, σ)	Unbiased	ReLU	ABS
Optdigits	(0.8,0.0)	0.917 \pm 0.042	0.950 \pm 0.019	0.961 \pm 0.006
	(0.8,0.01)	0.917 \pm 0.042	0.950 \pm 0.019	0.961 \pm 0.006
	(0.8,0.05)	0.914 \pm 0.031	0.953 \pm 0.005	0.961 \pm 0.007
	(0.8,0.1)	0.914 \pm 0.031	0.953 \pm 0.005	0.961 \pm 0.007
	(0.8,0.5)	0.875 \pm 0.044	0.933 \pm 0.020	0.942 \pm 0.018
	(0.9,0.0)	0.923 \pm 0.048	0.949 \pm 0.015	0.966 \pm 0.007
	(0.9,0.01)	0.923 \pm 0.048	0.949 \pm 0.015	0.966 \pm 0.007
	(0.9,0.05)	0.918 \pm 0.029	0.946 \pm 0.024	0.962 \pm 0.011
	(0.9,0.1)	0.918 \pm 0.029	0.946 \pm 0.024	0.962 \pm 0.011
	(0.9,0.5)	0.877 \pm 0.046	0.917 \pm 0.031	0.945 \pm 0.014
	(1.0,0.0)	0.925 \pm 0.052	0.954 \pm 0.017	0.965 \pm 0.007
	(1.0,0.01)	0.925 \pm 0.052	0.954 \pm 0.017	0.965 \pm 0.007
	(1.0,0.05)	0.886 \pm 0.072	0.959 \pm 0.012	0.970 \pm 0.006
	(1.0,0.1)	0.886 \pm 0.072	0.959 \pm 0.012	0.970 \pm 0.006
	(1.0,0.5)	0.872 \pm 0.052	0.927 \pm 0.024	0.949 \pm 0.016
	(1.1,0.0)	0.921 \pm 0.058	0.957 \pm 0.012	0.970 \pm 0.006
	(1.1,0.01)	0.921 \pm 0.058	0.957 \pm 0.012	0.970 \pm 0.006
	(1.1,0.05)	0.908 \pm 0.055	0.955 \pm 0.020	0.971 \pm 0.007
	(1.1,0.1)	0.908 \pm 0.055	0.955 \pm 0.020	0.971 \pm 0.007
	(1.1,0.5)	0.870 \pm 0.052	0.947 \pm 0.019	0.953 \pm 0.012
	(1.2,0.0)	0.910 \pm 0.057	0.970 \pm 0.008	0.974 \pm 0.007
	(1.2,0.01)	0.910 \pm 0.057	0.970 \pm 0.008	0.974 \pm 0.007
	(1.2,0.05)	0.919 \pm 0.058	0.964 \pm 0.009	0.972 \pm 0.006
	(1.2,0.1)	0.919 \pm 0.058	0.964 \pm 0.009	0.972 \pm 0.006
	(1.2,0.5)	0.892 \pm 0.051	0.944 \pm 0.013	0.953 \pm 0.013

Table 17: The detail of accuracy (mean \pm std) on in Fig 10.

Dataset	(ϵ, σ)	Unbiased	ReLU	ABS
Pendigits	(0.8,0.0)	0.870 \pm 0.086	0.986 \pm 0.004	0.987 \pm 0.002
	(0.8,0.01)	0.870 \pm 0.086	0.986 \pm 0.004	0.987 \pm 0.002
	(0.8,0.05)	0.870 \pm 0.076	0.987 \pm 0.005	0.988 \pm 0.004
	(0.8,0.1)	0.870 \pm 0.076	0.987 \pm 0.005	0.988 \pm 0.004
	(0.8,0.5)	0.908 \pm 0.070	0.977 \pm 0.008	0.983 \pm 0.005
	(0.9,0.0)	0.870 \pm 0.100	0.988 \pm 0.003	0.988 \pm 0.003
	(0.9,0.01)	0.870 \pm 0.100	0.988 \pm 0.003	0.988 \pm 0.003
	(0.9,0.05)	0.894 \pm 0.053	0.987 \pm 0.004	0.989 \pm 0.003
	(0.9,0.1)	0.894 \pm 0.053	0.987 \pm 0.004	0.989 \pm 0.003
	(0.9,0.5)	0.941 \pm 0.020	0.976 \pm 0.007	0.986 \pm 0.004
	(1.0,0.0)	0.927 \pm 0.081	0.987 \pm 0.003	0.991 \pm 0.003
	(1.0,0.01)	0.927 \pm 0.081	0.987 \pm 0.003	0.991 \pm 0.003
	(1.0,0.05)	0.954 \pm 0.038	0.987 \pm 0.004	0.991 \pm 0.003
	(1.0,0.1)	0.954 \pm 0.038	0.987 \pm 0.004	0.991 \pm 0.003
	(1.0,0.5)	0.951 \pm 0.026	0.981 \pm 0.007	0.986 \pm 0.004
	(1.1,0.0)	0.964 \pm 0.042	0.989 \pm 0.003	0.990 \pm 0.002
	(1.1,0.01)	0.964 \pm 0.042	0.989 \pm 0.003	0.990 \pm 0.002
	(1.1,0.05)	0.959 \pm 0.034	0.989 \pm 0.003	0.991 \pm 0.003
	(1.1,0.1)	0.959 \pm 0.034	0.989 \pm 0.003	0.991 \pm 0.003
	(1.1,0.5)	0.938 \pm 0.027	0.982 \pm 0.008	0.986 \pm 0.004
	(1.2,0.0)	0.964 \pm 0.036	0.990 \pm 0.004	0.992 \pm 0.002
	(1.2,0.01)	0.964 \pm 0.036	0.990 \pm 0.004	0.992 \pm 0.002
	(1.2,0.05)	0.964 \pm 0.037	0.989 \pm 0.004	0.991 \pm 0.002
	(1.2,0.1)	0.964 \pm 0.037	0.989 \pm 0.004	0.991 \pm 0.002
	(1.2,0.5)	0.924 \pm 0.031	0.981 \pm 0.006	0.984 \pm 0.004

Table 18: The detail of accuracy (mean \pm std) in Fig 11.

Dataset	(ϵ, σ)	Unbiased	ReLU	ABS
Letter	(0.8,0.0)	0.737 \pm 0.037	0.929 \pm 0.004	0.943 \pm 0.005
	(0.8,0.01)	0.737 \pm 0.037	0.929 \pm 0.004	0.943 \pm 0.005
	(0.8,0.05)	0.769 \pm 0.035	0.930 \pm 0.004	0.943 \pm 0.004
	(0.8,0.1)	0.769 \pm 0.035	0.930 \pm 0.004	0.943 \pm 0.004
	(0.8,0.5)	0.797 \pm 0.034	0.913 \pm 0.004	0.933 \pm 0.004
	(0.9,0.0)	0.774 \pm 0.023	0.933 \pm 0.004	0.947 \pm 0.005
	(0.9,0.01)	0.774 \pm 0.023	0.933 \pm 0.004	0.947 \pm 0.005
	(0.9,0.05)	0.782 \pm 0.042	0.932 \pm 0.007	0.948 \pm 0.005
	(0.9,0.1)	0.782 \pm 0.042	0.932 \pm 0.007	0.948 \pm 0.005
	(0.9,0.5)	0.807 \pm 0.036	0.919 \pm 0.007	0.936 \pm 0.005
	(1.0,0.0)	0.752 \pm 0.067	0.934 \pm 0.007	0.948 \pm 0.005
	(1.0,0.01)	0.752 \pm 0.067	0.934 \pm 0.007	0.948 \pm 0.005
	(1.0,0.05)	0.750 \pm 0.054	0.934 \pm 0.003	0.949 \pm 0.004
	(1.0,0.1)	0.750 \pm 0.054	0.934 \pm 0.003	0.949 \pm 0.004
	(1.0,0.5)	0.831 \pm 0.043	0.920 \pm 0.005	0.939 \pm 0.005
	(1.1,0.0)	0.779 \pm 0.048	0.933 \pm 0.007	0.951 \pm 0.001
	(1.1,0.01)	0.779 \pm 0.048	0.933 \pm 0.007	0.951 \pm 0.001
	(1.1,0.05)	0.817 \pm 0.053	0.937 \pm 0.005	0.951 \pm 0.005
	(1.1,0.1)	0.817 \pm 0.053	0.937 \pm 0.005	0.951 \pm 0.005
	(1.1,0.5)	0.771 \pm 0.030	0.918 \pm 0.006	0.941 \pm 0.004
	(1.2,0.0)	0.745 \pm 0.059	0.936 \pm 0.007	0.952 \pm 0.005
	(1.2,0.01)	0.745 \pm 0.059	0.936 \pm 0.007	0.952 \pm 0.005
	(1.2,0.05)	0.749 \pm 0.042	0.936 \pm 0.007	0.952 \pm 0.004
	(1.2,0.1)	0.749 \pm 0.042	0.936 \pm 0.007	0.952 \pm 0.004
(1.2,0.5)	0.736 \pm 0.024	0.920 \pm 0.003	0.942 \pm 0.006	

Table 19: The detail of accuracy (mean \pm std) in Fig 12.

Dataset	(ϵ, σ)	Unbiased	ReLU	ABS
PMU-UD	(0.8,0.0)	0.873 \pm 0.066	0.973 \pm 0.008	0.975 \pm 0.010
	(0.8,0.01)	0.873 \pm 0.066	0.973 \pm 0.008	0.975 \pm 0.010
	(0.8,0.05)	0.870 \pm 0.064	0.953 \pm 0.020	0.971 \pm 0.009
	(0.8,0.1)	0.870 \pm 0.064	0.953 \pm 0.020	0.971 \pm 0.009
	(0.8,0.5)	0.862 \pm 0.058	0.950 \pm 0.019	0.964 \pm 0.011
	(0.9,0.0)	0.875 \pm 0.085	0.960 \pm 0.032	0.975 \pm 0.009
	(0.9,0.01)	0.875 \pm 0.085	0.960 \pm 0.032	0.975 \pm 0.009
	(0.9,0.05)	0.872 \pm 0.083	0.959 \pm 0.017	0.977 \pm 0.009
	(0.9,0.1)	0.872 \pm 0.083	0.959 \pm 0.017	0.977 \pm 0.009
	(0.9,0.5)	0.863 \pm 0.072	0.955 \pm 0.006	0.967 \pm 0.009
	(1.0,0.0)	0.892 \pm 0.092	0.970 \pm 0.018	0.978 \pm 0.007
	(1.0,0.01)	0.892 \pm 0.092	0.970 \pm 0.018	0.978 \pm 0.007
	(1.0,0.05)	0.898 \pm 0.069	0.978 \pm 0.005	0.976 \pm 0.007
	(1.0,0.1)	0.898 \pm 0.069	0.978 \pm 0.005	0.976 \pm 0.007
	(1.0,0.5)	0.872 \pm 0.068	0.955 \pm 0.023	0.965 \pm 0.014
	(1.1,0.0)	0.904 \pm 0.074	0.978 \pm 0.009	0.974 \pm 0.012
	(1.1,0.01)	0.904 \pm 0.074	0.978 \pm 0.009	0.974 \pm 0.012
	(1.1,0.05)	0.901 \pm 0.080	0.979 \pm 0.008	0.980 \pm 0.007
	(1.1,0.1)	0.901 \pm 0.080	0.979 \pm 0.008	0.980 \pm 0.007
	(1.1,0.5)	0.889 \pm 0.075	0.959 \pm 0.011	0.968 \pm 0.014
	(1.2,0.0)	0.912 \pm 0.045	0.981 \pm 0.009	0.977 \pm 0.014
	(1.2,0.01)	0.912 \pm 0.045	0.981 \pm 0.009	0.977 \pm 0.014
	(1.2,0.05)	0.900 \pm 0.052	0.978 \pm 0.002	0.980 \pm 0.006
	(1.2,0.1)	0.900 \pm 0.052	0.978 \pm 0.002	0.980 \pm 0.006
(1.2,0.5)	0.906 \pm 0.072	0.950 \pm 0.011	0.967 \pm 0.013	

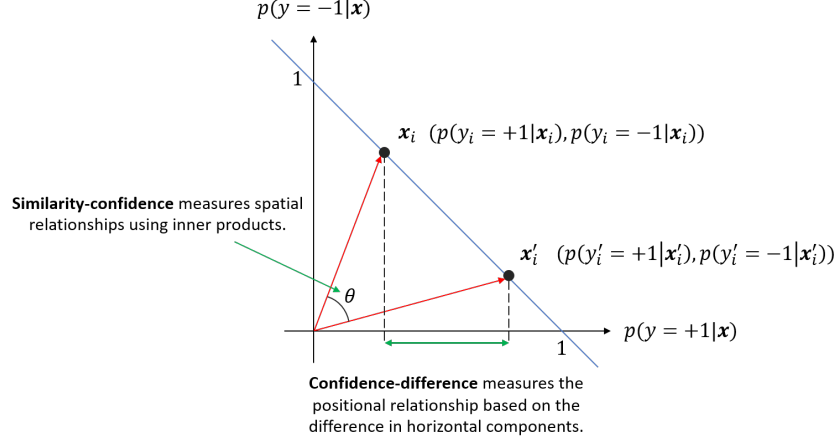


Figure 13: Geometric Interpretation of Similarity-Confidence and Confidence-Difference.

F Geometric Interpretation of Sconf and ConfDiff

In this section, we provide a geometric interpretation of similarity-confidence and confidence-difference. Based on the definition of similarity-confidence, the following equation holds.

$$\begin{aligned}
 s(\mathbf{x}, \mathbf{x}') &= p(y = y' | \mathbf{x}, \mathbf{x}') \\
 &= p(y = y' = +1 | \mathbf{x}, \mathbf{x}') + p(y = y' = -1 | \mathbf{x}, \mathbf{x}') \\
 &= \frac{p(\mathbf{x}, y = +1, \mathbf{x}', y' = +1) + p(\mathbf{x}, y = -1, \mathbf{x}', y' = -1)}{p(\mathbf{x}, \mathbf{x}')} \\
 &= \frac{p(\mathbf{x}, y = +1)p(\mathbf{x}', y' = +1) + p(\mathbf{x}, y = -1)p(\mathbf{x}', y' = -1)}{p(\mathbf{x})p(\mathbf{x}')} \\
 &= p(y = +1 | \mathbf{x})p(y' = +1 | \mathbf{x}') + p(y = -1 | \mathbf{x})p(y' = -1 | \mathbf{x}') \\
 &= p(y = +1 | \mathbf{x})p(y' = +1 | \mathbf{x}') + (1 - p(y = +1 | \mathbf{x}))(1 - p(y' = +1 | \mathbf{x}'))
 \end{aligned}$$

According to this result, in Fig. 13, similarity-confidence computes the inner product of their confidences between two samples using the inner product of their confidences. In contrast, confidence-difference is based on the difference along the horizontal axis in Fig. 13. Therefore, both similarity-confidence and confidence-difference can be interpreted as measuring the relative position of confidence values between two samples. However, since they measure it in different ways, the label information encoded in the data pairs is considered to be fundamentally different.